The Regulation of Fibroblast Growth Factor 23 in Autosomal Dominant Polycystic Kidney Disease

---

Dissertation

zur

Erlangung der naturwissenschaftlichen Doktorwürde

(Dr. sc. nat.)

vorgelegt der

Mathematisch-naturwissenschaftlichen Fakultät

der

Universität Zürich

von

Daniela Spichtig

von

Sachseln OW

Promotionskomitee

Prof. Dr. med. Carsten A. Wagner (Vorsitz)
Prof. Orson W. Moe, MD, PhD
Prof. Dr. med. Philippe Jaeger
Prof. Olivier Devuyst, MD, PhD

Zürich, 2015

Contents

Zusammenfassung

Der Fibroblasten Wachstumsfaktor 23 (FGF23) wird vom Knochen sezerniert und gelangt über die Blutgefässe in die Nieren, in welchen er die Phosphatkonzentration des Blutes und den Vitamin D_3 Metabolismus reguliert. Patienten im 2. und 3. Stadium der chronischen Nierenerkrankung (CKD) haben erhöhte FGF23 Blutwerte, welche im Endstadium von CKD wesentlich zu kardiovaskulären Komplikationen und zur erhöhten Sterblichkeit beitragen. Die polyzystische Nierenerkrankung (ADPKD) führt zu CKD, wobei jedoch erhöhte FGF23 Blutwerte bereits bei normaler Nierenfunktion vorliegen. Die Regulierung von FGF23 in ADPKD und CKD ist zu weiten Teilen unbekannt. In dieser Studie wurden PKD Tiermodelle verwendet um die Regulation von FGF23 in CKD zu untersuchen. Fgf23 war in PKD Ratten, ähnlich wie bei ADPKD Patienten, erhöht bevor die Nierenfunktion abnahm. Trotz erhöhter Fgf23 Blutwerte waren keine Veränderungen in Bezug auf die Phosphat- oder die Vitamin D_3 Konzentrationen im Blut zu beobachten. Die Signalkaskade, welche von Fgf23 in der Niere ausgelöst wird, war intakt. Daraus geht hervor, dass die Nieren von PKD Ratten resistent gegenüber Fgf23 sind. Wir zeigten, dass die *Fgf23* Expression in PKD Ratten und Mäusen statt im Knochen in der Niere erhöht war. Anschliessend evaluierten wir Sauerstoffarmut oder Entzündungsfaktoren als zwei mögliche Ursachen, welche die Regulation der Fgf23 Expression in der Niere und im Knochen beeinflussen. In primären Mausosteozyten erhöhte der Entzündungsfaktor Tumornekrosefaktor (Tnfα), nicht aber die Sauerstoffarmut, die *Fgf23* Expression. In PKD Nieren war die *Tnfα* Expression erhöht und zusätzlich begleitet von einer erhöhten Expression des nuklären Rezeptors *Nurr1*. Nurr1 stimuliert Fgf23 Expression im Knochen. Die Blockierung von Tnfα in PKD Mäusen resultierte in der Reduktion der Fgf23 Blutwerte sowie der Reduktion der renalen *Fgf23* und *Nurr1* Expression. Mit dieser Studie konnten wir aufzeigen, dass der Entzündungsfaktor Tnfα eine wichtige Rolle spielt in der Regulation von Fgf23 Expression in der Niere und im Knochen.

Abstract

Fibroblast growth factor 23 (FGF23) is a bone derived endocrine factor which regulates phosphate homeostasis and vitamin D_3 metabolism in the kidney. FGF23 rises in chronic kidney disease (CKD) stage G2 to G3 and contributes significantly to cardiovascular disease and all cause mortality in endstage renal disease. Autosomal dominant polycystic kidney disease (ADPKD) is a cause for CKD where the increase in FGF23 precedes the first measurable decline in renal function. The mechanisms governing FGF23 production and effects in kidney disease are largely unknown. In this study we investigated the regulation of Fgf23 in PKD using the Han:SPRD rat and *Pkd1* conditional KO mouse model. We found highly elevated Fgf23 levels in Han:SPRD *cy/+* rats while renal function was still normal. Despite the high Fgf23 levels, phosphate handling and vitamin D_3 metabolism were unchanged and the Fgf23 signaling cascade was intact indicating resistance to Fgf23. We evaluated the source of Fgf23 and found that *Fgf23* expression in kidney but not in bone was increased. In PKD kidneys, the cells lining the cysts expressed Fgf23. This triggered the question of the regulation of Fgf23 expression in bone and *de novo* Fgf23 expression in kidney. We investigated the effect of hypoxia and the inflammatory cytokine Tnfα on *Fgf23* expression in bone cells. Tnfα but not hypoxia regulated *Fgf23* expression in primary mouse osteocytes. In PKD kidneys, elevated *Tnfα* and *Tgfβ* expression levels were paralleled by increased expression of the orphan nuclear receptor *Nurr1*. Nurr1 is involved in the Pth dependent upregulation of Fgf23 in bone. In PKD kidneys, Nurr1 was predominantly localized in the nucleus and often overlapped with Fgf23 protein expression. Neutralization of Tnfα reduced Fgf23 plasma levels in PKD and healthy animals and decreased the renal expression of inflammatory cytokines. Furthermore application of anti-Tnfα antibodies tended to result in lower renal *Fgf23* and *Nurr1* expression. This study provides strong evidence that the inflammatory cytokine Tnfα modulates Fgf23 expression in cystic kidneys as well as in osteocytes.

Chapter 1

Introduction

1.1 The biological function of phosphorus

Phosphorus is a key element in various biological processes such as energy production, cell signaling, mineralization of the endoskeleton as well as membrane and protein synthesis [1–6]. In a balanced diet, humans consume daily approximately 20 mg/kg phosphorus from which 16 mg/kg is absorbed by the intestine [7]. The pancreas as well as the intestine secret 3 mg/kg phosphorus into the intestine in the form of digestive juice that results in a daily net phosphorus absorption into the circulation of 13 mg/kg and net phosphorus excretion into the feces of 7 mg/kg [7]. Additionally, there is a constant bone turnover which amounts to 3 $\frac{mg}{kg*day}$ [7]. In mammals, phosphorus occurs in the form of mono- or divalent inorganic phosphate (Pi) ($H_2PO_4^-$ and HPO_4^{2-}) or organic phosphates which are combinations of phosphate and lipids, carbohydrates, or proteins [8]. The average plasma Pi concentration in children is between 1.3 and 2.3 mmol/l and in adults between 0.8 and 1.5 mmol/l [8, 9]. The high extracellular Pi concentration in young mammals is important for normal growth and bone mineralization [9, 10]. In adults 80-90 % of phosphate is found in the form of hydroxyapatite in bone and 9% in the form of organic phosphate in skeletal muscle [4, 5, 8]. Phosphate which is not deposited in bone is mostly localized intracellularly in the form of organic phosphate and to a minor fraction in the form of Pi [8]. With an estimated concentration of up to 100 mmol/l, Pi is the main intracellular anion [8].

Disturbances of phosphate homeostasis lead to severe physiological problems. An acute negative phosphate balance causes leukocyte and erythrocyte dysfunction due to impairment of ATP synthesis as well as altered cardiac function and myopathy [8, 11, 12]. Chronic

phosphate deficiency results in impaired bone mineralization and therefore causes rickets and osteomalcia [13, 14]. On the other hand hyperphosphatemia leads to ectopic calcification of soft tissues and vasculature which in turn causes inflammation and cardiovascular disease [15, 16]. An acute and severe increase of serum phosphate levels is accompanied by a drop in the serum calcium concentration which leads to tetany [17]. To prevent unbalanced phosphate homeostasis plasma Pi is tightly regulated by intestinal absorption, renal excretion and bone turnover [18–20]. In this organ orchestra, hormones adjust serum phosphate levels mainly by regulating phosphate reabsorption in the kidney.

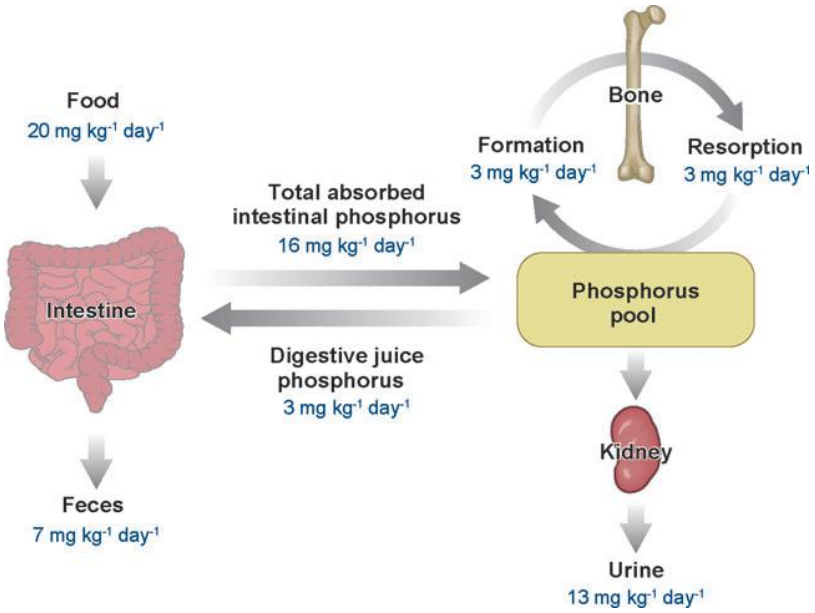

Figure 1.1: Quantitative phosphate homeostasis in humans. Intestine and kidneys are the main organs regulating phosphate absorption and excretion in the human body. Bone is in absolute need of phosphate to maintain its structural integrity and serves at the same time as an internal phosphate storage pool. Adapted from Berndt et al. (2007) [6].

1.2 Phosphate reabsorption in the kidney by sodium-dependent phosphate co-transporters

Phosphate reabsorption in the kidney takes place along the proximal tubule where sodium-dependent phosphate co-transporters NaPi-IIa (SLC34A1) and NaPi-IIc (SLC34A3) of the SLC34 family as well as PiT-2 of the SLC20 family are responsible for phosphate reabsorption at the apical membrane of proximal tubule epithelia [21–26]. NaPi-IIa is expressed along the entire proximal tubule whereas NaPi-IIc and PiT-2 are predominantly expressed in the S1 segment [26–28]. Both SLC34 members transport divalent Pi ($HPO_4{}^{2-}$) but with

a different stoichiometry: NaPi-IIa is electrogenic and transports 1Pi:3Na^+ and NaPi-IIc is electroneutral and transports 1Pi:2Na^+ [29]. PiT-2 transports monovalent Pi ($H_2PO_4^-$) with a ratio of 1Pi:2Na^+ (Figure 1.2) [29]. The sodium gradient for the secondary active sodium-dependent phosphate co-transport is maintained by the Na-K-ATPase which is localized at the basolateral side of proximal tubule cells [30]. The exit pathway for Pi at the basolateral side is so far unknown (Figure 1.2).

The importance of NaPi-IIa and NaPi-IIc in terms of phosphate transport in the kidney depends on the species [31]. Human mutations of *SLC34A3* (NaPi-IIc) gene cause hereditary hypophosphatemic rickets with hypercalciuria (HHRH) and human mutations of *SLC34A1* (NaPi-IIa) gene lead to idiopathic infantile hypercalcemia which is characterized by primary renal phosphate wasting and hypercalcemia [31–34]. This suggests that both NaPi-IIa and NaPi-IIc play an important role in human phosphate homeostasis [31]. *NaPi-IIc*$^{-/-}$ as well as kidney specific conditional NaPi-IIc KO mice have similar plasma phosphate levels and display normal bone growth compared with wild type animals [35, 36]. In contrast, mice lacking NaPi-IIa display hypophosphatemia but surprisingly they do not suffer from hypophosphatemic rickets [31, 37]. *NaPi-IIa*$^{-/-}$ and *NaPi-IIc*$^{-/-}$ double KO animals suffer from severe hypophosphatemia accompanied by rickets which is similar to the HHRH phenotype in humans [31, 38]. High Pi diet can rescue both HHRH and *NaPi-IIa*$^{-/-}$, *NaPi-IIc*$^{-/-}$ double KO mice phenotypes [31, 38]. These findings propose that NaPi-IIc in mice is less important in mediating phosphate homeostasis compared to NaPi-IIc in humans [31]. Due to the fact that NaPi-IIc is not able to rescue the hypophosphatemic phenotype in *NaPi-IIa*$^{-/-}$ mice, NaPi-IIa plays a more important role in phosphate homeostasis compared to NaPi-IIc [31]. But nevertheless there is a synergism between NaPi-IIa and NaPi-IIc because loss of both proteins is necessary to cause severe hypophosphatemia and rickets in mice [31]. The importance of NaPi-IIa in mice is also reflected by the phosphate transport activity in the kidney. NaPi-IIa accounts for approximately 70% and NaPi-IIc for 30% of phosphate transport activity in mouse kidneys [25, 37].

The abundance of NaPi-IIa protein at the brush border membrane determines the rate of renal phosphate reabsorption [39]. Hence, the protein can be regulated at the biosynthesis level, the rate of insertion into the apical membrane, or by endocytotic retrieval from

the membrane [39]. Currently, the endocytotic regulation process is the most examined one [39]. It has been shown that receptor mediated endocytosis of NaPi-IIa including clathrin-coated vesicles, early and late endosomes and lysosomal degradation is an important process to reduce its abundance on the brush border membrane [39, 40]. Sodium hydrogen exchanger regulatory factor 1 (NHERF1) interacts with the c-terminal PDZ binding motif of NaPi-IIa [41, 42]. Phosphorylation of NHERF1 protein leads to dissociation of the NaPi-IIa-NHERF1 complex and to endocytotic retrieval of NaPi-IIa from the apical membrane [41]. Dietary phosphate intake, parathyroid hormone (PTH), and fibroblast growth factor 23 (FGF23) are key regulators of phosphate homeostasis and are able to modulate abundance of NaPi co-transporter mRNA and protein levels [43–45]. The interplay of these mediators is discussed in the following section.

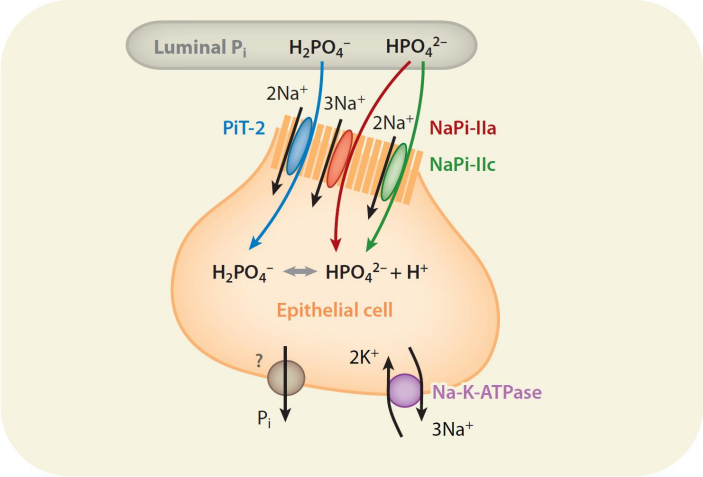

Figure 1.2: Concept of phosphate reabsorption. Phosphate reabsorption by sodium-dependent phosphate cotransporter PiT-2, NaPi-IIa, and NaPi-IIc takes place at the brush border membrane of proximal tubule epithelia. On the basolateral side the Na-K-ATPase maintains the Na^+ gradient which enables the phosphate transport. The exit mechanism of phosphate on the basolateral side is unknown. Adapted from Biber et al. (2013) [30].

1.3 Hormonal regulation of phosphate homeostasis

PTH, $1,25(OH)_2$ vitamin D_3, FGF23 and Klotho build an endocrine network that tightly regulates phosphate homeostasis (Figure 1.3) [46]. In this section I will discuss the role of PTH and vitamin D_3 in phosphate homeostasis whereas FGF23 and Klotho are explained in more detail in the following section.

The parathyroid gland primarily functions as a calciostat and releases in response to low calcium levels PTH into the circulation [47]. In addition to calcium, PTH governs serum phosphate levels mainly by the regulation of phosphate transporters in the proximal tubule [44, 48]. Oral phosphate loading in humans leads within 45 minutes to increased serum PTH levels [48]. In the kidney, PTH activates the PTH receptor (PTHR), a G-protein coupled receptor, which leads to the activation of protein kinase A (PKA) and protein kinase C (PKC) and the subsequent internalization of sodium phosphate co-transporters [41, 44, 49]. Phosphorylation-deficient PTHR causes a sustained increase in cAMP production and therefore PKA is constitutively activated which leads in mice to permanent reduction of serum phosphate levels [50]. $PTH^{-/-}$ KO animals suffer from abnormal bone development, renal calcium loss, and phosphate retention as well as reduced $1,25(OH)_2$ vitamin D_3 and FGF23 levels [47, 51, 52]. $1,25(OH)_2$ vitamin D_3 is the activated form of vitamin D_3 and is metabolized in the kidney [47]. The production of $1,25(OH)_2$ vitamin D_3 is regulated by the expression and activity of *Cyp27b1* and *Cyp24a1* which encode the 1α-hydroxylase (vitamin D_3 activating enzyme) and the 24-hydroxlyase (vitamin D_3 inactivating enzyme), respectively [47]. In $PTH^{-/-}/Hyp$ double KO animals, exogenous PTH stimulates $1,25(OH)_2$ vitamin D_3 production independently of FGF23 [52]. In these mice the expression of *Cyp27b1* is completely abolished while the *Cyp24a1* expression is significantly increased compared with *Hyp* mice (a mouse model of FGF23 excess) [52]. In return, PTH supplementation of $PTH^{-/-}/Hyp$ double KO animals increases *Cyp27b1* expression and reduces *Cyp24a1* expression [52]. Taken all together, PTH promotes calcium retention and phosphate excretion in the kidney and stimulates $1,25(OH)_2$ vitamin D_3 production in the kidney and FGF23 expression in bone (Figure 1.3) [46].

The main function of $1,25(OH)_2$ vitamin D_3 is the regulation of bone and mineral metabolism but it is also involved in other biological processes such as macrophage differentiation and modification of T-lymphocyte activity [53]. $1,25(OH)_2$ vitamin D_3 mainly acts through the vitamin D receptor (VDR) which is expressed in many tissues, among them kidney, intestine, bone, and parathyroid gland [53]. VDR is a cytoplasmic protein and is upon $1,25(OH)_2$ vitamin D_3 activation translocated to the nucleus where it binds to the retinoid X receptor (RXR) [47, 54, 55]. Within the nucleus the $1,25(OH)_2$ vitamin D_3/VDR-RXR complex regulates gene expression by binding to vitamin D response elements [56].

VDR$^{-/-}$ KO animals have a shortened life span and display extremely low serum phosphate and FGF23 levels whereas PTH and 1,25(OH)$_2$ vitamin D$_3$ are elevated [57]. The *PTH* gene promoter has a vitamin D response element. Binding of the 1,25(OH)$_2$ vitamin D$_3$/VDR-RXR complex to the vitamin D response element suppresses *PTH* expression [58]. Further 1,25(OH)$_2$ vitamin D$_3$ increases dietary phosphate reabsorption in the intestine [47]. Overall 1,25(OH)$_2$ vitamin D$_3$ increases serum phosphate levels [47].

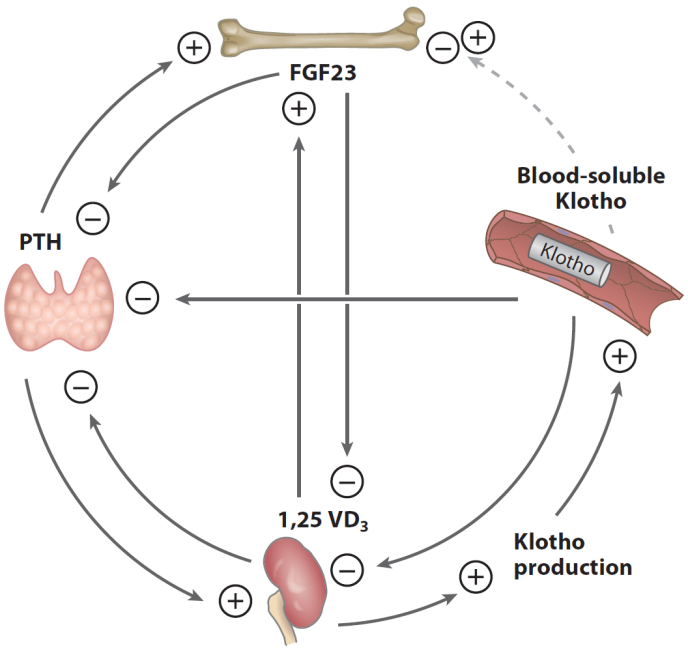

Figure 1.3: Endocrine regulation of phosphate metabolism. The principle regulators of phosphate homeostasis FGF23, PTH, vitamin D and soluble Klotho are regulating each other by multiple negative feedback loops to tightly regulate phosphate serum levels. Adapted from Hu et al. (2013) [46].

1.4 Fibroblast growth factor 23 (FGF23)

Within the large fibroblast growth factor super family, FGF23 belongs together with FGF15/19 and FGF21 to the fibroblast growth factor subfamily 19 [59, 60]. The members of this family are missing a heparin binding sequence and function therefore as endocrine factors [60]. FGF15/19 and FGF21 play a unique role in energy and bile acid homeostasis as well as glucose and lipid metabolism whereas FGF23 is a key player in the regulation of mineral homeostasis and vitamin D$_3$ metabolism [61, 62]. Human *FGF23* is localized on chromosome 12p13 and encodes FGF23, a secreted, glycosylated 32kDa protein, which consists of 251 amino acids [59]. The homologue mouse gene shares 72% amino acid

identity with human *FGF23* and lies on chromosome 6 [59]. The promoter region of human, mouse, and rat FGF23 is highly conserved and has several putative binding sites, among them a vitamin D_3 responsive element [63]. The protein consists of a hydrophobic signaling sequence, a N-terminal FGF homology region and a C-terminal receptor binding region (see Figure 1.4) [46, 59, 64]. FGF23 is mainly expressed in bone and to a much lower extend in thymus, brain, and heart [59, 61, 62, 65].

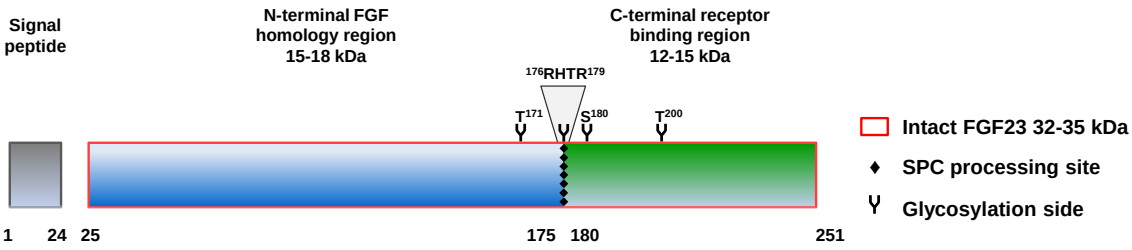

Figure 1.4: Schematic structure of the intact FGF23 protein. Signal peptide (grey) tags FGF23 as a secreted protein, N-terminal FGF homology region (blue), and C-terminal receptor binding region (green). The amino sequence ^{176}RHTR^{179} is a subtilisin-like proprotein convertase (SPC) cleavage site where FGF23 can be processed in an inactive C- and N-terminal fragment. Adapted from Hu et al. (2013) and Bhattacharyya et al. (2012). [46, 64, 66]

1.4.1 FGF23-FGF receptor (FGFR)-Klotho complex

Four *FGFR* genes (*FGFR1-FGFR4*) encode seven different receptor tyrosin kinases [60]. FGFR receptors are structured in an extracellular ligand-binding domain with three immunoglobulin domains, a transmembrane domain, and an intracellular tyrosine kinase domain [60]. Alternative splicing of the *FGFR1-3* immunoglobulin domains generates two proteins (e.g. FGFR1b and FGFR1c) with different ligand-binding specificity [60]. FGFR receptors are widely expressed all over the body and as FGF signaling is mostly autocrine and paracrine the local FGF expression set determines the degree of signaling [62]. The binding of FGF-FGFR needs heparan sulfate (HS), a polysaccarid with variably sulfated repeating disaccharide units [67]. HS is structurally similar to heparin which can replace HS in the FGF-FGFR complex formation [67]. Heparin or HS interacts with its nonreducing ends with both FGF and FGFR which leads to the formation of a stable 1:1:1 FGF:FGFR:heparin ternary complex [68]. For receptor dimerization the recruitment of a second FGF:FGFR:heparin/HS ternary complex is necessary and is initiated either by direct FGFR:FGFR contacts or by secondary interaction between FGF of one ternary

complex with FGFR in the other ternary complex or by indirect heparin/HS mediated FGFR-FGFR contacts [68]. As mentioned in the previous section, FGF23 is an endocrine factor and distinguished from the other auto- and paracrine acting FGFs by the altered heparin binding sequence (HBS) [67]. The HBS of FGF23 has a very poor binding affinity to HS and thus the pericellular HS is neither able to trap and immobilize FGF23 in the extracellular matrix nor form the necessary complex with FGFR for signal transduction [67]. Consequently, FGF23 has an endocrine mode of action and needs the co-ligand Klotho for FGFR signaling whose expression pattern determines the FGF23 target organs [69]. *Klotho* was originally discovered as a gene which prevents premature aging and is mainly expressed in kidney and brain and to a lower extend in pituitary, placenta, skeletal muscle, urinary bladder, aorta, pancreas, testis, ovary, colon and thyroid gland [70]. In mouse and human, *Klotho* encodes either a single transmembrane or by alternative splicing a shortened secreted protein [71, 72]. The membrane-bound Klotho protein consists of a short N-terminal signaling sequence, an extracellular domain with two internal repeats (KL1 and KL2), a single transmembrane domain and a short intracellular domain [72]. The extracellular domain of membrane Klotho can be shed by the two metalloproteases ADAM10 and ADAM17 in a 68kDa (KL1) or a 130kDa (KL1+KL2) fragment [73]. Klotho is essential for FGF23 signaling through FGFR receptors and therefore its expression determinates the target organs of FGF23 [69, 74]. In immunoprecipitation experiments it has been shown that Klotho binds most of the FGFR receptor isoforms but nevertheless the affinity of Klotho with FGFR c isoforms is much stronger compared to b isoforms [74]. Further FGFR2 has a lower affinity for interaction with Klotho compared with FGFR1, FGFR3 and FGFR4 [74]. FGF23 itself does not interact with Klotho or FGFR alone, it only binds FGFR1c, FGFR3c, and FGFR4 in combination with Klotho [74]. The necessity of Klotho for FGF23 signaling could also be demonstrated by blocking Klotho *in vivo*. The injection of an anti-Klotho antibody in wild type mice leads after 4 hours to the upregulation of *Cyp27b1* and downregulation of *Cyp24a1* gene expression followed after 9 and 24 hours by increasing $1,25(OH)_2$ vitamin D_3, phosphate, and FGF23 serum concentration [69]. Klotho converts FGFR receptors into a FGF23 responsive receptor with non-mitogenic character (Figure 1.5) [69].

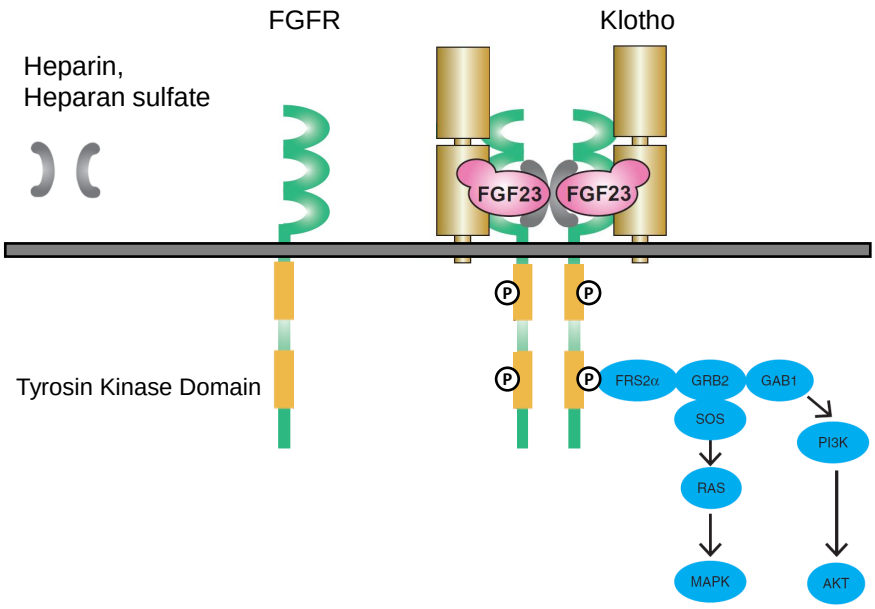

Figure 1.5: Schematic illustration of FGF23-Klotho-FGFR receptor complex. Receptor activation leads to dimerization and cross-phosphorylation of FGFR tyrosine kinase domains and activates the downstream signaling molecules. Downstream signaling occurs mainly through the MAPK and AKT pathway. FRS2α, fibroblast growth factor receptor substrate 2α; GRB2, growth factor receptor-bound protein 2; GAB1, GRB2-associated binding protein 1; PI3K, phosphoinositide-3 kinase; AKT, v-akt murine thymoma viral oncogene; SOS, son of sevenless; RAS, rat sarcoma; MAPK, mitogen-activated protein kinase. Adapted from Urakawa et al. (2006) and Tenhagen et al. (2012) [69, 75].

1.4.2 FGF23 action in the kidney

The high expression levels of Klotho and the presence of several FGFR receptors in the kidney makes the kidney to the main target organ of FGF23 [70, 76]. It is well established that FGF23 in the kidney inhibits phosphate reabsorption and vitamin D_3 synthesis [61, 65, 77–79] but there is growing evidence that FGF23 additionally impacts sodium retention and calcium reabsorption [80, 81]. In this section I will focus on the effects of FGF23 in the kidney regarding phosphate reabsorption and vitamin D_3 metabolism.

FGF23 signaling is dependent on the presence of the Klotho-FGFR receptor complex [69]. In the kidney Klotho is mostly expressed in the distal convoluted tubule and as shown by several groups to a lower extent in the proximal tubule where phosphate reabsorption takes place (see section 1.2) [82, 83]. The proximal tubule expresses FGFR1 and FGFR3 as well as FGFR4 but not FGFR2 receptors [84]. $FGFR3^{-/-}$ and $FGFR4^{-/-}$ KO mice lower the serum phosphate level in response to FGF23 administration, but $FGFR1^{-/-}$ KO mice do not [84]. This suggests that FGF23 signaling in the proximal tubule happens

predominantly by binding of FGF23 to the Klotho-FGFR1 receptor complex and FGFR3 and FGFR4 play a minor role [84]. This is further supported by the fact that phosphate wasting in the *Hyp* mice, a model of FGF23 excess, is not inhibited by the ablation of either FGFR3 or FGFR4 receptors [85]. Finally, kidney specific $FGFR1^{-/-}/FGFR4^{-/-}$ double KO mice have elevated serum phosphate and FGF23 levels and do not respond to exogenously added FGF23 [86]. Therefore FGFR1 displays a key function in mediating FGF23 dependent phosphaturia which is supported by FGFR3 and FGFR4 [84–87]. The binding of FGF23 to the corresponding Klotho-FGFR receptor complex in cultured proximal tubular cells activates in a dose and time dependent manner the extracellular signaling regulated kinase (ERK1/2) protein [69, 83]. Downstream of ERK1/2, serum glucocorticoid regulated kinase 1 (SGK1) is phosphorylated by P-ERK1/2 which is prevented by an ERK1/2 inhibitor [83]. Phospho-SGK1 in turn phosphorylates NHERF1 which results in the internalization and lysosomal degradation of the sodium phosphate co-transporter NaPi-IIa from the brush border membrane [41, 83]. Lack of Klotho abolishes this process which proves that the effect of FGF23 on NaPi-IIa internalization is Klotho dependent [83].

FGF23 decreases plasma concentration of $1,25(OH)_2$ vitamin D_3 by downregulation of 1α-hydroxylase and upregulation of 24-hydroxylase gene and protein expression in the kidney [77, 79]. It has been shown that the regulation of vitamin D_3 metabolism is dependent on the MAPK signaling pathway [88–90]. *In vitro* and *in vivo* application of the MAPK inhibitor blocks the effects of FGF23 on the downregulation of 1α-hydroxylase and upregulation of 24-hydroxylase [88–90]. Due to high FGF23 serum concentration MAPK signaling in *Hyp* mice is constitutively activated [89, 90]. Long term blockade of MAPK signaling pathways in *Hyp* mice restores normal $1.25(OH)_2$ vitamin D_3 serum levels [90].

1.4.3 FGF23 action in the parathyroid gland

The parathyroid gland expresses Klotho as well as FGFR1 and FGFR3 which makes the gland a target organ of FGF23 [91]. Administration of FGF23 in rats for 5 days leads to an upregulation of Klotho protein and a downregulation of *PTH* gene expression in the parathyroid gland as well as decreased serum PTH levels [91]. Short term intravenous FGF23 administration in rats downregulates serum PTH levels within 10 minutes whereas

intraperitoneal FGF23 administration needs 40 minutes to downregulate PTH serum and mRNA levels [91]. The regulation of PTH expression by FGF23 is dependent on MAPK signaling pathways and therefore is inhibited by an ERK1/2 inhibitor which prevents the reduction of serum PTH concentration in rats after FGF23 administration [91]. Similarly, cultured bovine parathyroid gland cells are in a dose and time dependent manner sensitive to FGF23 treatment and are increasing early growth response protein 1 (*Egr-1*) expression within an hour whereas *PTH* expression is downregulated after 12 hours [92]. Additionally, parathyroid cells treated with FGF23 display a higher *Cyp27b1* expression compared with vehicle treated cells [92]. In rats with chronic kidney disease (CKD) which was either induced by adenine diet or 5/6 nephrectomy, FGF23 treatment does not activate ERK1/2 and PTH expression as observed in wild type animals [93, 94]. Further on in the hyperplastic parathyroid gland of CKD animals Klotho and FGFR1 mRNA and protein levels are decreased [93, 94]. The absence of the functional FGF23 receptor explains the observed resistance of the parathyroid gland against FGF23 [93, 94]. The same event sequence is observed in humans with CKD where hyperplasia of the parathyroid gland is accompanied by a decrease in Klotho and FGFR1 expression and a subsequent resistance of the parathryoid against FGF23 [95, 96]. Parathyroid specific deletion of Klotho reveals a Klotho independent effect of FGF23 on PTH in the parathyroid gland [97]. *PTH-KL*$^{-/-}$ mice are able to response to increased FGF23 concentration within 15 minutes by activating a FGFR1-calcineurin dependent pathway which downregulates serum PTH levels [97]. *PTH-KL*$^{-/-}$ mice with adenine induced CKD were not able to decrease serum PTH levels in a calcineurin dependent manner similar to CKD mice and rats expressing Klotho in the parathyroid gland [97]. The way FGF23 activates FGFR1 receptors in the absence of Klotho is not yet known.

1.4.4 FGF23 processing

FGF23 inactivation by SPC cleavage

In *FGF23* transfected COS-7 cells, endogenous furin type convertase, a member of the subtilisin-like proprotein convertase (SPC) family, is responsible for FGF23 cleavage at the SPC cleavage site motive RXXR at position ^{176}RHTR^{179} (see Figure 1.4) [65, 98]. Furin inhibitors block FGF23 hydrolysis in a dose dependent manner [65]. Autosomal dominant

hypophosphatemic rickets (ADHR) is caused by missense mutations in *FGF23* gene [98]. Patients carrying an ADHR mutation suffer from hypophosphatemia and consequently from osteomalcia or rickets [99]. In ADHR mutations, the arginine (R) residues within the SPC cleavage site RXXR motive are missing [98]. Transfection of different cell lines with either wildtype or ADHR mutated *FGF23* showed that changes in the RXXR motive makes FGF23 less sensitive to proteolytic cleavage [64, 65, 100]. Hence, conditioned media of wild type transfected cells contained beside full-length FGF23 also FGF23 fragments whereas conditioned media of ADHR mutated FGF23 contained only the full-length FGF23 [64, 65, 100]. In mice, administration of full-length FGF23 protein but not C- or N-term fragments leads to renal phosphate wasting which means that proteolytic cleavage inactivates FGF23 [64]. Further ADHR mutations change the O-glycosylation pattern of FGF23 [64] but have no effect on the secretion of FGF23 into the cell supernatant and the interaction of FGF23 with heparin [100].

Mucin-type O glycosylation of FGF23

FGF23 has four possible O-glycosylation sites localized either around the SPC cleavage site at position 162-175 (1 site) as well as at position 176-178 (2 sites) or in a more C-terminal fragment (199-228, 1 site) [64]. Mucin-type O-glycosylation is initiated by enzymes of the UDP-GalNAc:polypeptide N-acetylgalactosaminyltransferase (GalNAc transferases) family which add N-acetylgalactosamine (GalNAc) to serine or threonine residues [101]. FGF23 O-glycosylation at position T^{171} can be performed by different isoforms of GalNAc transferases whereas the O-glycosylation of T^{178} within the SPC cleavage site is only initiated by the GalNAc-T3 isoform [102]. *In vitro* studies have shown that O-glycosylation by GalNAc-T3 at T^{178} following sialylation of the sugar prevents FGF23 from SPC cleavage [102]. Mutations in the *GALNT3* gene causes familial tumoral calcinosis which manifests itself by hyperphosphatemia and ectopic calcifications [103–105]. The lack of O-glycosylation at T^{178} of FGF23 leads to the immediate degradation of the protein already within the cell [102]. Hence, patients affected by mutations in the *GALNT3* gene have highly elevated plasma levels of C-term FGF23 whereas levels of intact FGF23 are very low [105, 106]. The amount of intact FGF23 is not sufficient to induce appropriate phosphaturia in the kidney and is the reason for hyperphosphatemia in these patients [105, 106].

Due to reduced FGF23 signaling, patients tend to have higher 1,25 $(OH)_2$ vitamin D_3 levels which promote hyperphosphatemia by increased Pi uptake in the intestine [105, 106]. In the *Galnt3* KO mouse model it has been shown that *FGF23* gene expression in bone is 14-fold increased but due to the fast degradation, FGF23 plasma levels are half of that of wild type mice [107]. Interestingly, *Klotho* gene expression in kidneys of *Galnt3* KO mice is also elevated which suggests that Klotho itself is regulated by serum Pi or FGF23 levels [107]. O-glycosylation of FGF23 by GalNAc-T3 is a critical step in the course of FGF23 processing by preventing premature inactivation of the protein by SPCs.

Phosphorylation of FGF23

Fam20C is a secreted as well as golgi-localized protein kinase which recognizes SXE (serine-X-glutamic acid) motives [108, 109]. This motive is found in several secreted proteins, among them the group of small integrin-binding ligand, N-linked glycoproteins (SIBLING) [108]. The following five highly phosphorylated proteins belong to the SIBLING family: osteopontin (OPN), dentin matrix protein 1 (DMP-1), bone sialoprotein (BSP), matrix extracellular phosphoglycoprotein (MEPE), and dentin sialophosphoprotein [108]. Fam20C phosphorylates SIBLING proteins *in vitro* in a time dependent manner whereas inactivating mutations of Fam20C are failing to do so [108, 109]. In humans, mutations in Fam20C lead to the autosomal recessive Raine syndrome which results most often in death after birth [110, 111]. Genetic defects in the *FAM20C* gene are causing osteosclerotic bone dysplasia including an increase of bone density in all bones, most prominent in the skull [110]. It could be shown that most of the *FAM20C* mutations are affecting either the secretion or the kinase activity of the protein [108, 109]. Therefore decreased phosphorylation of SIBLING proteins by FAM20C may contribute to the bone dysplasia phenotype of Raine syndrome patients [108, 109]. Patients affected by non-lethal *FAM20C* mutations as well as tissue specific conditional *Fam20C* KO animals display hypophosphatemia as well as elevated FGF23 expression levels [112, 113]. An *in vitro* study demonstrated that FAM20C phosphorylates FGF23 S^{180} and thereby inhibits O-glycosylation of FGF23 by GALNT3 [114]. These results suggest that the regulation of FGF23 processing is a dynamic interplay between phosphorylation and O-glycosylation of FGF23. O-glycosylation increases the secretion of the active form of FGF23 whereas phosphorylation promotes the cleavage

of FGF23 by furin and therefore the secretion of inactive N- and C-terminal FGF23 fragments [114]. This interplay is disturbed in indivdiuals with viable *FAM20C* mutations as well as in *Fam20C* KO animals and therefore intact serum FGF23 concentrations are increased [114].

1.4.5 Regulation of FGF23 expression in bone

Local regulation of FGF23 expression in bone by Phex and Dmp-1

The phosphate-regulating gene with homologies to endopeptidases on the X chromosome (Phex) shares high homologies with the membrane-bound metalloendopetpidase family and is mainly expressed in bone [115]. Mutations in *PHEX* causes X-linked hypophosphatemia (XLH) which is characterized by rickets and hypophosphatemia due to impaired phosphate reabsorption in the kidney [115]. The *Hyp* mouse is the homologous animal model for XLH and suffers similar to humans from hypophosphatemia, impaired bone mineralization, high serum PTH, and FGF23 as well as low 1,25$(OH)_2$ vitamin D_3 levels [79, 115–117]. Mutations in *Phex* selectively increase *FGF23* gene expression in bone and cause therefore the phosphate wasting phenotype observed in *Hyp* mice [117]. Despite the presence of hyerphosphatemia in *Hyp*/*FGF23*$^{-/-}$ double KO mice, the mineralization of long bones is impaired which suggest that Phex has additional functions which are not linked to FGF23 expression [117].

Dmp-1 belongs to the SIBLING protein family and is mainly expressed in mineralized tissues and to a lower extent in nonmineralized tissues such as kidney, pancreas and brain [118, 119]. Dmp-1 is secreted to the extracellular matrix where it is processed by Bmp-1 into a C-terminal 57kDa and a N-terminal 37kDa fragment [120, 121]. Mutations in *DMP-1* lead to autosomal dominant hypophosphatemic rickets (ADHR) [118]. ADHR manifests itself as rickets and progressive lower limb deformity as well as hypophosphatemia, high serum FGF23, and normal PTH and 1,25$(OH)_2$ vitamin D_3 levels [118]. *Dmp-1* KO mice display a similar phenotype to human ADHR and suffer from severe hypophosphatemia due to increased renal phosphate clearance and increased serum PTH and FGF23 levels whereas 1,25$(OH)_2$ vitamin D_3 levels are normal [118]. The increased serum FGF23 levels are accompanied by increased *FGF23* gene expression in bone and more specifically in osteocytes which is also the main place of DMP-1 production [118, 122]. The upregulation

of osteoblastic markers such as alkaline phosphatase and collagen type 1 expression as well as the disorganization of osteocyte lacunae and the reduced bone mineralization in *Dmp-1* KO mice demonstrates that Dmp-1 deposition in the extracellular matrix is important for normal ostoblast-to-osteocyte differentiation as well as matrix mineralization [118]. Double *Phex*/*Dmp-1* KO mice have non additive effects regarding FGF23 gene and protein expression and share their biochemical profile as well as the bone phenotype [123]. The phenotypic similarity of *Hyp* and *Dmp-1* KO mice suggests that they regulate FGF23 expression through a common pathway [123]. Indeed pathway analysis of gene arrays of *Hyp*, *Dmp-1* and *Hyp*/*Dmp-1* KO mice reveals activated FGFR1 signaling pathways in all three mouse models [123]. Inhibition of FGFR1 in differentiated wild type mouse bone marrow stromal cells reduces *FGF23* expression as well as *FGF23* promoter activity [123]. The involvement of FGFR1 in the regulation of *FGF23* expression is also shown in the short term treatment of *Hyp* mice with a selective, pan-specific FGFR inhibitor which reduces FGF23 gene and protein expression in bone [124]. Overexpression of full length or C-term Dmp-1 in *Dmp-1* KO animals strongly decreases FGF23 expression and rescues the *Dmp-1* KO phenotype which indicates that the essential functional domains of Dmp-1 are within the C-terminal fragment [125]. To the contrary, overexpression of C-term Dmp-1 in *Hyp* mice significantly impairs bone mineralization and doubles serum FGF23 levels despite a 40% reduction in *FGF23* gene expression [125]. Measuring the ratio between full length and C-term FGF23 serum levels reveals that *Hyp* mice have proportionally higher intact FGF23 than wild type mice and this ratio is even more increased in *Hyp* mice overexpressing C-term Dmp-1 [125]. The increased ratio explains the FGF23 accumulation in serum despite the reduced mRNA expression and attributes an important role to Phex and Dmp-1 in the degradation process of the FGF23 protein [125]. The function of C-term Dmp-1 is Phex dependent and the two proteins coordinate FGF23 production and bone mineralization [125]. A hypothetical model could be that C-term Dmp-1 binds with its acidic serine- and aspartate-rich motif (ASARM) to Phex and this interaction inhibits *FGF23* expression (Figure 1.6) [125]. The N-terminal Dmp-1 fragment binds to matrix metalloproteinase 9 (MMP-9) and influences FGF23 protein degradation [125, 126].

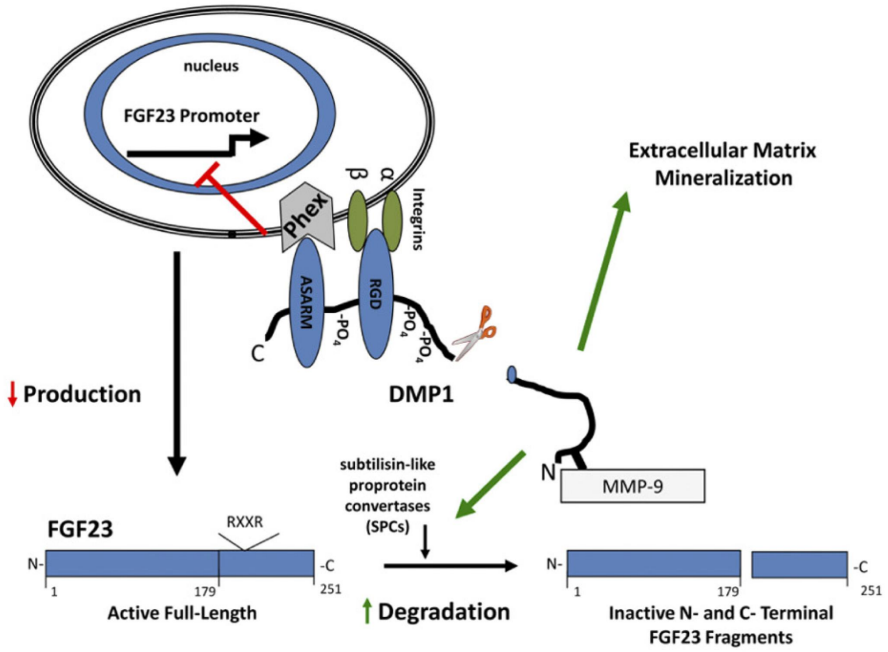

Figure 1.6: Regulation of FGF23 expression by Dmp-1 and Phex in mice. The C-term Dmp-1 fragment binds to the ASARM sequence of Phex and thereby inhibits FGF23 expression while the N-term Dmp-1 fragment binds to MMP-9 which increases the degradation of FGF23. Adapted from Martin et al. (2012) [125].

Systemic regulation of FGF23 expression in bone

Many systemic factors were described to affect FGF23 expression in bone, among them 1,25(OH)$_2$ vitamin D$_3$, PTH, iron as well as soluble Klotho [127]. 1,25(OH)$_2$ vitamin D$_3$ is by far the best investigated factor which upregulates *Fgf23* gene expression in bone. Administration of 1,25(OH)$_2$ vitamin D$_3$ in mice leads to elevation of Fgf23 and reduction of PTH serum concentration and is accompanied by an increase in *Fgf23* gene expression exclusively in bone [63, 77, 128]. The 1,25(OH)$_2$ vitamin D$_3$-induced change in Fgf23 expression is independent of changes in PTH levels [63]. *Gcm2* KO animals have low serum PTH and 1,25(OH)$_2$ vitamin D$_3$ levels due to an abnormal development of the parathyroid gland [63]. Administration of 1,25(OH)$_2$ vitamin D$_3$ to *Gcm2* KO mice also increases FGF23 expression [63]. In the *Hyp* mouse model, 1,25(OH)$_2$ vitamin D$_3$ is able to double the already increased Fgf23 levels [63]. In rat osteosarcoma cell lines such as UMR-106 and Ros 17/2.8 cells, 1,25(OH)$_2$ vitamin D$_3$ leads to a dose and time dependent increase in *Fgf23* mRNA transcripts with a maximum peak after 24 hours [63, 128]. A promoter activity assay performed in Ros17/2.8 rat osteosarcoma cells revealed that 1,25(OH)$_2$ vitamin D$_3$ is a potent stimulator of *Fgf23* promoter activity whereas Pi and calcium failed

to do so [63]. Promoter mutants indicate that the vitamin D responsive region at *FGF23* promoter position -1240 to -1161 is necessary for the activation of 1,25$(OH)_2$ vitamin D_3-induced *Fgf23* transcription [63]. Vitamin D receptor (VDR) is essential for increased Fgf23 promoter activity following 1,25$(OH)_2$ vitamin D_3 stimulation. Ros17/2.8 cells over-expressing VDR mutants do not have the same potency to induce 1,25$(OH)_2$ vitamin D_3 dependent FGF23 promoter activity compared to wild type cells [63].

PC2 mice suffer from primary hyperparathyroidism and have highly elevated serum calcium, PTH, and Fgf23 levels whereas serum phosphate levels are decreased [129]. After parathyroidectomy of *PC2* mice, calcium, phosphate PTH and Fgf23 serum concentrations return to a normal level [129]. This observation suggests that PTH stimulates FGF23 secretion and therefore coordinates the lowering of serum calcium and phosphate levels under hypercalcemic conditions to prevent ectopic calcification [129]. A similar observation was made in parathyroidectomized wild type and CKD rats which showed reduced circulating FGF23 and calcium levels as well as increased phosphate levels compared to sham operated rats [130, 131]. The administration of physiological PTH doses to parathyroidectomized rats normalized Fgf23 levels whereas the administration of supraphysiological PTH doses led to strongly elevated Fgf23 levels [130]. Parathyroidectomized mice and rats show the importance of PTH for Fgf23 secretion but unfortunately do not explain the molecular mechanism of how PTH increases FGF23 levels. *Ex vivo* stimulation of calvarias from wild type and uremic rats with PTH had no effect on Fgf23 gene and protein expression whereas 1,25$(OH)_2$ vitamin D_3 did increase Fgf23 levels [132]. To the contrary, PTH increases *Fgf23* mRNA expression in UMR-106 rat osteosarcoma cells [131, 133]. Thereby PTH activates protein kinase A (PKA) and induces expression of the nuclear receptor related 1 protein (Nurr1) expression, a nuclear orphan receptor, also known as nuclear receptor subfamily 4 group A member 2 (NR4A2) which leads to the subsequent increase in *Fgf23* gene expression [133–135]. Transient Nurr1 overexpression in UMR-106 cells showed that Nurr1 in the absence of PTH is able to increase FGF23 promoter activity and induces *Fgf23* gene expression [133]. In addition, downregulation of Nurr1 by shRNA prevents the PTH induced *FGF23* expression in UMR-106 cells [133]. Within the *FGF23* promoter Nurr1 binds to the NBRE binding element and activates *FGF23* expression [133]. This supposes that PTH activates PTH receptors in osyteocytes which increases cAMP

and PKA which leads to an increase in Nurr1 expression which then again is responsible for an increase in *Fgf23* gene expression [133]. An alternative intracellular pathway for PTH dependent *Fgf23* expression was reported by Lavi-Moshayoff et al. (2010). In this model PTH is supposed to decrease *Sost* gene expression which is followed by a reduced sclerostin protein production (product of *Sost* gene) [131]. Reduction in sclerostin leads to the activation of the Wnt signaling pathway and releases β-catenin which increases *Fgf23* expression [131].

Iron deficiency causes an increase of Fgf23 mRNA and protein levels in wild type as well as ADHR mice [136]. To keep serum Pi levels in a normal range wild type mice compensate the increased Fgf23 expression by increased proteolytic cleavage and consequently inactivation of Fgf23 [136]. In ADHR mice, the increased FGF23 protein stability does not allow Fgf23 inactivation and therefore results in Fgf23 induced hypophosphatemia [136]. UMR-106 rat osteosarcoma cells treated for 48 hours with the iron chelator deferoxamine increase *Fgf23* gene expression in a dose dependent manner [136]. The increase in *FGF23* transcripts in response to low iron is dependent on MAP kinase and Hif1α and therefore can be blocked by a MAP kinase inhibitor or stabilized by a Hif1α activator [136]. Anemia in Gambian children is a frequent feature and goes along with increased FGF23 and 1,25$(OH)_2$ vitamin D_3 levels whereas serum PTH and phosphate levels were normal [137]. In these children hemoglobin levels are inversely correlated with serum FGF23 levels [137]. Iron deficiency is the primary cause for anemia in Gambian children throughout the year for what reason Braithwaite et al. (2012) postulate that on one hand the low hemoglobin level represents the poor iron status of these children and on the other hand low iron levels could be an additional reason for elevated FGF23 beside the chronically low calcium intake in this population group [137]. Women with iron deficiency anemia due to heavy uterine bleeding have strongly elevated c-term FGF23 levels [138]. Administration of a single dose iron dextran or ferric carboxymaltose increases not only hemoglobin and iron indices but also lowers c-term FGF23 levels [138]. Further evidence that iron influences FGF23 gene and protein expression was produced by the fact that iron deficiency in wild type and ADHR female breeders during pregnancy and breastfeeding leads to increased Fgf23 expression in their pubs [139]. Additional to iron deficiency hypoxia can upregulate *Fgf23* gene expression in UMR-106 rat osteosarcoma cells [139]. The exact link between

iron deficiency and transcriptional regulation of FGF23 is not yet completely understood and needs further evaluation.

The impact of circulating Klotho on *Fgf23* expression in bone is not well explored. Nevertheless, a *de novo* translocation between chromosome 9 and 13 led in the affected patient to inappropriate high circulating Klotho levels [140]. The patient suffered from $1,25(OH)_2$ vitamin D_3 treatment independent increased FGF23 levels, elevated PTH levels, and hypophosphatemia [140]. This observation triggered the hypothesis that circulating Klotho directly regulates *FGF23* expression in bone [140, 141]. Wild type mice treated with an adeno-associated virus producing circulating Klotho which was driven by a liver specific thyroxine-binding globulin promoter exhibit low serum phosphate and calcium levels due to the circulating Klotho dependent upregulation of Fgf23 mRNA and protein expression in bone [141]. The activity of the circulating Klotho was tested in NIH3T3 mouse fibroblast cells where it was able to activate only in presence of Fgf23 FGFR signaling [141]. Whether activated FGFR-Klotho-Fgf23 signaling in bone is responsible for elevated *Fgf23* expression or whether there is an other circulating Klotho specific receptor is unclear and needs further investigations.

1.5 FGF23 and inflammation

In recent years several studies have shown an association between inflammation and FGF23. In the Chronic Renal Insufficiency Cohort (CRIC) the inflammatory marker IL-6 and tumor necrosis factor alpha (TNFα) are increasing with ascending FGF23 quartiles and significantly correlate with FGF23 levels independently of renal function and measures of mineral metabolism [142]. Among the study participants with severe inflammation FGF23 was a strong and independent risk factor for severe inflammation, but PTH or Pi were not [142]. In the Reasons for Geographic and Racial Differences in Stroke Study (REGARDS) ascending FGF23 quartiles in non CKD patients were as well associated with markers of inflammation such as IL-6 and IL-10 [143]. Interestingly, *FGF23* gene expression is increased in chondrocytes from patients with osteoarthritis, a disease characterized by inflammation [144]. Additionally, children affected by inflammatory bowel disease (IBD) have elevated circulating FGF23 protein levels that decrease in the remission phase [145]. In a small IBD patient population, the treatment with infliximab, an anti-TNFα

antibody, normalized FGF23 levels [145]. Trinitrobenzene sulfonic acid (TNBS) induced colitis in mice is accompanied by an upregulation of *Tnfα* expression in colon and leads to a decrease of *Phex* expression in bone [146]. The downregulation of *Phex* gene expression is Tnfα dependent and can be reversed by the administration of an anti-Tnfα antibody [146]. Further, Phex promoter activity in transfected UMR-106 cells is reduced by Tnfα in a time and dose dependent manner [146]. Phex is known to inhibit *FGF23* expression in bone and therefore a TNFα induced reduction of *Phex* expression could be responsible for the elevated FGF23 levels observed in childern with IBD [145].

Inflammatory stimuli such as TNFα, IL-1β and lipopolysaccharide (LPS) increased *FGF23* expression in *ex vivo* cultured human trabecular bone as well as in IDG-SW3 cells, a mouse osteocyte cell line [147]. Similar as in mice with IBD, Tnfα stimulation of IDG-SW3 cells resulted in the downregulation of *Phex* gene expression [147]. Additionally, Tnfα increases *Galnt3* expression, the gene which encodes the protein responsible for O-glycosylation of FGF23 [147]. Further evidence that FGF23 is involved in inflammation originates from microarray data of the $Col4a3^{-/-}$, *Hyp* and $FGF23^{Tg}$ mice, three models of FGF23 excess [148]. In the kidneys of these three animal strains 31 genes were detected to be regulated in at least two out of the three models of FGF23 excess [148]. An Ingenuity Pathway Analysis performed with these 31 genes suggests an important role of the activation of transforming growth factor beta (Tgfβ), Tnfα, nuclear factor of kappa light polypeptide gene enhancer in B-cells 1 (NFκB), IL-1β, interferon, and platelet derived growth factor (PDGF) which is consistent with activation of inflammatory processes [148]. Intraperitonal injection of LPS, E. coli or S. aureus in mice leads to an elevation of FGF23 serum concentration [149]. In these mice, thymus, spleen, bone marrow, liver, and kidney but not bone were evaluated as source of FGF23, out of them spleen was the only organ with elevated *FGF23* expression levels [149]. Within the spleen bone marrow derived dendritic cells (BMDC) and to a lower extent macrophages were able to express *FGF23* in response to LPS, but lymphocytes were not [149]. In BMDC *FGF23* expression was prevented by a Nfκ B inhibitor [149]. There is growing evidence that FGF23 is involved in inflammatory processes but further studies are needed to define the physiological role of FGF23 within the inflammatory response.

1.6 Chronic kidney disease (CKD)

CKD is a collective term for heterogeneous disorders affecting kidney structure and function over a period of more than 3 months [150]. The presence of CKD is bound to a drop in GFR (see Table 1.1), an increase in albuminuria (see Table 1.2) and the presence of systemic diseases or pathological anatomic findings within the kidney [150]. CKD progression is promoted by risk factors such as hypertension, diabetes mellitus type 2, obesity, inherited kidney diseases, and cardiovascular disease [151, 152]. Therefore, prevention of these disease mediators by control of blood pressure, dietary intake of protein, salt, and minerals as well as glycemic control are effective in slowing down disease progression and delay end stage renal disease (ESRD) [150]. In an advanced CKD stage (GFR category 5), patients reach end stage renal disease (ESRD) and rely on renal replacement therapy such as dialysis or kidney transplantation [150].

The prevalence of CKD worldwide is estimated to be 8-16% [152]. According to the Global Burden of Disease study 2013, CKD ranks with an age-standardized annual death rate of 15.8 per 100'000 (CI 13.5-17.1) at position 19 in the list of causes of total number of global deaths [153]. Especially at the time when patients reach ESRD and when renal replacement therapy is initiated, the mortality of CKD patients increases strongly [154]. The large number of CKD patients causes health care cost in a not negligible range. For example, the US Medicare social health insurance spends annually about $44.6 billion for health costs of CKD patients older than 65 years [151]. This number does not include ESRD patients. This represents approximately 20% of the overall health cost covered by the insurance in this age class [151]. Furthermore, ESRD patients of all ages cost Medicare $28.6 billion which corresponds to 5.6% of their total expenses [151]. To reduce costs caused by CKD, it is important to raise the consciousness of people for CKD and prevent the disease progression by medication and adequate lifestyle [150, 152]. Additionally, better understanding of the disease itself and identification of risk factors responsible for the high mortality rate of the CKD population is necessary to improve CKD outcome [155].

1.6.1 Disturbance of mineral homeostasis in CKD

The decrease of renal function in the course of CKD entails stepwise changes in mineral homeostasis (see Figure 1.7) [156–158]. The gradual decrease of soluble Klotho in urine

Table 1.1: GFR categories in CKD. Adapted from Levin et al. (2014) [150].

GFR category	**GFR (ml/min per 1.73m^2)**	**Terms**
G1	> 90	Normal or high
G2	60 - 89	Mildly decreased*
G3a	45 - 59	Mildly to moderately
G3b	30 - 44	Moderately to severely decreased
G4	15 - 29	Severely decreased
G5	< 15	Kidney failure

Abbreviations: CKD, chronic kidney disease; GFR, glomerular filtration rate.
* Relative to young adult level
In the absence of evidence of kidney damage, neither GFR category G1 or G2 fulfill the criteria for CKD

Table 1.2: Albuminuria categories in CKD. Adapted from Levin et al. (2014) [150].

		ACR (approximate equivalent)		
Category	AER (mg/24h)	(mg/mmol)	(mg/g)	Terms
A1	< 30	< 3	< 30	Normal to mildly increased
A2	30 - 300	3 - 30	30 - 300	Moderately increased*
A3	> 300	> 30	> 300	Severely increased**

Abbreviations: ACR, albumin-to-creatinine ratio; AER, albumin excretion rate; CKD, chronic kidney disease.
*Relative to young adult level.
**Including nephrotic syndrome (albumin excretion usually >2200mg/24 h (ACR > 2220 mg/g; > 220mg/mmol)).

and serum from CKD patients starting at CKD stage G1 belongs to the first events happening in the sequence of changes in mineral homeostasis [46, 158, 159]. Subsequently, FGF23 significantly raises at an eGFR threshold of 57.8 ml/min per 1.73 m^2 [157]. The *Col4a3*$^{-/-}$ KO mouse, a CKD animal model, displays as well an early increase in FGF23 in the course of CKD [160]. Interestingly, FGF23 gene expression in bone of these animals is unchanged at early CKD stages and increases just at the time when the mice are reaching ESRD [160]. Thus, it is unclear whether the early rise in FGF23 is due to enhanced stability of FGF23 protein because of posttranslational modification or due to the expression of FGF23 in other organs than bone [160]. The elevated FGF23 is thought to suppress 1,25$(OH)_2$ vitamin D_3 synthesis and initiate the pathogenesis of secondary hyperparathyroidism [156, 157]. The dependence of low 1,25$(OH)_2$ vitamin D_3 levels in CKD on FGF23 levels is demonstrated in a CKD rat model where a single injection of anti-FGF23 antibody is able to normalize 1,25$(OH)_2$ vitamin D_3 levels [161]. The low 1,25$(OH)_2$ vitamin D_3 levels further contribute to the reduction of Klotho expression [162, 163]. The GFR threshold for PTH lies at 46.9 ml/min per 1.73 m^2 and occurs later in the course of CKD compared to the rise in FGF23 [157]. This is also illustrated by the fact that in CKD stage G2 to G3a the most common pattern is high FGF23 (FGF23 $\geq$ 100RU/ml) combined with normal PTH levels (PTH $<$ 65 pg/ml) whereas in CKD stage G3b to G4 the predominant pattern is high FGF23 (FGF23 $\geq$ 100RU/ml) combined with high PTH levels (PTH $\geq$ 65 pg/ml) [157]. Therefore, the rises in FGF23 levels precedes the increase of PTH in CKD [157]. Hyperphosphatemia occurs even later in the course of CKD [156, 157]. Serum phosphate is decreasing in an initial phase (eGFR $>$ 59.1ml/min per 1.73 m^2) which goes along with the increase in FGF23 and the fractional excretion of phosphate as well as the decrease in 1,25$(OH)_2$ vitamin D_3 [157]. In the second phase, there is a shift where serum phosphate levels gradually increase with eGFR $<$ 59.1ml/min per 1.73 m^2 [157]. Hyperphosphatemia is present only in advanced CKD stages [156, 157]. The "Trade-off hypothesis" according to Bricker et al. (1972) suggests that reduced eGFR in CKD represents a reduction in nephron mass and therefore the total remaining nephrons have a reduced phosphate clearance [164]. To maintain phosphate clearance in spite of the reduced eGFR, the remaining nephrons have to excrete more phosphate per unit [164]. The implementation of the "Trade-off hypothesis" into the changes in mineral homeostasis

in CKD suggests that Klotho deficiency demands an increased phosphate clearance per nephron which is achieved by elevation of FGF23 levels [165]. This adaptation involves the trade-off of continuous decreasing $1,25(OH)_2$ vitamin D_3 levels and the consequential development of secondary hyperparathyroidism [165]. Recently it has been shown that FGF23 levels, similar to phosphate levels, are highly associated with the relative risk of death in ESRD patients undergoing hemodialysis [155, 166]. This association between FGF23 and mortality is independent of serum phosphate levels and considerably stronger compared to the association between mortality and serum phosphate levels [166]. Hence, FGF23 excess in CKD is important for the maintenance of phosphate balance in reaction to reduced phosphate clearance but at the same time FGF23 excess is responsible for the development of secondary hyperparathyroidism as well as linked to the increased mortality in ESRD patients [165].

The reduction of FGF23 levels in early CKD is important to normalize vitamin D_3 levels, prevent secondary hyperparathyroidism, and reduce mortality. The achievement of this goal with simultaneous control of serum phosphate levels is challenging and so far not possible. Efforts to block FGF23 action in the kidney have not been completely successful in selectively blocking its effect on vitamin D_3 synthesis but preserving its phosphaturic action which is beneficial in preventing hyperphosphatemia. The administration of anti-FGF23 antibodies in rodents suffering from CKD normalizes $1,25(OH)_2$ vitamin D_3 levels and prevents secondary hyperparathyroidism but on the other hand it leads to hyperphosphatemia [161, 167]. Hyperphosphatemia causes vascular calcification and increases mortality in CKD rats [167]. Other strategies to target FGF23 include inhibiting the signaling cascade at various levels in the kidney. This was done primarily in the *Hyp* mouse, a model of FGF23 excess due to mutation in the *Phex* gene [65, 115]. Because of constitutive activated ERK1/2 signaling caused by FGF23 excess, these rodents suffer from hypophosphatemia, impaired bone mineralisation and vitamin D_3 deficiency [89, 90, 116, 168, 169]. Long term blocking of FGFR receptors with a panspecific FGFR inhibitor in *Hyp* mice corrects hypophosphatemia and leads to enhanced bone mineralization [124]. Short and long term inhibition of ERK1/2 signaling in *Hyp* mice reduces expression of the transcription factor *Egr-1* and normalizes $1,25(OH)_2$ vitamin D_3 levels [89, 90]. Furthermore, the treatment partially corrects hypophosphatemia by upregulating NaPi-IIa protein abundance

at the brush border membrane [89, 90] and improves bone mineralization [90]. Additionally, the ERK1/2 blockade in *Hyp* mice leads to an increase in FGF23 gene expression in bone and to an increase in circulating FGF23 levels [90]. The effect of increased FGF23 expression in bone on the mortality of the *Hyp* mouse was not evaluated. *Hyp* mice lacking one allele of FGF23 have a 40% reduction in FGF23 plasma levels compared to Hyp mice [117]. Similar to ERK1/2 blockade, 1,25(OH)$_2$ vitamin D$_3$ levels are corrected in *Hyp/FGF23*$^{+/-}$ mice whereas hypophosphatemia remains [117]. Therefore, the effect of FGF23 on renal 1,25(OH)$_2$ vitamin D$_3$ production and renal phosphate reabsorption underlies different regulations [90]. These studies show that the intervention in phosphate homeostasis in CKD is extremely delicate and the system of adaption and maladaption in CKD is complex [170]. Hence, FGF23 regulation and its action in CKD as well as the mechanism how mortality is influenced by FGF23 has to be elucidated to modulate and influence CKD outcome in the future.

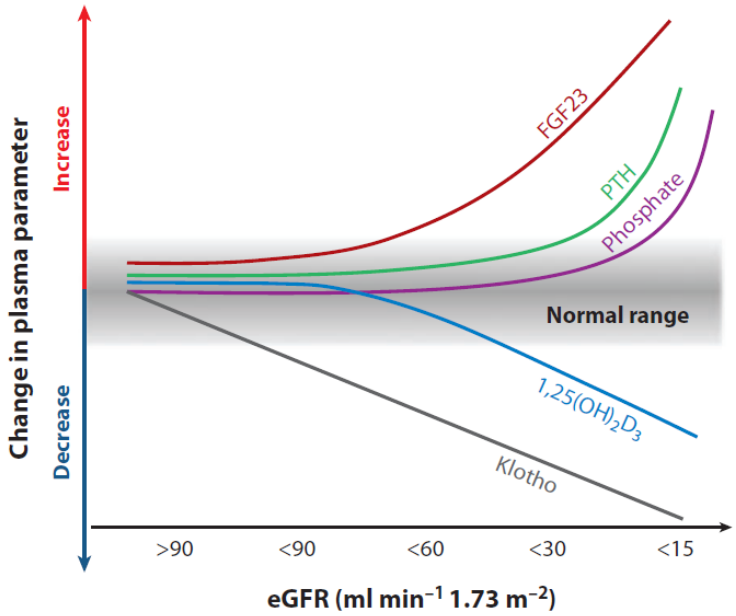

Figure 1.7: Disregulation of mineral homeostasis in CKD. Proposed time profile of changes in Klotho, serum phosphate levels and hormones relevant to mineral metabolism in CKD. The x-axis represents the decline in renal function from stage 1 to 5 of CKD based on eGFR. Adapted from Hu et al. (2013) [46].

1.7 Autosomal dominant polycystic kidney disease

Autosomal dominant polycystic kidney disease (ADPKD) is a monogenetic disorder and occurs worldwide with a prevalence of 1 to 1000 [171]. ADPKD is caused by mutations in the *PKD1* (85%) or *PKD2* (15%) genes which encode the polycystin 1 (PC1) and polycystin 2 (PC2) protein, respectively [172–177]. Patients affected by ADPKD suffer from bilateral kidney enlargement where functional renal tissue is progressively replaced by growing cysts [177]. Although the size of cysts within and between the kidneys is highly variable, the kidney enlargement proceeds at a steady rate specific for each patient [177]. ADPKD is a cause for CKD and the progression of the disease leads to ESRD [151]. In the US, ADPKD patients represent approximatly 6% of the ESRD population [151]. In ADPKD, smaller kidney volumes are related to lower changes in GFR whereas in larger kidneys the decline in GFR is accelerated [177]. This means that ADPKD patients compensate the loss of renal units resulting from cyst growth with hyperfiltration, thereby keeping GFR over a long period of time constant [178]. Therefore eGFR is not an accurate predictor for disease progression in early ADPKD [177, 178]. Hypertension is an accompanying symptom of ADPKD which occurs before the decline in GFR [179–181]. Hypertension in ADPKD is associated with the magnitude of renal structural abnormalities for this reason hypertensive ADPKD patients have a larger kidney volume than non-hypertensive ADPKD patients [180]. In this context, hypertension is most probably due to the compression of renal vasculature by growing cysts which causes bilateral renal ischemia and activates the renin-angiotensin-aldosterone system [179, 180, 182]. Another feature of ADPKD are liver cysts which are particularly prevalent in older ADPKD patients and more frequent in patients with large kidney volumes [183]. Women and in particular women who underwent pregnancy are more affected by liver cysts than men [183].

ADPKD patients with a preserved renal function and CKD stage 1 or 2 have 4-fold increased FGF23 levels compared with non-diabetic patients or patients with diabetes mellitus type 2 and a similar CKD stage, whereas PTH and 1,25$(OH)_2$ vitamin D_3 levels still remain in the normal range [184]. The elevated FGF23 is functionally active as demonstrated by a positive correlation between serum phosphate levels and tubular maximal phosphate reabsorption per eGFR [184]. The early rise in FGF23 is a specific manifes-

tation in ADPKD and cannot be explained by the loss of renal function as discussed in section 1.6.1 because in this patient population the eGFR is still preserved [184]. Interestingly, only ADPKD patients with normal soluble Klotho levels show a mild decrease in plasma phosphate levels whereas the majority of ADPKD patients have low serum Klotho levels [184, 185]. Klotho is the obligate co-receptor for FGF23 signaling and its absence can account for the FGF23 resistance observed in ADPKD patients [184, 185].

The course of ADPKD is extremely heterogeneous and largely depends on the type of mutation and on the gender [186–188]. Patients carrying a mutation in *PKD1* gene reach death or ESRD at a median age of 53-58.1 whereas patients with mutations in *PKD2* gene have a median age of 69.1-79.7 at ESRD [186–188]. A similar trend is observed for the diagnosis of hypertension which is made in *PKD1* mutation carriers at a mean age of 38.6 and in *PKD2* mutation carriers at a mean age of 48.6 [186]. Furthermore, truncating *PKD1* mutations such as frameshift, nonsense, or splice mutations and large rearrangements are leading to an earlier onset of ESRD (median age 55.6) than non-truncating mutations such as in-frame and missense mutations (age 67.9) [186].

Genetic testing and imaging methods allow ADPKD diagnosis before a detectable decline in renal function occurs, thus ADPKD is a useful model to study the whole process of CKD development [189].

1.7.1 Function of PC1 and PC2

Although the genes related to ADPKD have been known for two decades the exact function of PC1 and PC2 is not completely understood. PC1 is a large glycosylated protein with a long extracellular N-terminal region (2550 amino acids), an eleven transmembrane domain (1500 amino acids), and a short C-terminus (225 amino acids) [175]. Within the extracellular part of the protein multiple domains such as leucine reach repeats, a C type lectin domain, immunoglobulin-like repeat, and type III fibronectin related domains were identified [175]. These structures are important for the interaction with other cells and the extracellular matrix as well as with signaling molecules [175]. The intracellular domain contains several phosphorylation sites for tyrosine kinases and PKC [175]. PC2 consists of 968 amino acids and is an integral membrane protein with 6 transmembrane regions and an intracellular N- and C-terminus [176]. PC2 is a nonselective cation channel with a

high permeability to Ca^{2+} and it shows high sequence similarity with transient receptor potential channels and voltage gated Ca^{2+} channels [190–192].

PC1 and PC2 are co-localized at the primary cilia, cell-cell or cell-matrix adhesion sites [193, 194]. The C-terminal cytoplasmic tails of PC1 and PC2 interact with each other at a coil-coiled domain and form a heterodimeric complex [195]. This polycystin complex enables PC2 to function as an ion channel [192, 195]. Additionally, PC2 proteins are able to form homodimers by binding to a specific C-terminal cytoplasmic region which is different from the PC1-PC2 interaction site [195]. Mutations in the C-terminal domain of PC1 and PC2 reduce the binding affinity of the two proteins to each other and therefore, by causing miss-localization or inadequate pore formation, prevent the formation of a functional channel [192]. In the primary cilia, PC1 and PC2 transduce external mechanical flow stimuli into a intracellular calcium signal [196]. Thereby the large extracellular domain of PC1 acts as a mechano-fluid stress sensor and senses the bending of the primary cilia in response to fluid flow [196]. The subsequent activation of the PC2 Ca^{2+} channel by PC1 transforms the mechanical signal into a chemical response and leads to a local Ca^{2+} influx into the primary cilium [196]. The change in the intracellular Ca^{2+} concentration triggers intraorganellar Ca^{2+} release within the cytoplasm through Ca^{2+}-induced Ca^{2+} release [196]. *In vitro* experiments showed that renal cells lacking PC1 are not able to respond to fluid flow and lose their ability to act as a mechanosensory organelle [197].

The study of *Pkd1* KO models showed that PC1-PC2 signaling is important in kidney as well as pancreas, cardiovascular, cartilage, and bone development [198–200]. Homozygous *Pkd1* KO mice show normal histological development until day E14.5 but thereafter progressive tubule dilatation and subsequent cyst formation lead most of the animals to die at an embryonic stage [198–200]. In the developing kidney, PC1 expression increases strongly from E15.5 to E18.5 and can be localized to mesenchymal cells and endothelial cells in the nephrogenic zone as well as the differentiating tubules of the nephron and the collecting duct system [200]. This matches the time and place where cyst development occurs in *Pkd1* KO animals and identifies PC1 as a critical protein influencing renal tubule maturation [198–200]. Mutations which lead to a partially functional PC1 protein have a reduced rate of cyst formation but the onset of cyst developing is comparable to *Pkd1* null mice [199]. This suggests that the type of mutation influences disease progression in mice

like in humans as mentioned above [199]. Besides kidney phenotype, mice lacking *Pkd1* display a markedly impaired skeletogenesis which finds expression in osteochondrodysplasia and delayed endochondral and intramembranous bone formation [199, 200]. There is no bone phenotype in human ADPKD patients which most likely is due to the fact that homozygous individuals die in utero [199].

To bypass the early mortality in *Pkd1* KO mice and the fact that heterozygous animals rarely develop cysts before 6 months, conditional *Pkd1* KO animals were generated by the group of Gregory Germino [201]. In this mouse model PC1 exons 2-4 are flanked by unidirectional loxP sites [201]. Mice homozygous for the floxed *Pkd1* ($Pkd1^{fl/fl}$) allele are viable, fertile, and born at the expected Mendelian ratio [201]. In the presence of Cre recombinase the floxed *Pkd1* sequence is excised which leads to a complete null allele and renal cyst formation [201]. Therefore the floxed *Pkd1* mouse strain serves as a model to investigate the effect of temporally and spatially inactivation of the *Pkd1* gene [201]. For example, the $Pkd1^{fl/fl}$ mouse in combination with a tamoxifen inducible Cre driven by the beta-actin promoter allows a distinct temporally inactivation of *Pkd1* in the whole mouse whereas $Pkd1^{fl/fl}$ in combination with a kidney specific cadherin Cre leads to an inactivation of *Pkd1* specifically in parts of the kidney [202, 203]. The time point of *Pkd1* inactivation defines the kinetics of kidney cyst formation, an induction till day 12 post partum results in severe cystic disease within 3 weeks whereas an induction after day 14 results in a late onset cystic disease where cysts appear after 3 month and become severe after 6 month [202, 203]. The slow PKD disease progression model is an ideal system to study the sequential hormonal changes observed in CKD.

Chapter 2

Hypothesis and aims

This project is based on the clinical observation that ADPKD patients have elevated plasma FGF23 levels while their renal function is still normal [184]. The reason for this abnormal regulation of FGF23 is so far unknown.
The aims of this study are:

1. Examine the role of high Fgf23 in PKD rodent models (Han:SPRD rats *cy/+* and *Pkd1* conditional KO mice)

2. Investigate the regulation of Fgf23 expression in bone and the *de novo* Fgf23 expression in kidney cell culture

3. Test the hypothesis that local hypoxia or inflammation triggers ectopic Fgf23 expression

Chapter 3

Experimental Studies

3.1 Renal expression of FGF23 and peripheral resistance to elevated FGF23 in rodent models of polycystic kidney disease

Daniela Spichtig[1*], Hongbo Zhang[1*], Nilufar Mohebbi[1,2], Ivana Pavik[1], Katja Petzold[1], Gerti Stange[1], Lanja Saleh[3], Ilka Edenhofer[1], Stephan Segerer[1,2], Jürg Biber[1], Philippe Jaeger[4], Andreas L. Serra[1,2#], and Carsten A. Wagner[1#]

[1]Institute of Physiology and Zurich Center for Integrative Human Physiology (ZIHP), University of Zurich, Zurich Switzerland,
[2]Division of Nephrology, University Hospital Zurich, Switzerland,
[3]Department of Clinical Chemistry, University Hospital Zurich, Switzerland,
[4]Center for Nephrology, Royal Free Hospital, University College London, UK

*D. Spichtig and H. Zhang contributed equally to this study and share first authorship
#A. L. Serra and C. A. Wagner contributed equally to this study and share last authorship

Published in: Kidney International 2014, Jun;85(6):1340-50. doi: 10.1038/ki.2013.526.

Own contribution:
Daniela Spichtig (DS) contributed to Figure 3.1 - 3.4 and 3.8 - 3.10 as well as to Supplementary Figure 3.11 - 3.14 and 3.16 - 3.17. The manuscript inclusive figures was drafted by DS.

3.1.1 Abstract

Fibroblast growth factor 23 (FGF23) regulates phosphate homeostasis and is linked to cardiovascular disease and all-cause mortality in chronic kidney disease. FGF23 rises in

patients with CKD stages 2-3 whereas in patients with autosomal dominant polycystic kidney disease (ADPKD), the increase of FGF23 precedes the first measurable decline in renal function. The mechanisms governing FGF23 production and effects in kidney disease are largely unknown. We examined the correlation between FGF23 and its effects on mineral homeostasis in two PKD animal models. Plasma FGF23 levels were 10-fold increased in 4 weeks old cy/+ Han:SPRD rats, whereas plasma urea and creatinine concentrations were similar to controls. Plasma calcium and phosphate levels as well as TmP/GFR were similar in PKD and control rats at all time points. Expression and activity of renal phosphate transporters, the vitamin D_3 metabolizing enzymes, and the FGF23 co-ligand Klotho in the kidney were similar in PKD and control rats at 2, 4 and 8 weeks, indicating resistance to FGF23. However, phosphorylation of the FRS2α protein was enhanced. In PKD kidneys FGF23 mRNA was highly expressed and FGF23 protein was detected in cells lining renal cysts. FGF23 expression in bone and spleen was similar in PKD and healthy animals. Similarly, in an inducible Pkd1 knockout mouse model plasma FGF23 levels were elevated, FGF23 was expressed in kidneys whereas renal phosphate excretion was normal. Thus, the polycystic kidney produces FGF23 but is resistant to it.

3.1.2 Introduction

Systemic phosphate homeostasis is regulated by a variety of factors including dietary intake, intestinal absorption, skeletal turnover, renal excretion, and systemic acid-base status as well as by many hormones. Among them parathyroid hormone (PTH), vitamin D_3, and fibroblast growth factor 23 (FGF23) act in concert at various levels of systemic phosphate homeostasis [39, 40, 204–211].

FGF23 is a recently discovered member of the fibroblast growth factor family and is mainly expressed in bone and to a lesser extent in spleen, and brain but not in kidney [59, 65]. The kidney is the major target regulating phosphate reabsorption as well as vitamin D_3 metabolism [69, 77]. FGF23 acts on the distal convoluted tubule which may lead to the triggering of a cascade that reduces proximal tubular phosphate reabsorption [212, 213]. Alternatively in the proximal tubule FGF23 activates ERK1/2 and SGK1 phosphorylation (SGK1) [83]. Phospho-SGK1 enables the phosphorylation of the sodium hydrogen exchanger regulatory factor (NHERF1) thereby allowing the internalization of the sodium

phosphate cotransporter NaPi-IIa from the brush border membrane [83]. Consequently the reabsorption of phosphate from the glomerular filtrate will decrease [83, 212, 213]. Furthermore, FGF23 reduces the plasma concentration of 1,25(OH)$_2$ vitamin D$_3$ through downregulation of Cyp27b1 (1α-hydroxylase) in the proximal tubule, the responsible enzyme for the 1α-hydroxylation of 25(OH) vitamin D$_3$, and the upregulation of Cyp24a1 (24-OHase), the responsible enzyme for the degradation of active 1,25(OH)$_2$ vitamin D$_3$ [69, 77].

The severe disturbance of phosphate homeostasis accounts for morbidity and mortality in patients with endstage renal disease [155]. FGF23 is elevated in patients with CKD stages 2 and 3 whereas PTH increases significantly later [156, 157, 214, 215]. In haemodialysis patients FGF23 contributes to the excessive morbidity and mortality independently of serum phosphate and PTH levels [155]. Moreover, CKD patients suffer from low vitamin D$_3$ which may be caused at least in part by high FGF23 levels [156–158]. Similarly, rats with progressive kidney disease showed elevated FGF23 levels [161]. In these animals, a neutralizing FGF23 antibody led to hyperphosphatemia and normalized 1,25(OH)$_2$ vitamin D$_3$ levels [161].

ADPKD is a slowly progressive disease that is manifested by the replacement of functional renal tissue with growing cysts [171]. The responsible mutations lie in the PKD1 and PKD2 genes, encoding the two transmembrane proteins polycystin-1 (PC1) and polycystin-2 (PC2), respectively [172–176]. ADPKD patients have 4-fold increased FGF23 levels even before renal function declines [184]. Among these patients, only those with normal soluble α-Klotho, showed a mild decrease in plasma phosphate values [184, 185].

The Han:SPRD rat is a well-established PKD animal model with a mutation in the Pkdr1 gene that encodes the SamCystein protein [216, 217]. The slow progression of cystic kidney disease with a significant increase of creatinine and urea serum concentrations after 8 weeks is typical for heterozygous male animals (cy/+) [218]. Cysts in the cy/+ animals originate mainly from the proximal tubule similar to mice with a deletion in the Pkd1 gene [218, 219]. The PKD model has been widely used for examining mechanisms and therapies for ADPKD [220–223].

We investigated the regulation of renal phosphate handling, FGF23 expression, and production in two PKD animal models. We found that the polycystic kidney produces FGF23

but is resistant to it.

3.1.3 Results

Plasma concentrations of FGF23 and PTH

FGF23 plasma concentrations were increased in cy/+ Han:SPRD rats compared with wild type (+/+) animals at all time points studied (Figure 3.1a). At week 2, the difference in FGF23 concentration between cy/+ (55 ± 27pg/ml) and +/+ animals (35 ± 11 pg/ml) was 20 pg/ml (95% CI 0.5 − 39 pg/ml). FGF23 plasma levels further increased in cy/+ animals to 549 pg/ml after 4 weeks (mean difference 497 pg/ml, 95% CI 444 − 549 pg/ml). FGF23 concentration in cy/+ animals remained approximately 10-fold higher at 6 and 8 weeks compared with controls. PTH plasma concentrations were similar in cy/+ and +/+ animals at 2 weeks (Figure 3.1b) whereas after 4 weeks, PTH levels of cy/+ animals were 2-fold elevated (141 ± 16 pg/ml) compared with +/+ animals (63 ± 6 pg/ml) (mean difference 78 pg/ml, 95 % CI 64 − 92pg/ml). PTH concentration in cy/+ animals remained 2-fold higher at 6 and 8 weeks.

The renal function parameters plasma creatinine and urea were similar for cy/+ and +/+ animals from birth to week 4, thereafter the values were higher in cy/+ compared with +/+ animals (Figure 3.1c and d). The estimated change of plasma creatinine per week in cy/+ animals was 2 μmol/l (95 % CI 1 − 3 μmol/l) and 0.8 μmol/l (95 % CI 0.7 − 1 μmol/l) in +/+ animals. For urea, the estimated change per week was 0.6 mmol/l (95% CI 0.4 − 0.9 mmol/l) in cy/+ animals and 0.1 mmol/l (95% CI 0.1 − 0.2 mmol/l) in +/+ animals. At week 4, we measured plasma phosphate and calcium as well as TmP/GFR and creatinine clearance of cy/+ and control Han:SPRD rats after an overnight fast (Supplementary Figure 3.11). All parameters were similar in both groups.

FGF23 expression in cystic kidneys

In order to identify the source(s) of elevated FGF23 in cy/+ Han:SPRD rats, we extracted mRNA from bone, kidney, spleen, heart, and liver and assessed FGF23 mRNA expression by semi-quantitative real-time PCR. In bone, FGF23 expression increased over time in cy/+ and healthy animals but there were no differences between the groups at all time points studied (Figure 3.2a). In addition, we detected stable FGF23 mRNA expression

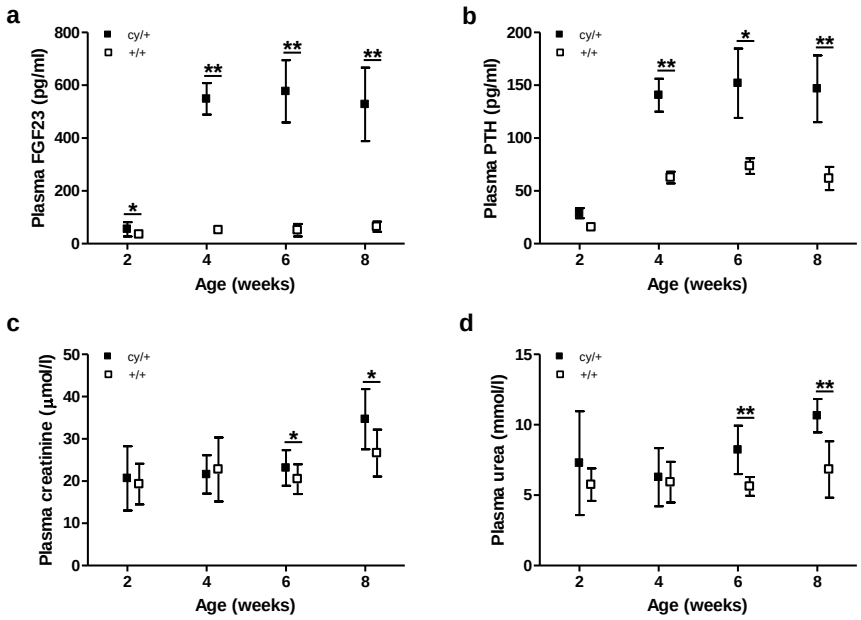

Figure 3.1: FGF23, PTH and renal function. Plasma concentrations of FGF23 (a), PTH (b), creatinine (c) and urea (d) after 2, 4, 6, and 8 weeks in cy/+ (black squares) and +/+ (white squares) Han:SPRD rats (mean ±SD); number of animals (median), cy/+ = 11.5, +/+ = 11; * $p<0.05$ and ** $p<0.001$

in spleen whereas no FGF23 mRNA expression was found in liver and heart tissue in both animal groups (results not shown). In polycystic kidneys increasing levels of FGF23 mRNA were detectable after 4 weeks. However, in healthy kidneys no FGF23 mRNA expression was detected (Figure 3.2a). FGF23 protein expression was detected by immunohistochemistry in cells lining the cysts in kidneys from cy/+ Han:SPRD rats but not in control kidneys (Figure 3.2b-f). Dmp1 and Fam20c modulate FGF23 expression in bone. We detected mRNA of both molecules in rat kidney at high levels. Fam20c expression was similar in cy/+ and control rats but Dmp1 expression was increased in kidneys from 8 weeks old cy/+ rats (Supplementary Figure 3.12).

1,25(OH)$_2$ vitamin D$_3$ metabolism

Plasma 1,25(OH)2 vitamin D3 levels were similar among cy/+ and control animals at 2, 4, and 8 weeks (Figure 3.3a). In both groups 1,25(OH)$_2$ vitamin D$_3$ levels decreased similarly over time. The relative mRNA expression of vitamin D receptor (VDR) is similar in both groups whereas there is a reduction of VDR from week 4 to 8 in cy/+ animals (Figure 3.3b). In addition, the relative mRNA expression of Cyp27b1 and Cyp24a1, the

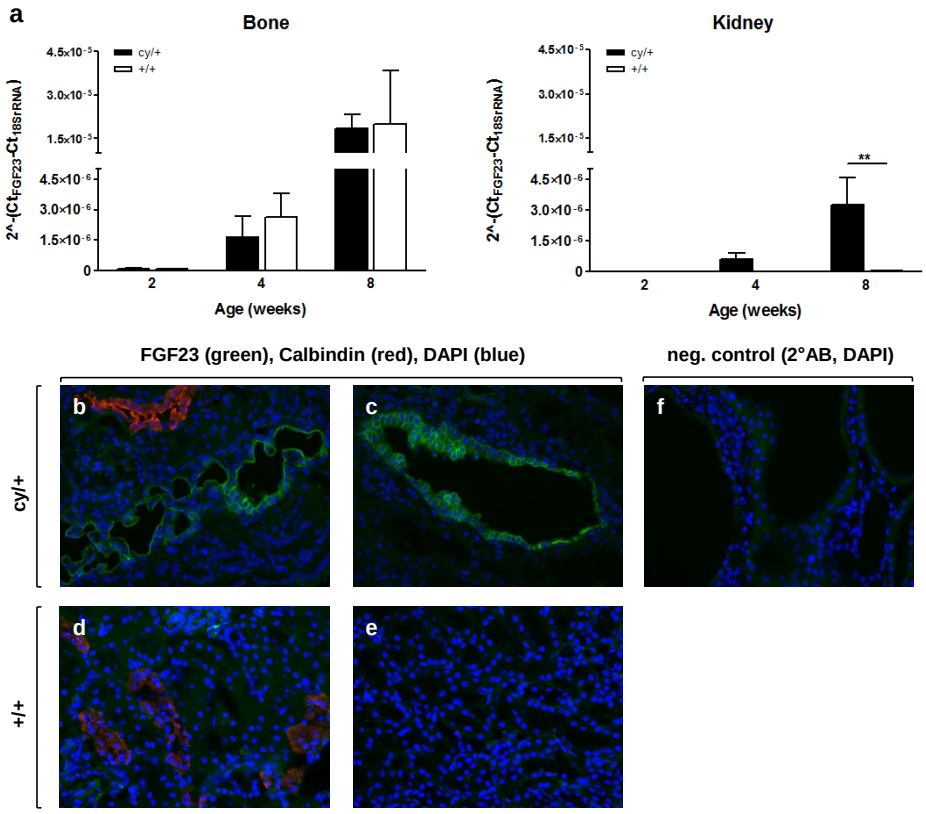

Figure 3.2: FGF23 expression in kidney. (a) Relative mRNA expression of FGF23 to 18S rRNA in bone and kidney after 2, 4, and 8 weeks in cy/+ (black bars) and +/+ (white bars) Han:SPRD rats (mean ±SD); number of animals (median), cy/+ = 6, +/+ = 5.5; ** $p<0.001$. Immunohistochemistry for FGF23 (green), calbindin D28k (red), a marker for distal convoluted tubules and connecting tubules, and DAPI (blue, cell nuclei): (b,c) kidneys from 8 week old cy/+ rats, (d,e) kidneys from 8 week old control rats, (f) kidney from 8 week old cy/+ rat incubated with secondary antibodies alone. Original magnification 400 x.

major enzymes responsible for vitamin D_3 metabolism was measured (Figures 3.3c and d). The mRNA expression of the catabolic enzyme Cyp24a1 was higher at 2 weeks in cy/+ animals. However, the expression of Cyp24a1 was similar in cy/+ and +/+ animals after 4 and 8 weeks. For the anabolic enzyme Cyp27b1, we detected similar mRNA expression levels in the cy/+ and +/+ groups at all time points studied.

Renal phosphate and calcium handling

To evaluate the biological effect of high FGF23 plasma levels, we measured phosphate and calcium concentrations in blood and urine. The plasma phosphate and calcium levels as well as the renal excretion of calcium and phosphate were similar among cy/+ and +/+ animals at all time points studied (Figure 3.4).

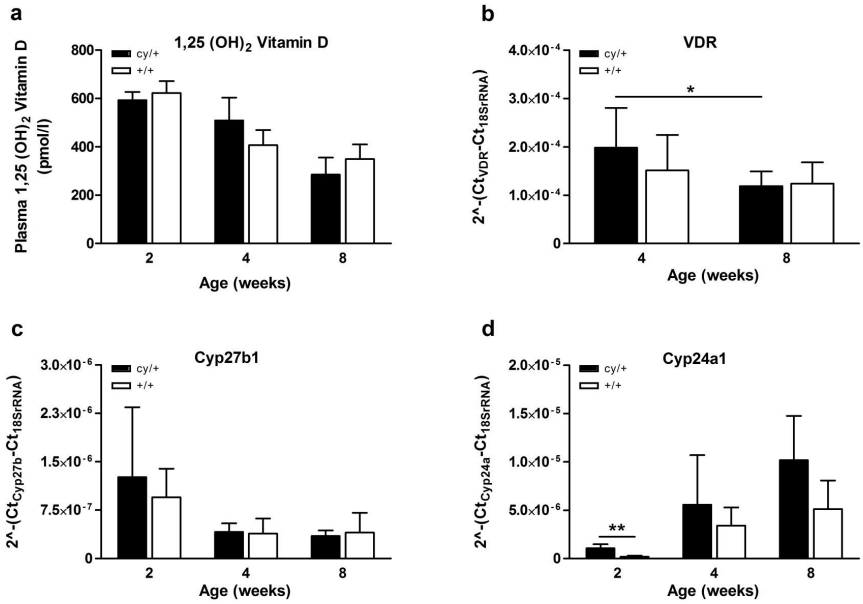

Figure 3.3: Vitamin D_3 metabolism. Plasma concentration of $1,25(OH)_2$ Vitamin D_3 (a), relative mRNA expression of the vitamin D receptor (VDR) (b) as well as Cyp27b1 (c) and Cyp24a1 (d) enzymes in the kidney to 18S rRNA after 2, 4, and 8 weeks in cy/+ (black bars) and +/+ (white bars) Han:SPRD rats (mean ±SD); number of animals (median), cy/+ = 6, +/+ = 5; * $p<0.05$ and ** $p<0.001$.

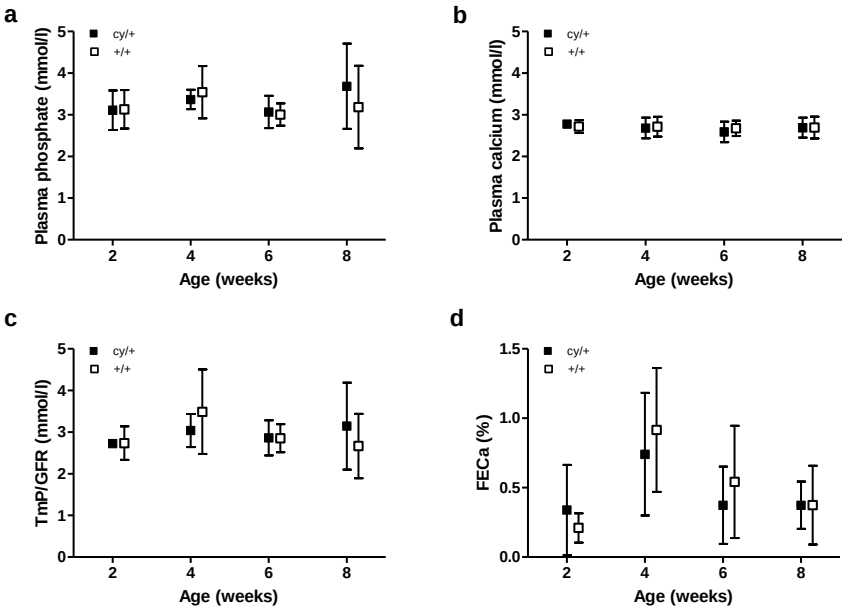

Figure 3.4: Renal phosphate and calcium handling. Plasma concentrations of phosphate (a) and calcium (b) as well as TmP/GFR (c) and FECa ratio (d) after 2, 4, 6, and 8 weeks in cy/+ (black squares) and +/+ (white squares) Han:SPRD rats (mean ±SD); number of animals (median), cy/+ = 11.5, +/+ =11; * $p<0.05$.

Phosphate cotransporters NaPi-IIa and NaPi-IIc

The renal phosphate cotransporters NaPi-IIa and NaPi-IIc are downregulated by high levels of FGF23. In our study, the mRNA and protein expression levels of NaPi-IIa and NaPi-IIc were similar in both groups at 2, 4, and 8 weeks (Figures 3.5 and 3.6). Immunolocalization of NaPi-IIa protein in kidney sections of 4 and 8 weeks old cy/+ and +/+ animals demonstrated expression of NaPi-IIa protein in the brush border membrane of proximal tubules and smaller cysts as evident from colocalization with actin (Supplementary Figure 3.13). At these time points, basolateral NaPi-IIa staining was absent, whereas a prior report demonstrated aberrant NaPi-IIa localization in 32 weeks old Han:SPRD rats [224].

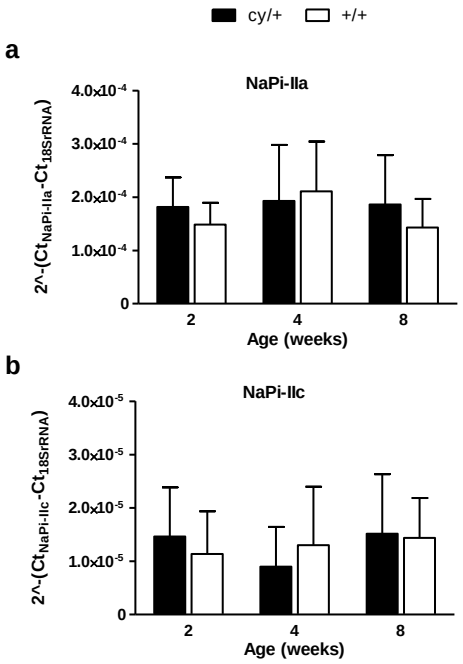

Figure 3.5: Phosphate transporter mRNA expression. Relative mRNA expression of NaPi-IIa (a) and NaPi-IIc (b) to 18S rRNA after 2, 4, and 8 weeks in cy/+ (black bars) and +/+ (white bars) Han:SPRD rats (mean ±SD); number of animals (median), cy/+ = 6, +/+ = 6; * $p<0.05$.

Phosphate and glucose transport activities

We tested the sodium-dependent transport rate of ^{32}-labeled phosphate into brush border membrane vesicles in the absence and presence of phosphonoformic acid (PFA, 6 mM), an inhibitor of NaPi-IIa and NaPi-IIc, and found similar transport rates among cy/+ and

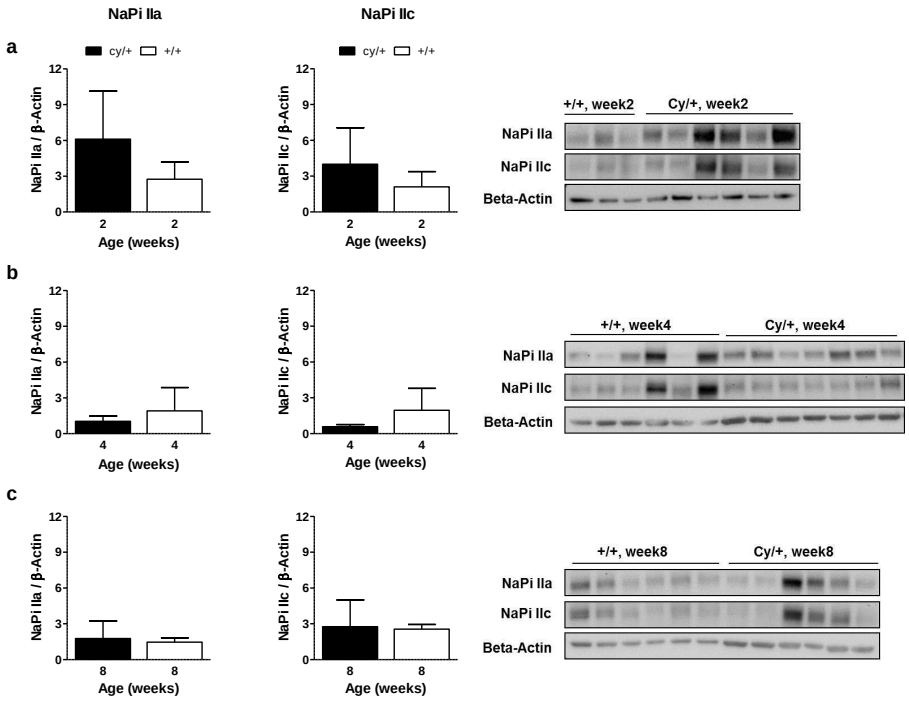

Figure 3.6: Phosphate transporter protein expression. Relative protein expression of NaPi-IIa and NaPi-IIc to β-actin after 2 (a), 4 (b), and 8 (c) weeks in cy/+ (black bars) and +/+ (white bars) Han:SPRD rats (mean $\pm$SD); number of animals (median), cy/+ = 6, +/+ = 6; * $p<0.05$.

control animals at 2 and 4 weeks (Figure 3.7). Na^+-dependent phosphate uptake in the absence of PFA was significantly increased in kidneys of 8 weeks old cy/+ rats. ^{3}-H glucose uptake was similar in both groups at all time points studied.

FGF23 and left ventricular hypertrophy (LVH)

High FGF23 plasma levels are associated with LVH [225]. We analyzed whether high FGF23 levels in 4 and 8 weeks old rats were associated with LVH but no difference was found for heart wall or septum thickness, heart to body weight or heart weight to tibia length (Supplementary Figure 3.14).

Klotho expression and FRS2a phosphorylation state

Since cy/+ animals appear to be resistant to the expected normal biological actions of FGF23 we examined whether Klotho availability or FGF23 signaling via the FGFR-1 receptor may be altered. We observed similar relative Klotho mRNA expression in cy/+ and +/+ animals at 2 and 4 weeks whereas at 8 weeks, Klotho mRNA expression was reduced in cy/+ animals (Figure 3.8a). Klotho protein abundance was similar in 8 weeks

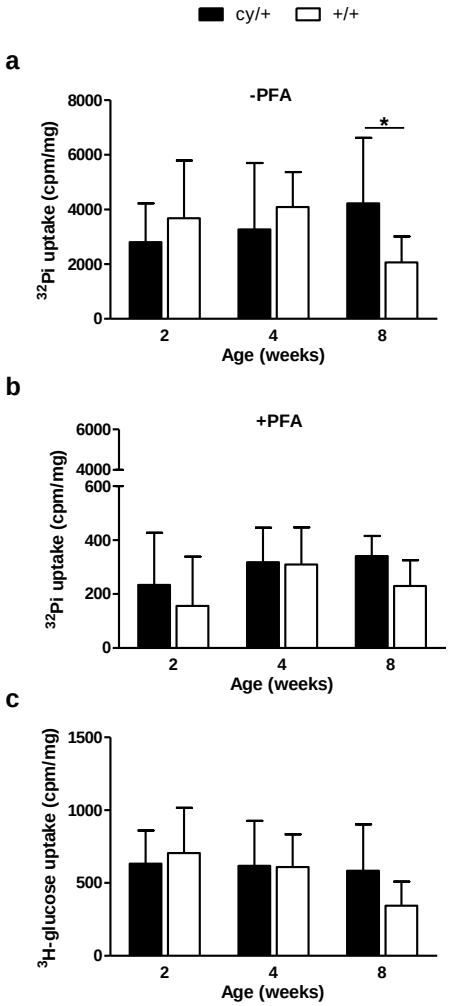

Figure 3.7: Phosphate and glucose uptake into renal brush border membrane vesicles. Phosphate uptake without (a) and with (b) PFA and glucose uptake (c) after 2, 4, and 8 weeks in cy/+ (black bars) and +/+ (white bars) Han:SPRD rats (mean ±SD); number of animals (median), cy/+ = 11, +/+ = 7; * $p<0.05$.

old cy/+ and +/+ animals (Figure 3.8b). Relative mRNA expression levels of FGFR-1 in kidney and bone were similar among cy/+ and +/+ animals (Supplementary Figure 3.15). The downstream signaling of FGF23, Klotho, and FGFR-1 complex leads to the phosphorylation of the FGF receptor substrate 2 alpha (FRS2a). Total FRS2a was similar in kidneys from 8 week old cy/+ and +/+ rats, whereas phosphorylated FRS2a protein was increased (Figure 3.8c).

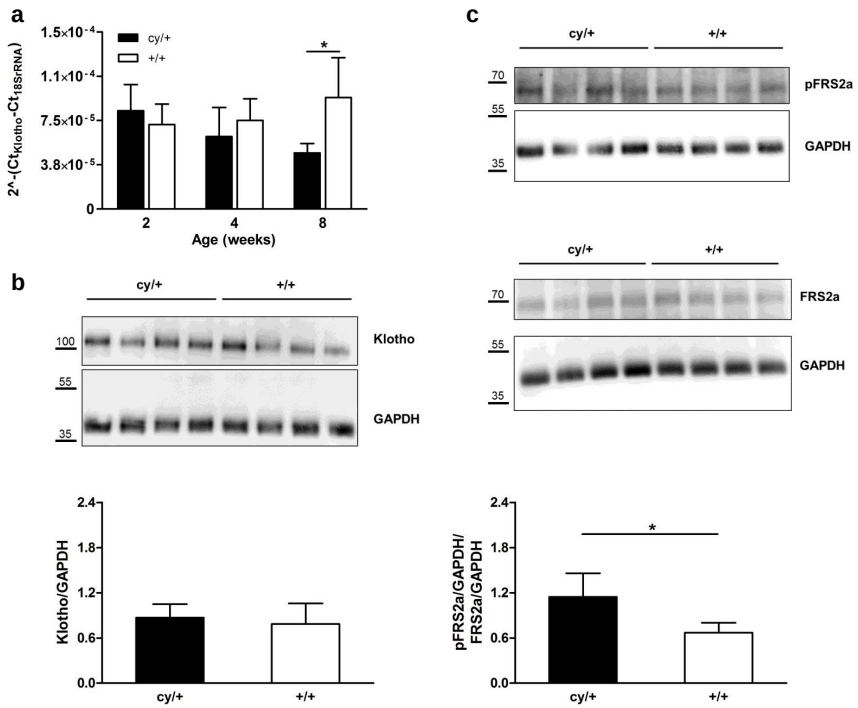

Figure 3.8: Klotho expression and phosphorylation state of FRS2a. Relative mRNA expression of Klotho in kidney (a) to 18S rRNA after 2, 4, and 8 weeks; relative protein expression of Klotho (b) and phosphorylation state of FRS2a (c) to GAPDH after 8 weeks in cy/+ (black bars) and +/+ (white bars) Han:SPRD rats (mean ±SD); number of animals (median), cy/+ = 4, +/+ = 4; * $p<0.05$.

Elevated plasma FGF23 and renal expression of FGF23 in conditional Pkd1 KO mice

We employed a second model of PKD, the conditional Pkd1 KO mice where deletion of Pkd1 gene can be induced. We induced Pkd1 deletion at days 15-19 after birth which result in a slow progression of cystic kidney disease [202]. Pkd1 mRNA was strongly reduced in kidneys and bone from 10 week old Pkd1$^{fl/fl}$, cre+ mice as compared to Pkd1$^{fl/fl}$, cre- mice (Supplementary Figure 3.16). Conditional Pkd1 KO elevated intact FGF23 plasma levels in 10 weeks old Pkd1$^{fl/fl}$, cre+ (277 ± 130 pg/ml) compared to Pkd1$^{fl/fl}$, cre- mice (199 ± 57 pg/ml) whereas TmP/GFR and creatinine clearance was similar in knockout and healthy animals (Figure 3.9). Intact PTH did not differ between Pkd1$^{fl/fl}$, cre+ (176 ± 71 pg/ml) and Pkd1$^{fl/fl}$, cre- (253 ± 126 pg/ml) mice (Figure 3.9). Similar to the rat model, Pkd1$^{fl/fl}$, cre+ mice expressed similar FGF23 mRNA levels in bone as the control mice. Kidneys from Pkd1$^{fl/fl}$, cre+ mice expressed FGF23 mRNA and protein but not kidneys from Pkd1$^{fl/fl}$, cre- (Figure 3.9 and Supplementary Figure 3.17).

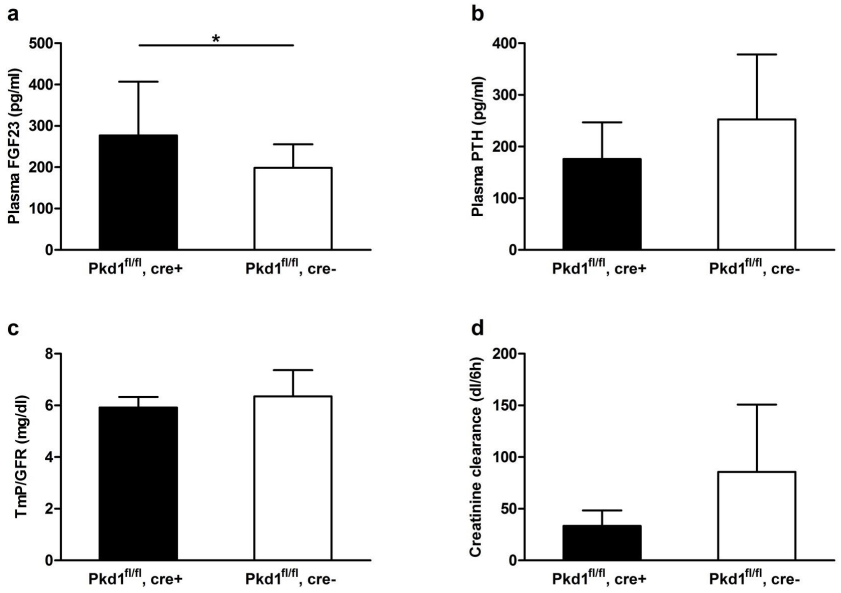

Figure 3.9: FGF23, PTH, TmP/GFR, and renal function in Pkd1$^{fl/fl}$ mice. Plasma intact FGF23 (a) and PTH (b) as well as TmP/GFR (c) and creatinine clearance (d) after 10 weeks in Pkd1$^{fl/fl}$, cre+ (black bars) and Pkd1$^{fl/fl}$, cre- (white bars) mice (mean ±SD); number of animals (median), Pkd1$^{fl/fl}$, cre+ = 7, Pkd1$^{fl/fl}$, cre- = 16; * p¡0.05.

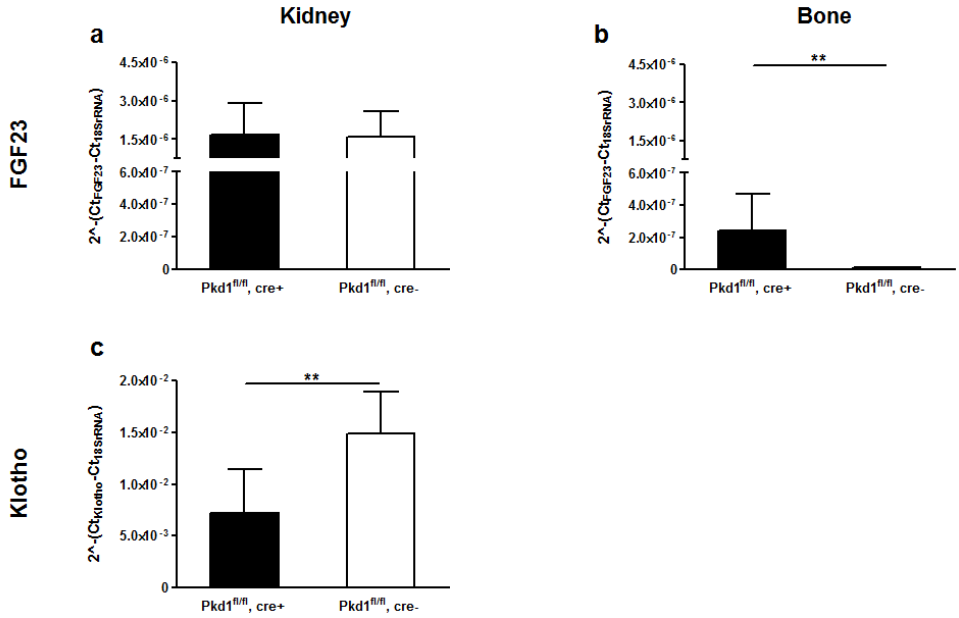

Figure 3.10: FGF23 and Klotho expression in bone and kidneys of Pkd1$^{fl/fl}$ mice. Relative mRNA expression of FGF23 in kidney (a) and bone (b) as well as Klotho in kidney (c) to 18S rRNA after 10 weeks in Pkd1$^{fl/fl}$, cre+ (black bars) and Pkd1$^{fl/fl}$, cre- (white bars) mice (mean ±SD), Pkd1$^{fl/fl}$, cre+ = 8, Pkd1$^{fl/fl}$, cre- = 15 * p<0.05 and ** p<0.001.

3.1.4 Discussion

Our study provides four major findings: i) the Han:SPRD rat model accurately reproduces the observed increase of FGF23 levels in the early disease course of human ADPKD with normal kidney function, ii) Han:SPRD rats show resistance to highly elevated FGF23 levels as evident from normal phosphatemia, unchanged renal phosphate excretion, preserved expression of renal phosphate cotransporters, increased PTH, normal $1,25(OH)_2$ vitamin D_3 levels, and normal expression of Cyp27b1, iii) expression of FGF23 in polycystic kidneys, and iv) reproduction of the major findings in a second model of ADPKD, the inducible Pkd1 KO mouse.

ADPKD patients with an estimated GFR of 60 ml/min/1.73m^2 and higher display strongly elevated FGF23 levels but only a small fraction of these patients present a reduction in renal phosphate reabsorption - albeit small - and a very mild hypophosphatemia [184]. In ADPKD patients with normal renal phosphate handling despite high FGF23 levels, reduced soluble Klotho levels were found whereas ADPKD patients that appeared to retain sensitivity to high FGF23 levels had preserved soluble Klotho levels [185]. However, the temporal sequence of rising FGF23 in PKD, the mechanisms underlying resistance to the biological actions of FGF23, and the source and cause of the elevated FGF23 levels remained unclear.

Herein, we demonstrate that intact FGF23 concentration in the cy/+ Han:SPRD rats increases early after birth before renal function decreases. The high FGF23 levels were accompanied by a 2-fold increase in PTH and normal $1,25(OH)_2$ vitamin D_3 levels. Plasma creatinine and urea indicated a decrease in renal function in cy/+ animals 6 weeks after birth and thereby 4 weeks after the rise in FGF23 and PTH [218] Similarly, the inducible Pkd1 KO mouse, a second ADPKD model, has elevated plasma FGF23 levels whereas creatinine clearance, TmP/GFR, and intact PTH were normal. Thus, Han:SPRD rats and Pkd1 KO mice illustrate an increase in FGF23 levels similar to that observed in young ADPKD patients with preserved renal function, thus allowing to approach the underlying mechanisms in more detail.

In healthy subjects and animals, a rise in FGF23 results in increased urinary excretion of phosphate through reduced expression of renal phosphate cotransporters, thus leading to a lowering of systemic serum phosphate concentrations; concomitant reduction in circu-

lating levels of active 1,25$(OH)_2$ vitamin D_3 levels occurs [47] which may participate in serum phosphate reduction.

ADPKD patients and the PKD rodent models are resistant to the elevated FGF23 as indicated by normophosphatemia, normal renal phosphate excretion, unchanged expression and activity of renal phosphate cotransporters, and apparently normal vitamin D_3 metabolism. Moreover, the expression and activity of the main renal phosphate cotransporters NaPi-IIa and NaPi-IIc are unchanged or elevated as indicated by immunoblotting, transport studies, and immunolocalization whereas in mice, overexpressing FGF23, NaPi-IIa mRNA and protein expressions are down regulated [226]. No left ventricular hypertrophy was detected suggesting either that FGF23 requires longer time periods, stronger elevation or that the heart is also resistant to high FGF23 levels.

Vitamin D_3 metabolism is similar in polycystic and control rats: indeed plasma 1,25$(OH)_2$ vitamin D_3 concentrations and mRNA expression of Cyp27b1 did not differ between both groups of animals. Cyp24a1 was upregulated at 2 weeks in PKD animals which could be due to an early rise of plasma FGF23 concentration, but this effect was only transient and not observed at later time points.

We further investigated underlying mechanisms of resistance and found normal expression of the FGFR-1 receptor mediating the biological effects of FGF23 in the kidney [69, 85]. Mice constitutively expressing FGF23 have no changes in FGFR-1 expression levels suggesting that FGF23 per se does not modulate FGFR-1 expression [226]. Klotho is required to elicit FGF23 signals via the FGFR1 receptor [69]. In our PKD model Klotho protein abundance was unchanged. The activation of the Klotho/FGFR-1 complex leads to the phosphorylation of FRS2a. In the HanSPRD model pFRS2a was increased in cy/+ kidneys suggesting that FGF23 signaling can be induced but may be blocked further downstream. PKD animals have also higher PTH levels than control animals which are in contrast to ADPDK patients with normal eGFR [184]. The elevation of PTH levels was also observed in other CKD rat models and may be due to the faster disease progression in animals compared with humans [157, 161]. Measurement of plasma PTH at shorter intervals or studies in another animal model with slower disease progression might overcome this gap. FGF23 suppresses PTH secretion in healthy rats but loss of Klotho expression in parathyroid glands may be involved in the induction of FGF23 resistance and secondary

hyperparathyroidism [91, 93].

We further analyzed the source(s) of elevated FGF23 by examining FGF23 mRNA expression in different organs such as bone as the major source of FGF23 in health, spleen, kidney, heart, and liver. In wildtype animals, we detected FGF23 mRNA expression mainly in bone, and very small amounts were also observed in spleen, whereas PKD rats and mice expressed FGF23 mRNA and protein also in the polycystic kidneys more precisely in the cells lining the cysts. In the rat and mouse PKD animal models FGF23 mRNA expression levels increased only in the polycystic kidneys whereas bone expressed similar mRNA levels in both groups suggesting that kidney may be the major source of elevation of FGF23 levels in PKD. Similarly, in diabetic nephropathy the kidney may become a source of FGF23 [227]. The mechanisms causing ectopic FGF23 expression in kidney are currently unknown. Interestingly, the kidney expresses several regulators of FGF23 secretion in bone such as Dmp1 and Fam20c and we found upregulation of Dmp1 in polycystic kidneys. In diabetic nephropathy, renal FGF23 expression was suppressed by ACE inhibition [227]. Several rodent models have been reported with elevated FGF23 levels induced by deletion of the OSR1 and SPAK protein kinases expressed in kidney [228, 229]. Whether these kinases contribute to elevated FGF23 levels in ADPKD models remains to be elucidated.

In summary, we found 10-fold elevated FGF23 levels in PKD animals and resistance of the target organs to its biological actions at early stage of polycystic kidney disease. The polycystic kidney may be a major source of FGF23 in this type of nephropathy.

3.1.5 Methods

Animals

The Han:SPRD rat colony was established in our animal facility from a litter which was obtained from the Rat Resource and Research Center (Columbia, MO) [223]. Male heterozygous cystic (cy/+) and wild-type (+/+) rats were used in this study. Pkd1 floxed/floxed ($Pkd1^{fl/fl}$) tamoxifen inducible cre mice were kindly provided by Gregory Germino [201]. Male and female $Pkd1^{fl/fl}$ cre+ and $Pkd1^{fl/fl}$ cre- mice were used. We induced recombinase activity at days 15, 17, and 19 by injecting pups with 100 μl tamoxifen (2.5mg/ml) in corn oil. All animal studies were performed according to protocols approved by the legal

authority (Veterinary Office of the Canton of Zurich).

Plasma and urine analysis

Blood and spot urine was collected from cy/+ and +/+ control rats at week 2, 4, 6, and 8 after birth. Some rats included in the week 6 group were sacrificed between 5 and 6 weeks after birth. Plasma and urine aliquots were rapidly frozen and stored at -80°C until measurement. Plasma concentrations of phosphate, calcium, and urea and urinary concentrations of phosphate and calcium were measured by the Institute of Clinical Chemistry at the University Hospital Zurich using standard methods. Pkd1$^{fl/fl}$ mice were fasted overnight before urine was collected for six hours in metabolic cages (Tecniplast®, Italy). Afterwards the mice were anesthetized with isoflurane and blood was collected from the heart. Urine and plasma laboratory analysis were performed by the Zurich Integrative Rodent Physiology (ZIRP) core facility.

The ratio of the maximum rate of tubular phosphate reabsorption to the glomerular filtration rate (TmP/GFR) was calculated as follows:

$TmP/GFR\ in\ mmol/L = P_P - [U_P \times P_{crea}/U_{crea}]$

where P_P, U_P, P_{crea} , and U_{crea} refer to the plasma and urinary concentration of phosphate and creatinine, respectively [230]. The fractional excretion of calcium was calculated according to the following equation:

$FECa = (U_{Ca} \times P_{crea})/(P_{Ca} \times U_{crea}) \times 100$

where P_{Ca}, U_{Ca}, P_{crea}, and U_{crea} refer to the plasma and urinary concentrations of calcium and creatinine, respectively. The plasma concentration of intact FGF23 (Kainos Laboratories, Tokyo, Japan), intact PTH (Immutopics International, California, USA) and 1,25$(OH)_2$ vitamin D_3 (Immunodiagnostic Systems, London, UK) were measured by enzyme-linked immunosorbent assays according to the manufacturer's protocols.

RNA extraction and RT-PCR

Rats were sacrificed at week 2, 4, and 8 for harvesting kidney, bone, liver, spleen, and heart. Mice were sacrificed at week 10 for harvesting kidneys and bone. The organs were rapidly frozen in liquid nitrogen. Total RNA was extracted using the Qiagen RNeasy Mini Kit (Qiagen, Hombrechtikon, Switzerland) or TRizol reagent for bone tissue (Invitrogen, Zug, Switzerland). Snap-frozen tissue slices were homogenized in a pestle homogenizer

(Potter-Elvehjem type) together with 1ml precooled RLT-Buffer supplemented with β-mercaptoethanol at a final concentration of 1%. Subsequently, 700 μl of the homogenate were used for RNA preparation, which was carried out according to the manufacturer's protocol. DNAse digestion was performed using the RNase-free DNAase Set (Qiagen; Hilden, Germany). Total RNA extractions were analyzed for quality, purity, and concentration using the NanoDrop ND-1000 spectrophotometer (Wilmington, DE, USA). RNA samples were diluted to a final concentration of 100 ng/μl and cDNA was prepared using the TaqMan Reverse Transcriptase Reagent Kit (Applied Biosystems, Roche; Forster City, CA, USA). In brief, in a reaction volume of 40 μl, 300 ng of RNA was used as template and mixed with the following final concentrations of RT buffer (1x), $MgCl_2$ (5.5 mM), random hexamers (2.5 μM), dNTP mix (500 μM each), RNase inhibitor (0.4 U/μl), multiscribe reverse transcriptase (1.25 U/μl) and RNAse-free water. Reverse transcription was performed with thermocycling conditions set at 25°C for 10 min, 48°C for 30 min, and 95°C for 5 min on a thermocyler (Biometra, Goettingen, Germany). Quantitative real-time PCR (qRT-PCR) was performed on the ABI PRISM 7700 Sequence Detection System (Applied Biosystems). Primers for all genes of interest (Supplementary Table 1) were designed using Primer Express software from Applied Biosystems. Primers were chosen to result in amplicons no longer than 150 bp spanning intron-exon boundaries to exclude genomic DNA contamination. The specificity of all primers was first tested on mRNA derived from kidney, bone or intestine and always resulted in a single product of the expected size (data not shown). Probes were labelled with the reporter dye FAM at the 5'-end and the quencher dye TAMRA at the 3'-end (Microsynth, Balgach, Switzerland). Real-Time PCR reactions were performed using TaqMan Universal PCR Master Mix (Applied Biosystems) as described [211].

^{32}P and ^{3}H-glucose-uptake in brush border membrane vesicles

Brush border membrane vesicles were prepared using the Mg^{2+}-precipitation technique [231, 232] and further used for western blotting and transport studies. The transport rate of ^{32}-labeled phosphate and tritium labeled glucose into renal brush border membrane vesicles was determined at 30 s and 120 min (equilibrium value) as described [231] at 25°C in the presence of inward gradients of 100 mM NaCl or 100 mM KCl and 0.1 mM

K_2HPO_4. All measurements were performed in triplicates.

Western blot analysis

After measurement of the protein concentration (Bio-Rad, Hercules, CA), 10 μg of renal brush border membrane for NaPi-IIa and NaPi-IIc and 20 μg or 2 μg, respectively, of total kidney homogenate for FRS2a/pFRS2a and Klotho was solubilized in loading buffer containing DTT and separated on 8% polyacrylamide gels. For immunoblotting, proteins were transferred electrophoretically to polyvinylidene fluoride membranes (Immobilon-P, Millipore, Bedford, MA, USA). After blocking with 5% milk powder in Tris-buffered saline/0.1% Tween-20 for 60 min, blots were incubated with the primary antibodies: rabbit polyclonal anti-NaPi-IIa (1:6000) [27, 233], rabbit polyclonal anti-NaPi-IIc (1:10000) [211], mouse monoclonal anti-β-actin antibody (42kD; Sigma, St. Louis, MO; 1:5000), mouse monoclonal anti-FRS2a (R&D Systems, USA; 1:1500), rabbit polyclonal anti-pFRS2a (Cell Signaling Technology, USA; 1:2000), rat monoclonal anti-Klotho (Clone KM2076, TransGenic Inc., Japan; 1:1000), and mouse monoclonal anti-GAPDH (Merck Millipore, USA; 1:20000) either for 2 h at room temperature or overnight at 4°C. Membranes were then incubated for 1 h at room temperature with secondary goat anti-rabbit, donkey anti-mouse or goat anti-rat antibodies (1:5000) linked to alkaline phosphatase (Promega, USA), HRP (Amersham, USA or R&D Systems, USA). The protein signal was detected with the appropriate substrates using the DIANA III-chemiluminescence detection system (Raytest, Straubenhardt, Germany). All images were analyzed using the software Advanced Image Data Analyser AIDA, Raytest to calculate the protein of interest/actin ratio.

Immunofluorescence staining

Rat kidneys were perfused in situ through the left heart ventricle with a fixative solution containing 3% paraformaldehyde in phosphate buffered saline (PBS). Mouse kidneys were immersed in a fixative solution containing formalin (10%). Kidneys were embedded in TissueTec and frozen in liquid nitrogen cooled by liquid propane. Five μm cryosections were cut. Slides were washed in PBS and incubated in 50 mM NH_4Cl in PBS for 20 min at room temperature to reduce free aldehyde groups. For FGF23 staining, slides were treated for 5 min with 0.5% SDS in PBS. Unspecific sites were blocked with 1% bovine

serum albumin (BSA) in PBS for 1 h at room temperature. Primary antibodies were diluted in 1% BSA in PBS (NaPi-IIa 1:1000; anti-FGF23 (R&D Systems, USA) 1:1000; anti-Calbindin (Swant, Switzerland) 1:20000) and kidney sections were incubated with the primary antibody over night at 4°C. After washing with PBS, sections were incubated with the corresponding secondary antibody (1:500) (anti-rabbit Alexa594 (Invitrogen, Switzerland), anti-rat NL493 (R&D Systems, USA); anti-mouse (DyLight 649, Jackson ImmunoResearch, Europe), phalloidin-FITC (1:200), and DAPI (Invitrogen,1:1000) for 1 h at room temperature. Slides were washed twice with PBS before being mounted with Dako glycergel mounting medium. Sections were visualised on a Leica DM 5500B fluorescence microscope and images processed with Adobe Photoshop CS5 extended.

Statistical analysis

Statistics were performed using unpaired Student‘s t-test (GraphPad Prism version 5.0, GraphPad, San Diego, CA). Random-effects models for longitudinal data were applied to analyse unbalanced repeated measures (SAS version 9.3, Cary, NC, USA). Data are provided as mean ± SD. $P < 0.05$ was considered significant.

3.1.6 Disclosure

All authors declared no competing interests.

3.1.7 Acknowledgments

This study was supported by grants from the Swiss National Science Foundation (No. 310000-118166) to A. Serra, the Swiss National Center for Competence in Research Kidney. CH to C. A. Wagner, and by a collaborative grant from the Zurich Center for Integrative Human Physiology (ZIHP) to J. Biber, A. Serra, and C. A. Wagner. H. Zhang. was partly supported by a doctoral scholarship from the China Scholarship Council (CSC). S. Segerer is supported by grants from the CKM and the Hartmann Müller-Stiftung. The use of the ZIRP Core facility for Rodent Physiology is gratefully acknowledged. We thank O. Devuyst for helpful comments.

3.1.8 Supplementary Data

Supplementary Methods

H&E staining

Hearts were fixed in 10% buffered formalin over night and embedded in paraffin. Sections were stained with Hematoxilin-Eosin following routine protocols.

Supplementary Figures

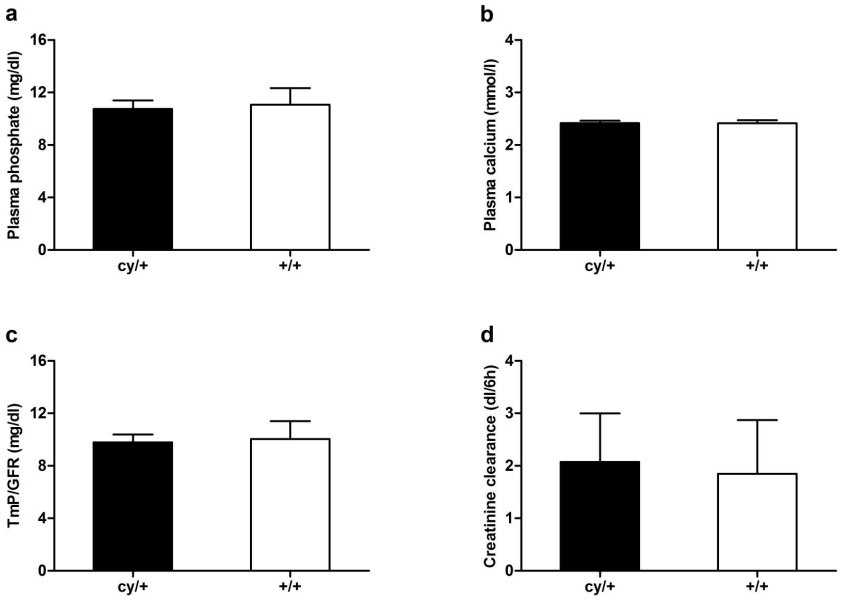

Figure 3.11: Renal function after fasting overnight of 4 weeks old HanSPRD rats. Plasma phosphate (a), plasma total calcium (b), TmP/GFR (c), and creatinine clearance after 4 weeks in cy/+ (black bars) and +/+ (white bars) HanSPRD rats (mean ±SD); number of animals (median), cy/+ n = 12, +/+ n = 8

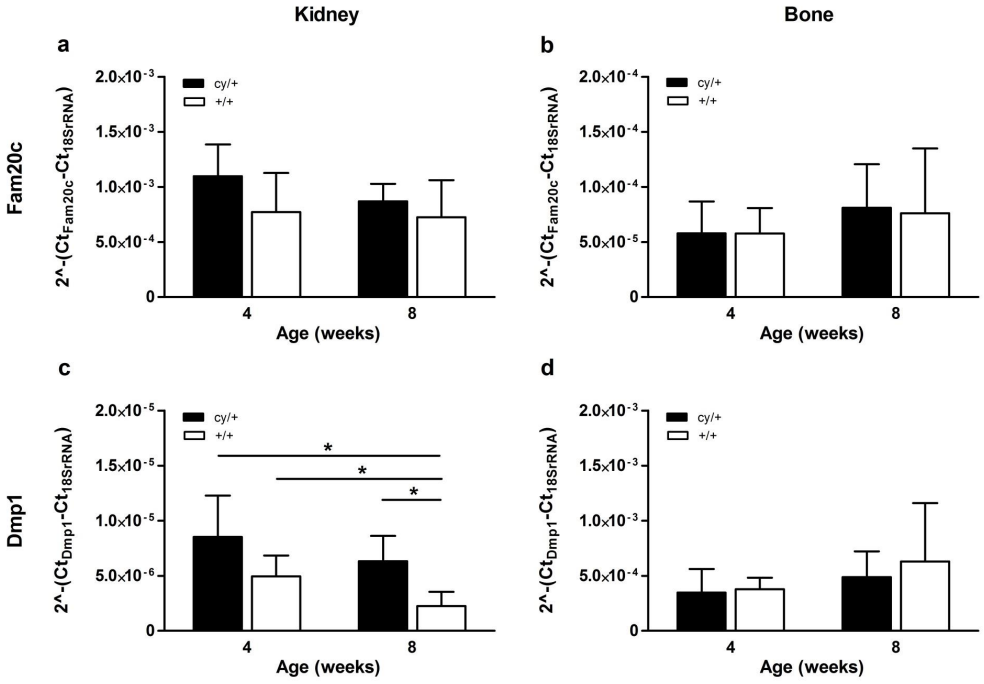

Figure 3.12: mRNA expression of FGF23 regulatory molecules in kidney and bone. Relative mRNA expression of Fam20c and Dmp1 in kidney (a, c) and bone (b, d) after 4 and 8 weeks in cy/+ (black bars) and +/+ (white bars) Han:SPRD rats (mean ±SD); number of animals (median), cy/+ n = 7, +/+ n = 5; * $p<0.05$

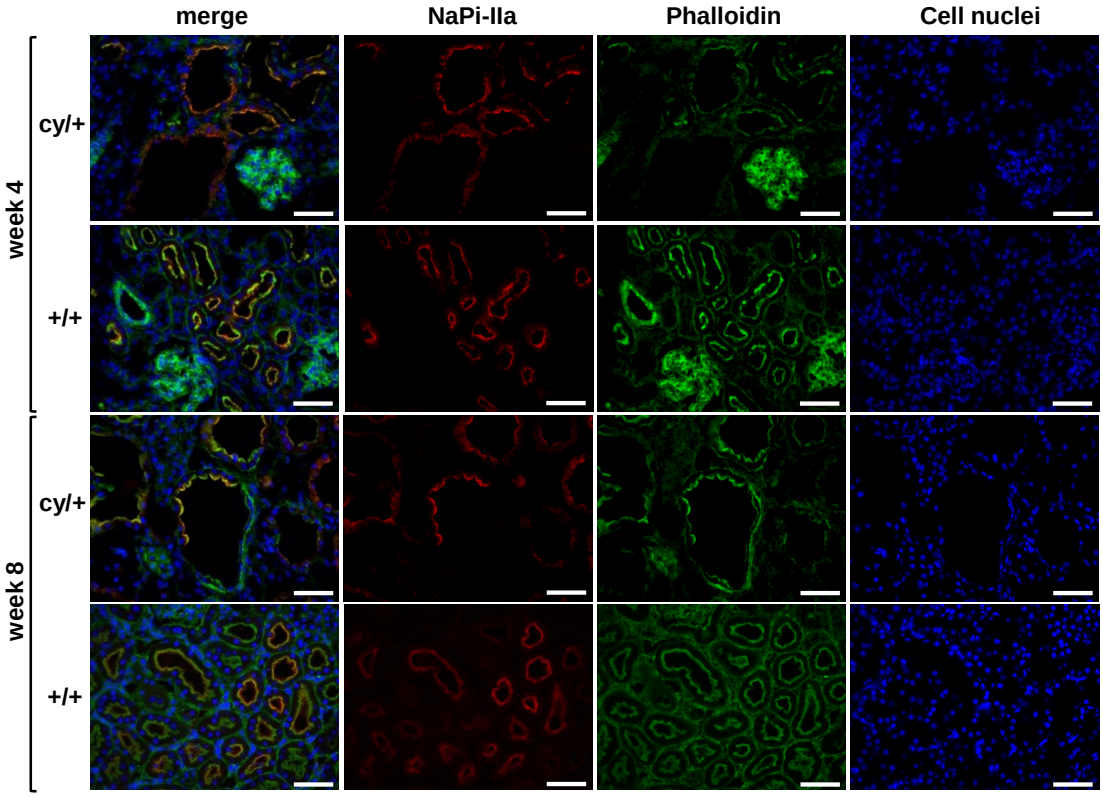

Figure 3.13: Immunolocalization of NaPi-IIa. Frozen kidney sections were stained with antibodies against NaPi-IIa (red), Phalloidin-FITC for actin (green), and DAPI (blue) in cy/+ and +/+ animals after 4 and 8 weeks. Scale bar 50 μm.

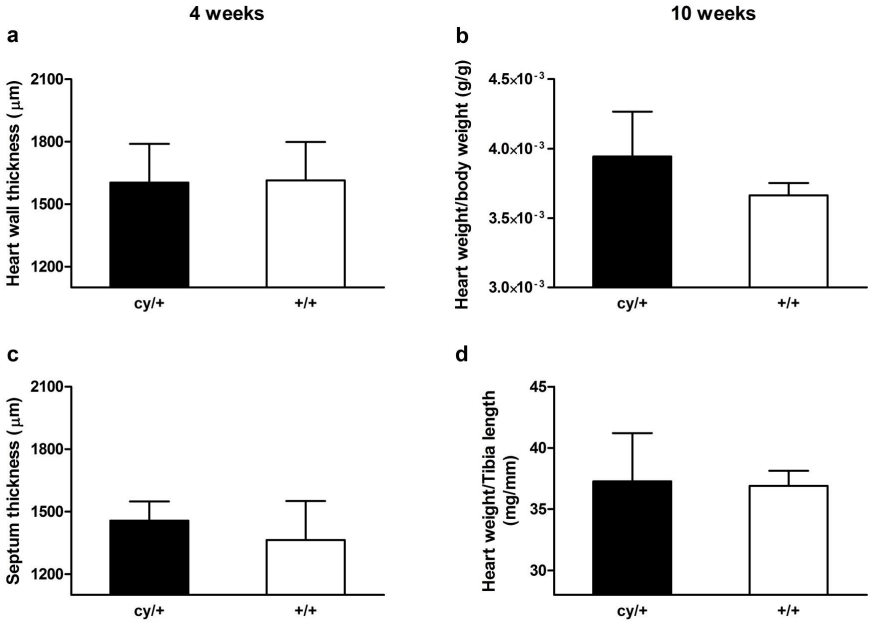

Figure 3.14: Heart wall thickness and heart weight. Heart wall (a) and septum thickness (c) of 4 weeks old HanSPRD rats; heart weight of 10 weeks old rats normalized to body weight (b) and tibia length (d); number of animals (median), cy/+ = 5, +/+ = 4

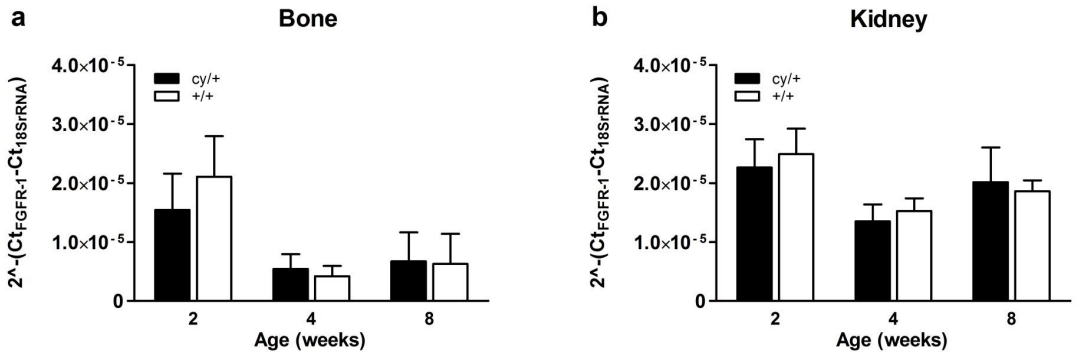

Figure 3.15: FGFR-1 mRNA expression. Relative mRNA expression of the FGF receptor 1 (FGFR-1) in bone (a) and kidney (b) to 18S rRNA after 2, 4, and 8 weeks in cy/+ (black bars) and +/+ (white bars) Han:SPRD rats (mean ±SD); number of animals (median), cy/+ n = 6, +/+ n = 5

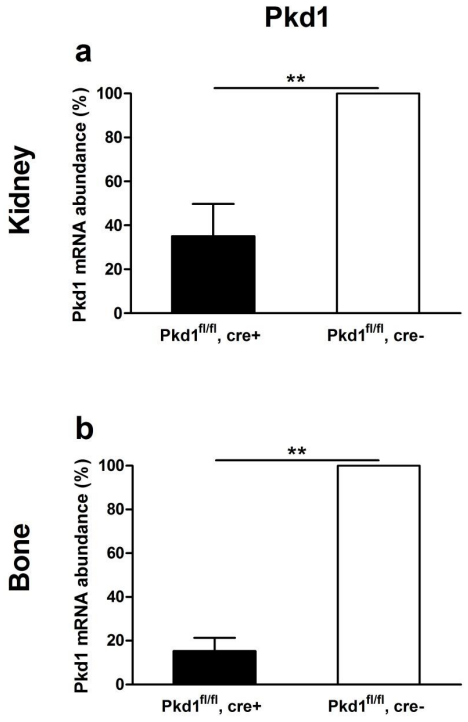

Figure 3.16: Pkd1 mRNA expression. Relative Pkd1 mRNA abundance in kidney (a) and bone (b) of 10 weeks old Pkd1fl/fl, cre+ (black bars) compared to Pkd1fl/fl, cre- (white bars) mice (mean ±SD); number of animals (median), $Pkd1^{fl/fl}$, cre+ n = 8, $Pkd1^{fl/fl}$, cre- n = 15; ** $p<0.001$

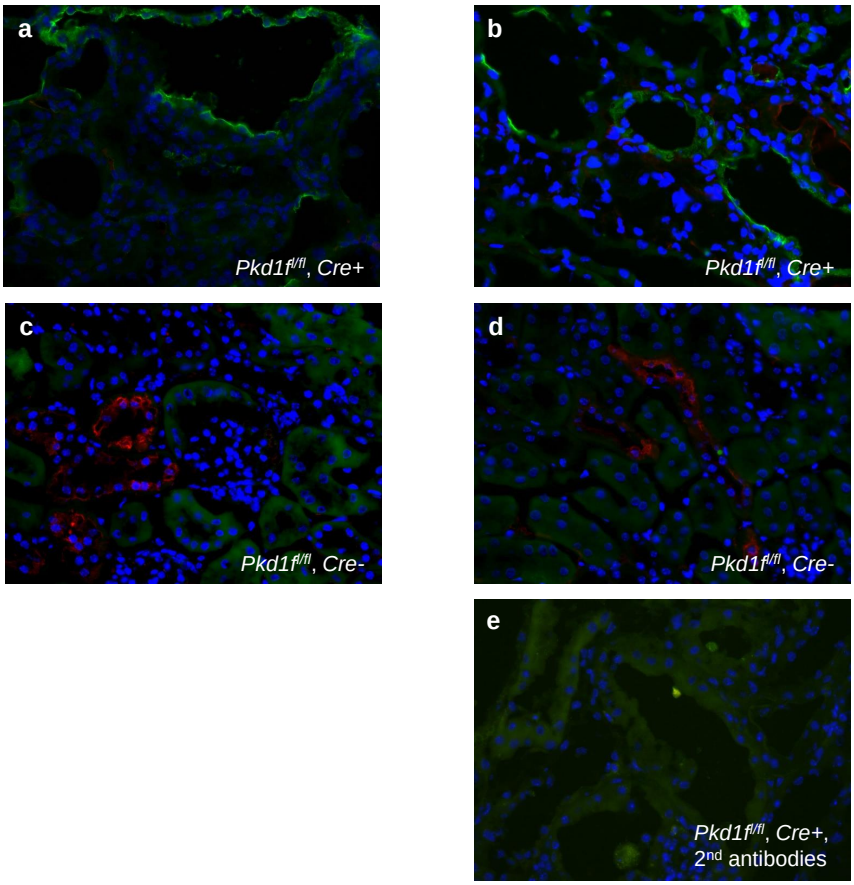

Figure 3.17: Expression of FGF23 in kidneys from Pkd$^{fl/fl}$, cre+ KO mice. Frozen kidney sections were stained for FGF23 (green), calbindin D28k, a marker of DCT and CNT segments (red), and DAPI (cell nuclei). In kidneys from Pkd1$^{fl/fl}$, cre+ mice strong FGF23 staining is observed in cells lining the cysts (a,b), no staining for FGF23 is observed in kidneys from Pkd1$^{fl/fl}$, cre- mice (c,d). Omission of primary antibodies in Pkd1$^{fl/fl}$, cre+ kidneys showed no staining (e). Original magnification 400 x.

Table 3.1: Primer and probe sequences used for RT-PCR

Gene	Type	Sequence
Rat NaPi-IIa (Slc34a1)	Fwd	5'-GGAATCACAGTDTCATTCGGATT-3'
	Rev	5'-ATGGCCTCTACCCTGGACATAG-3'
	Probe	5'-TGTCAACCAGAGACAAAAGAGGCTTCCACT-3'
Rat NaPi-IIc (Slc34a3)	Fwd	5'-GGGATCGGGATGAATTTCAGA-3'
	Rev	5'-GGGCCAGCTCACTCAGTCTCT-3'
	Probe	5'-ACGGCATCTTCAACTGGCTCACAGTGTT-3'
Rat FGF23	Fwd	5'-GCAACATTTTTGGATCGTATCA-3'
	Rev	5'-GATGCTTCGGTGACAGGTAGA-3'
	Probe	5'-AGATTCCGCCAGTGGACGCTAGAGA-3'
Rat Klotho	Fwd	5'-TATCTCAAGAAGTTCATAATGGAAAGC-3'
	Rev	5'-GAGGGACCATGCGGTGTA-3'
	Probe	5'-TAAAAGCCATCAGGCTGGATGGGG-3'
Rat FGFR1	Fwd	5'-GGTTGAAAAATGGCAAGGAA-3'
	Rev	5'-CCACGATGCAGGTGTAGTTG-3'
	Probe	5'-TCGGAGGCTACAAGGTTCGTTACGC-3'
Rat Cyp24a1	Fwd	5'-CAAATCAGTCAAACCCTGCAT-3'
	Rev	5'-GGCGTACAGTTCCTTCTTGG-3'
	Probe	5'-TACAGAGATATTCCCAGCAGCCCGG-3'
Rat Cyp27b1	Fwd	5'-TGGCAAACGAAGTTGCATAG-3'
	Rev	5'-AGCACCTCAAAATGGGTCAA-3'
	Probe	5'-CTACAAATGGCGTTGGCCCAGATC-3'
Rat Fam20c	Fwd	5'-CCATCGATGCCTTACTCCAC-3'
	Rev	5'-CCCGTAATTCTGGAAGGTCA-3'
	Probe	5'-CAGAAGATCACCAGTGTCGCCATGA-3'
Rat Dmp1	Fwd	5'-CTGTCCTGTGCTCTCCCTGT-3'
	Rev	5'-GCTGTCCGTGTGGTCACTATT-3'
	Probe	5'-TCTGAAAGCTCCGAAGAGAGGACGG-3'
Mouse Pkd1	Fwd	5'-GGCCAACCTCTCCTCAGTATC-3'
	Rev	5'-GAAGGGTACTGCTGCCACA-3'
	Probe	5'-CTGTGGTGAGGAATATGTCGCCTGC-3'
Mouse FGF23	Fwd	5'-TCGAAGGTTCCTTTGTATGGAT-3'
	Rev	5'-AGTGATGCTTCTGCGACAAGT-3'
	Probe	5'-TTTTTGGATCGCTTCACT-3'
Mouse Klotho	Fwd	5'-ACGTTCAAGTGGACACTACTCTCTC-3'
	Rev	5'-TTGGCTACAACCCCGTCTAC-3'
	Probe	5'-CCGAATGTCTATCTGTGGGATGTGCA-3'

3.2 Inflammation triggers renal expression of FGF23 and elevates systemic FGF23 levels in polycystic kidney disease

Daniela Spichtig[1], Nicole Gehring[1], Carla Bettoni[1], Désirée Schönenberger[1], Michal Rajski[1], David Hoogewijs[1], Michael Föller[2], Florian Lang[2], Roland H. Wenger[1], Ian Frew[1], and Carsten A. Wagner[1]

[1]Institute of Physiology, University of Zurich, Zurich Switzerland and National Center for Competence in Research NCCR Kidney.CH, Switzerland
[2]Institute of Physiology, University of Tübingen, Germany

Own contribution:
All animal and cell culture experiments, western blots, and histology were performed by Daniela Spichtig (DS). Enzyme-linked immunosorbent assays and gene expression analyses were partially performed by DS. The manuscript inclusive figures was drafted by DS.

3.2.1 Abstract

Fibroblast growth factor 23 (FGF23) regulates phosphate homeostasis and is directly linked to all-cause mortality in chronic kidney disease (CKD). In polycystic kidney disease (PKD) animal models plasma Fgf23 rises, however, *Fgf23* expression in bone is unchanged instead of the kidney becomes a site of *Fgf23* production. Since polycystic kidneys experience local hypoxia and inflammation, we examined whether hypoxia or inflammation affect Fgf23 expression in bone and polycystic kidneys. PKD kidneys had increased *Tnfα* and *Tgfβ* expression as well as increased phosphorylation of the NfκB subunit p65. Tnfα/NfκB signaling increases *Nurr1* expression, an orphan nuclear receptor involved in the Pth dependent regulation of *Fgf23* expression in bone. In PKD kidneys, *Nurr1* expression was upregulated and Nurr1 protein was predominantly localized in the cell nucleus. Nuclear Nurr1 overlapped with Fgf23 expression in the kidneys of PKD mice. Tnfα but not hypoxia stimulated *Fgf23* expression in primary mouse osteocytes and was paralleld by changes in *Nurr1* expression. Antibody-mediated neutralization of Tnfα in *Pkd1* conditional KO mice reduced renal *Tnfα* and *Tgfβ* mRNA expression and concomitantly decreased plasma Fgf23 levels. In conclusion, ectopic renal Fgf23 expression is triggered by Tnfα and Tnfα blockade normalizes expression of osteogenic markers and regulators of FGF23 expression in kidney along with plasma Fgf23 levels in PKD animals.

3.2.2 Introduction

Fibroblast growth factor 23 (Fgf23) is critical to maintain phosphate homeostasis and vitamin D_3 metabolism [59, 60]. The main target organ of Fgf23 is the kidney where Fgf23 binds in the presence of its obligate co-factor Klotho to the FGFR receptor and inhibits phosphate reabsorption as well as decreases 1,25$(OH)_2$ vitamin D_3 levels by reducing its synthesis and accelerating its degradation [69, 77]. Fgf23 is mainly expressed in bone and to a lower extent in thymus, spleen, brain, and heart [59, 61, 62, 65].

Many systemic factors regulate *Fgf23* gene expression among them 1,25$(OH)_2$ vitamin D_3, Pth as well as inflammatory cytokines such as TNFα and IL-1β [63, 130, 131, 133, 147]. In bone, 1,25$(OH)_2$ vitamin D_3 activates and translocates the vitamin D (VDR) receptor to the nucleus where it binds in form of the VDR/RXR heterodimeric complex to the vitamin D response element in the *Fgf23* promoter region and stimulates *Fgf23* expression [54–56, 63]. Pth has an other mode of action by which it activates the G protein coupled receptor PTHR on bone cells [134, 135]. This leads to a cAMP dependent activation of protein kinase A (PKA) and the subsequent induction of the nuclear receptor related 1 protein (Nurr1) expression [134, 135]. Nurr1 belongs to the nuclear orphan receptor family and is an early response gene which regulates target genes by binding to the nerve growth factor B response element (NBRE) in their promoter region [234–236]. Nurr1 physically interacts with the NBRE sequence in the FGF23 promoter region and activates *Fgf23* gene expression in UMR-106 rat osteosarcoma cells [133]. Apart from Pth, various factors such as membrane depolarization, brain and liver ischemia, as well as inflammatory cytokines such as tumor necrosis factor α (Tnfα) and interleukin 1β (IL-1β) stimulate *Nurr1* expression and are therefore potential regulators of *Fgf23* expression [234, 237–239]. Indeed, Tnfα, Il-1β, as well as lipopolysaccaride (LPS) stimulation increases *Fgf23* expression in IDG-SW3 osteocyte cells, macrophages, and dendritic cells [147, 149].

Chronic kidney disease (CKD) leads to a severe disturbance of mineral homeostasis which is one of the leading factors for morbidity and mortality in patients with endstage renal disease [155]. In the course of CKD, FGF23 levels rise before PTH and plasma phosphate concentrations and are independently associated with mortality [156, 157, 166]. The subsequent change of parameters of mineral homeostasis can be reproduced in the *Col4a3*$^{-/-}$ mouse, a CKD animal model [160]. The early rise of serum Fgf23 levels in *Col4a3*$^{-/-}$ mice

is not accompanied by an increase in *Fgf23* gene expression in bone [160]. Interestingly, ectopic Fgf23 gene and protein expression was reported in the kidneys of rats with diabetic nephropathy as well as in kidneys from animals with polycystic kidney disease (PKD), two models of CKD [227, 240]. The trigger for renal *Fgf23* expression is so far unknown.
In this study we evaluated hypoxia and inflammation, two common denominators of diabetic nephropathy and PKD, as possible factors regulating *Fgf23* expression in kidneys of *Pkd1* conditional KO mice as well as in bone cell culture models.

3.2.3 Results

Kidney weight, *Pkd1* knockdown and phosphate homeostasis

Cre recombinase activity of *Pkd1* conditional KO mice was activated by injection of tamoxifen (0.25mg/animal) at postnatal days 15, 17, and 19 to induce a slow PKD disease progression model [202]. At week 6, $Pkd1^{fl/fl}$, *cre+* animals had a two kidney per body weight (BW) ratio of 16 ± 2 mg/g BW which was similar compared to $Pkd1^{fl/fl}$, *cre-* animals (13 ± 1 mg/g BW) (Figure 3.18a). The two kidney per body weight ratio was dramatically increased in $Pkd1^{fl/fl}$, *cre+* animals (68 ± 36 mg/g BW) at week 12 due to massive bilateral cyst growth. After 6 and 12 weeks 19% and 74% residual *Pkd1* expression, respectively, was detected in $Pkd1^{fl/fl}$, *cre+* animals compared to *Pkd1* expression in $Pkd1^{fl/fl}$, *cre-* animals at week 6 (Figure 3.18 b) consistent with previous reports of compensatory increase of remaining Pkd1 expression in cystic epithelial cells [241].
Plasma Fgf23 and Pth levels were similar in $Pkd1^{fl/fl}$, *cre+* and $Pkd1^{fl/fl}$, *cre-* animals after 6 weeks (Figure 3.18 c and d). At week 12, plasma Fgf23 levels were significantly higher in $Pkd1^{fl/fl}$, *cre+* (255 ± 192 pg/ml) compared to $Pkd1^{fl/fl}$, *cre-* animals (87 ± 23 pg/ml). To the contrary, serum Pth levels decreased significantly after 12 weeks in $Pkd1^{fl/fl}$, *cre+* (57 ± 19 pg/ml) compared to $Pkd1^{fl/fl}$, *cre-* animals (237 ± 124 pg/ml). The ratio of maximal rate of tubular phosphate reabsorption per glomerular fitration rate (TmP/GFR) and blood urea nitrogen (BUN) did not differ between $Pkd1^{fl/fl}$, *cre+* and $Pkd1^{fl/fl}$, *cre-* animals at week 6 (Figure 3.18 e and f). At week 12, TmP/GFR was significantly decreased in $Pkd1^{fl/fl}$, *cre+* (4.6 ± 1.1 mg/dl) compared to $Pkd1^{fl/fl}$, *cre-* animals (6.3 ± 1.2 mg/dl) whereas at the same time point BUN significantly increased in $Pkd1^{fl/fl}$, *cre+* (148 ± 60 mg/dl) compared to $Pkd1^{fl/fl}$, *cre-* animals (60 ± 7 mg/dl).

There was no difference in the creatinine clearance between *Pkd1*$^{fl/fl}$, *cre+* and *Pkd1*$^{fl/fl}$, *cre-* animals at any time point studied (Figure 3.18 g). Taken together, these data indicate a state of chronic kidney disease in the 12 weeks old animals.

Renal expression of bone marker genes

We had previously reported renal Fgf23 mRNA and protein expression in 10 weeks old *Pkd1*$^{fl/fl}$, *cre+* animals [240]. Here, *Pkd1*$^{fl/fl}$, *cre+* animals at week 6 and *Pkd1*$^{fl/fl}$, *cre-* animals at week 6 and 12 did not express Fgf23 mRNA or protein whereas *Pkd1*$^{fl/fl}$, *cre+* animals at week 12 had a significant increase in renal *Fgf23* mRNA expression (Figure 3.19 a). At the same time *Fgf23* mRNA expression in bone was similar in *Pkd1*$^{fl/fl}$, *cre+* and *Pkd1*$^{fl/fl}$, *cre-* animals (Figure 3.19 b). Osteogenic marker genes such as *Runx2* and *Dmp-1* were upregulated in kidneys of *Pkd1*$^{fl/fl}$, *cre+* compared to *Pkd1*$^{fl/fl}$, *cre-* animals (Figure 3.19 c and e). The same genes were similarly expressed in bones of *Pkd1*$^{fl/fl}$, *cre+* and *Pkd1*$^{fl/fl}$, *cre-* animals (Figure 3.19 d and f).

Inflammation in PKD kidneys

Renal FGF23 expression was also reported in rats with diabetic nephropathy [227]. Two common denominators of diabetic nephropathy and PKD are local renal hypoxia and inflammation [242–247]. Moreover, hypoxia stimulated *Fgf23* expression in the UMR-106 rat osteosarcoma cell line [139]. Therefore we evaluated these two factors as potential triggers for renal and bone FGF23 expression. First, we assessed the presence of inflammation markers in the kidney. At week 6, renal *Tnfα* and *Tgfβ* mRNA expression was similar in *Pkd1*$^{fl/fl}$, *cre+* and *Pkd1*$^{fl/fl}$, *cre-* animals (Figure 3.20 a and b). In the course of PKD disease, *Tnfα* and *Tgfβ* mRNA expression increased significantly in *Pkd1*$^{fl/fl}$, *cre+* animals compared to *Pkd1*$^{fl/fl}$, *cre-* animals (Figure 3.20 a and b). Tnfα binding to Tnfα receptors activates the NfκB signaling pathway [248]. Figure 3.20 c shows the phosphorylation state of the NfκB subunit p65 as well as total NfκB p65 protein in the nuclear fraction of total kidney homogenates. The ratio of Phospho-NfκB p65 to NfκB p65 was significantly elevated in the kidneys of *Pkd1*$^{fl/fl}$, *cre+* compared to *Pkd1*$^{fl/fl}$, *cre-* animals.

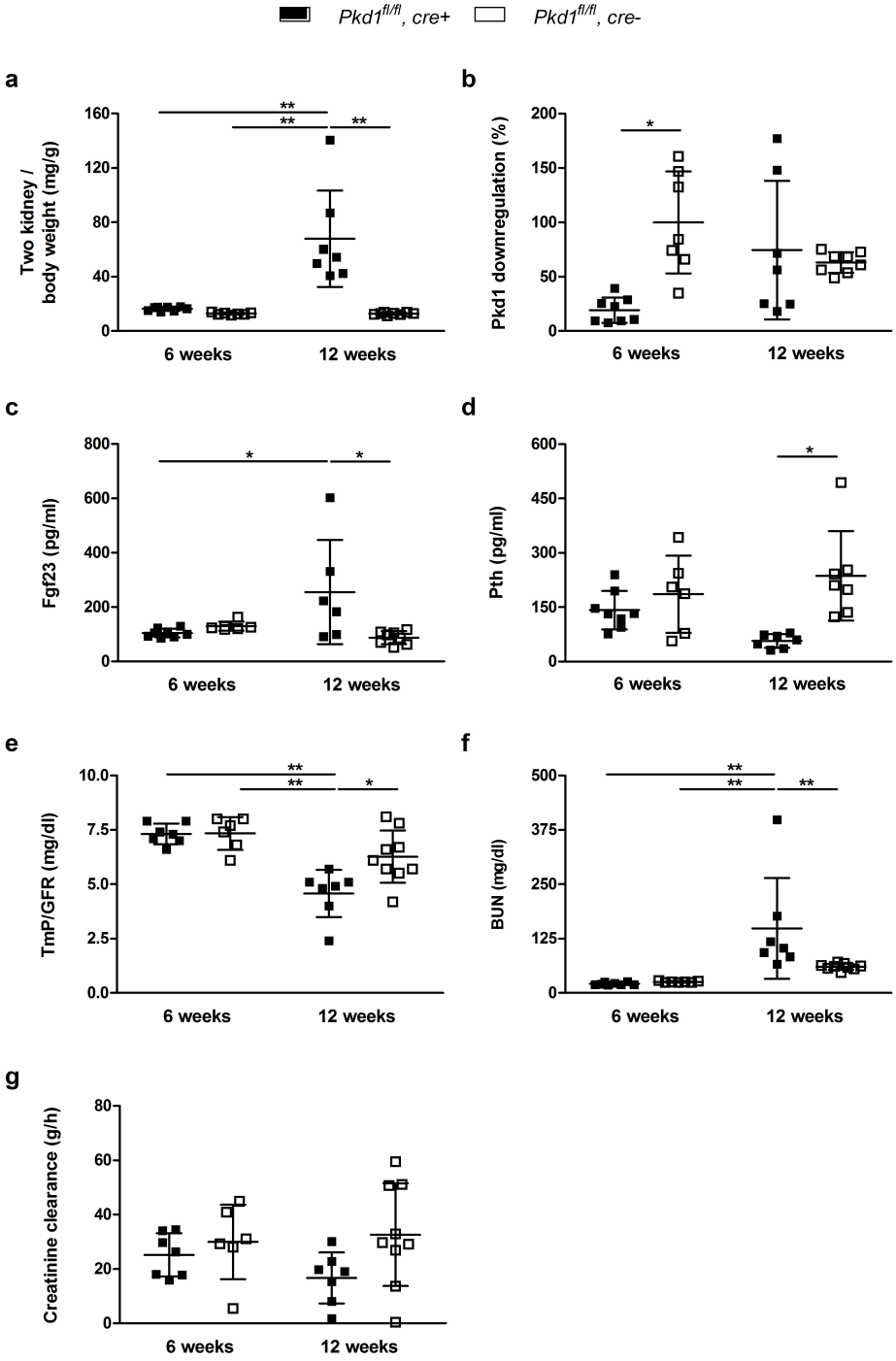

Figure 3.18: Baseline characteristics of *Pkd1* KO mice. Two kidney per body weight ratio (a), *Pkd1* mRNA expression normalized to $Pkd1^{fl/fl}$, *cre-* mice (6 weeks) (b), plasma Fgf23 (c), plasma Pth (d), TmP/GFR (e), BUN (f), and creatinine clearance (g) in $Pkd1^{fl/fl}$, *cre+* (black squares) and $Pkd1^{fl/fl}$, *cre-* (white squares) animals at the age of 6 and 12 weeks, respectively (mean ±SD). Number of animals per group 6-9; * $p<0.05$, ** $p<0.0001$.

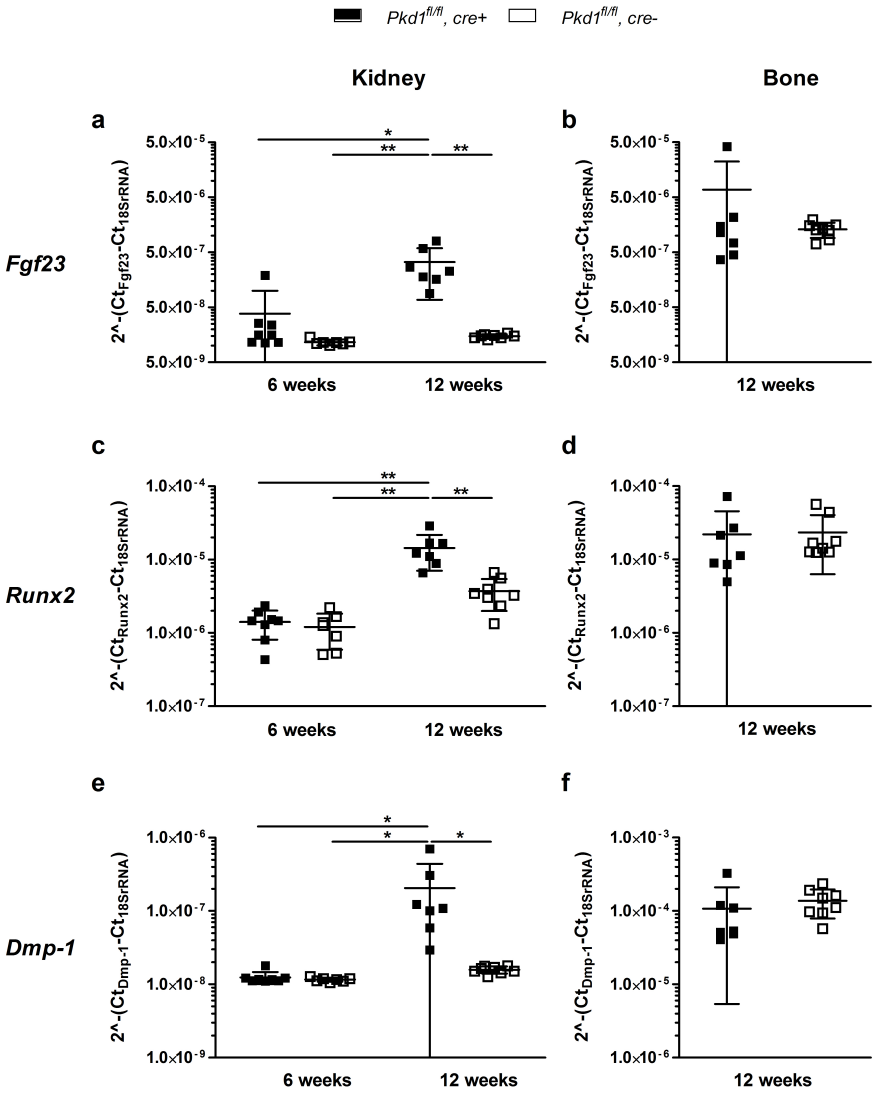

Figure 3.19: Expression of bone marker genes in kidney and bone of *Pkd1* KO mice. *Fgf23* (a, b), *Runx2* (c, d), and *Dmp-1* (e, f) mRNA expression relative to 18S rRNA in kidney and bone of $Pkd1^{fl/fl}$, *cre+* (black squares) and $Pkd1^{fl/fl}$, *cre-* (white squares) animals at the age of 6 and 12 weeks, respectively (mean ±SD). Number of animals per group 6-9; * $p<0.05$, ** $p<0.0001$.

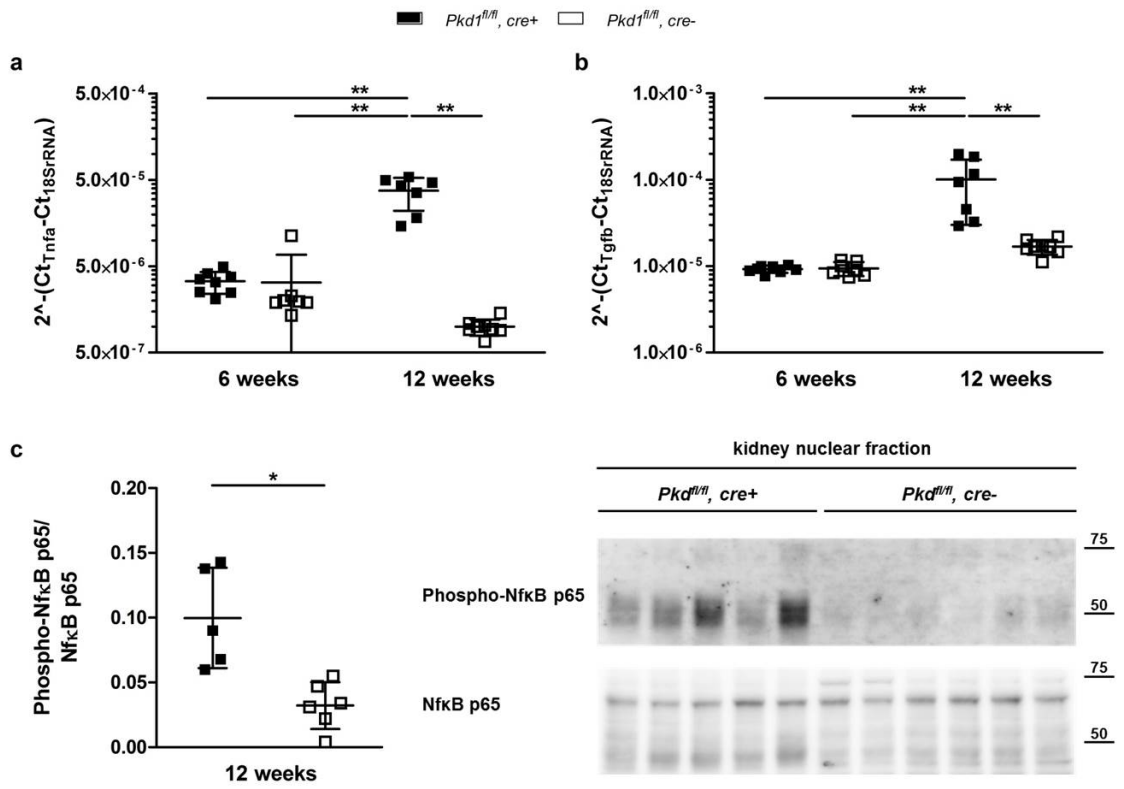

Figure 3.20: Inflammation markers in the kidney of *Pkd1* KO mice. Renal *Tnfα* (a) and *Tgfβ* (b) mRNA expression relative to 18S rRNA in $Pkd1^{fl/fl}$, *cre+* (black bars) and $Pkd1^{fl/fl}$, *cre-* (white bars) animals at the age of 6 and 12 weeks, respectively. Phosphorylation state of NfκB in the nuclear fraction of total kidney protein homogenates in $Pkd1^{fl/fl}$, *cre+* (black bars) and $Pkd1^{fl/fl}$, *cre-* (white bars) animals after 12 weeks (mean ±SD). Number of animals per group 6-9; * $p<0.05$, ** $p<0.0001$.

Expression and localization of Nurr1 in polycystic kidneys

The orphan nuclear receptor Nurr1 activates *Fgf23* mRNA expression in rat osteosarcoma cells [133]. *Nurr1* expression itself is stimulated by NfκB in response to Tnfα [239]. Nurr1 mRNA was detected in mouse kidney and bone (Figure 3.21). At week 6, renal *Nurr1* expression was similar in *Pkd1*$^{fl/fl}$*, cre+* and *Pkd1*$^{fl/fl}$*, cre-* animals. At week 12, renal *Nurr1* expression was significantly increased in *Pkd1*$^{fl/fl}$*, cre+* whereas *Nurr1* expression in bone was similar in PKD and control animals (Figure 3.21 a and b). Nurr1 is a orphan nuclear receptor and is active upon translocation to the nucleus where it binds to NERB sequences in the promotor region of target genes [234–236]. We found that Nurr1 in *Pkd1*$^{fl/fl}$*, cre+* kidneys was predominantly localized in the cell nucleus whereas Nurr1 in *Pkd1*$^{fl/fl}$*, cre-* animals was mainly distributed in the cytoplasm (Figure 3.21 c to j and Supplementary Figures 3.24 and 3.25). Further, nuclear Nurr1 staining in *Pkd1*$^{fl/fl}$*, cre+* animals is often but not exclusively co-localized with Fgf23 expressing cells. There was no Fgf23 protein expression in *Pkd1*$^{fl/fl}$*, cre-* animals. Staining of tissue section only with secondary antibodies revealed no staining (Figure 3.21 k).

Tnfα but not hypoxia stimulates *Fgf23* expression in bone cells

We cultured primary osteocytes from tibias and femurs of mice according to established protocols [249, 250]. Cells from digestion step 6-9 or cells and bone pieces from digestion step >9 expressed markers of osteocytes and were cultured for 2 weeks in osteogenic medium before supplemented for 24 hours either with 10 ng/ml Tnfα or 10 nM 1,25(OH)$_2$ vitamin D$_3$. Tnfα as well as 1,25(OH)$_2$ vitamin D$_3$ increased *Fgf23* mRNA expression in primary osteocytes (Figure 3.22 a). Further we investigated the expression of regulators of *Fgf23* gene expression or postranslational processing of Fgf23. Tnfα but not 1,25(OH)$_2$ vitamin D$_3$ increased the expression of the orphan nuclear receptor *Nurr1* as well as the expression of *Galnt3* (Figure 3.22 b and c). Galnt3 is important for the O-glycosylation of FGF23 preventing proteolytic cleavages of Fgf23 [102–105]. The expression of *Bmp-1*, involved in Dmp-1 cleavage, is moderately upregulated by 1,25(OH)$_2$ vitamin D$_3$ but not by Tnfα (Figure 3.22 d). Binding of Dmp-1 to the extracellular domain of Phex inhibits *Fgf23* gene expression [123, 125]. Upon Tnfα and 1,25(OH)$_2$ vitamin D$_3$ treatment *Dmp-1* expression was strongly decreased whereas *Phex* expression was only decreased by

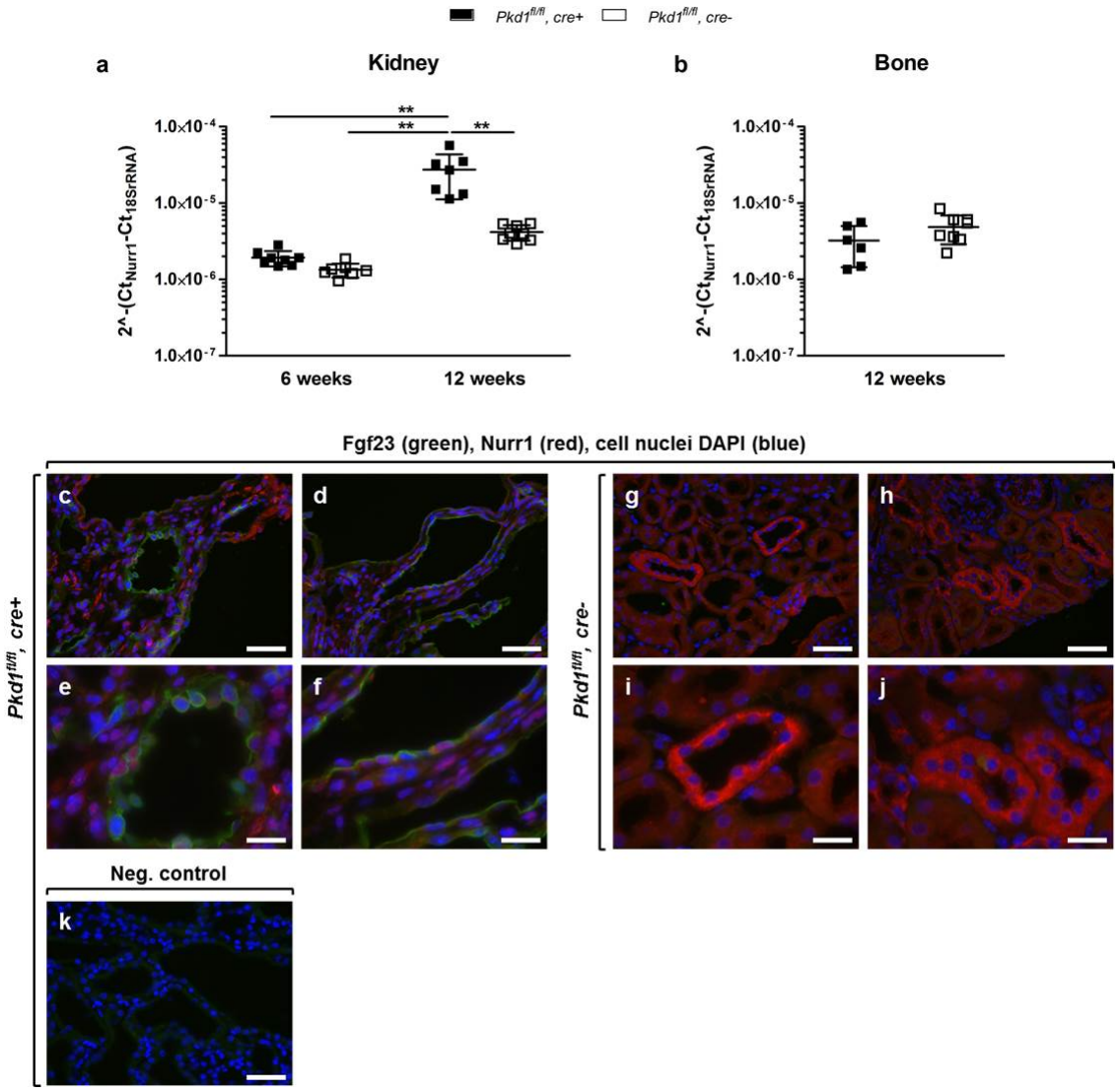

Figure 3.21: Expression and localization of Nurr1 in the kidney of *Pkd1* KO animals. *Nurr1* mRNA expression relative to 18S rRNA in kidney (a) and bone (b) of $Pkd1^{fl/fl}$, *cre+* (black squares) and $Pkd1^{fl/fl}$, *cre-* (white squares) animals at the age of 6 and 12 weeks, respectively. Number of animals per group 6-9; * $p<0.05$, ** $p<0.0001$. Immunofluorescense staining for FGF23 (green), Nurr1 (red), and DAPI (blue, cell nuclei): (c-f) kidneys from 12 weeks old $Pkd1^{fl/fl}$, *cre+* mice, (g-j) kidneys from 12 weeks old $Pkd1^{fl/fl}$, *cre-* mice, (k) kidney from 12 weeks old $Pkd1^{fl/fl}$, *cre+* mice incubated with secondary antibodies alone. Original magnification (c, d, g, h, k) 400x (scale bar 50 μm) and (e, f, i, j) 1000x (scale bar 20 μm).

1,25$(OH)_2$ vitamin D_3 but not by Tnfα (Figure 3.22 e and f).

MC3T3-E1 mouse preosteoblasts, used to study the effect of hypoxia, did not display intrinsic *Fgf23* expression. Nevertheless, after 2 or 3 weeks differentiation of MC3T3-E1 along the osteogenic lineage *Fgf23* mRNA expression was induced by 10 nM 1,25$(OH)_2$ vitamin D_3. However, 1,25$(OH)_2$ vitamin D_3 induced *Fgf23* mRNA expression was completely repressed when cells were cultured for 24 or 48 hours under hypoxic conditions (0.2% O_2) (Supplementary Figure 3.26 a). The two Hif1α target genes carbonic anhydrase 9 (Ca9) and prolyl hydroxylase domain containing protein 2 (Phd2) were upregulated in hypoxia and therefore confirmed the presence and effect of hypoxia (Supplementary Figure 3.26 b and c). Similarly, we did not see any effect of hypoxia on *Fgf23* mRNA expression in U2OS rat osteosarcoma cells as well as in primary osteoblast cells (not shown). Moreover, we evaluated *Fgf23* as Hif1α or Hif2α target gene by analyzing kidneys of Von Hippel-Lindau (*Vhl*) KO animals [251]. Lack of Vhl protein prevents Hif hydroxylation and degradation and activates hypoxia sensitive genes [252]. We quantified *Fgf23* expression in kidneys of *Vhl* KO animals as well as in primary kidney cells lacking Vhl but neither the kidneys of Vhl KO animals nor the cells lacking Vhl expressed *Fgf23* (not shown).

TNFα blockade in *Pkd1* KO mice suppresses Fgf23

In a next step we investigated the effect of Tnfα blockade on *Fgf23* expression in PKD kidneys and plasma. We injected a single dose of 0.5 mg anti-Tnfα antibody or isotypic IgG control into 12 weeks old $Pkd1^{fl/fl}$, *cre+* and $Pkd1^{fl/fl}$, *cre-* mice. After 24 hours, anti-Tnfα treated animals had a significant reduction of plasma Tnfα levels compared to the IgG control treated animals (Figure 3.23 a). There was no difference in plasma Tnfα levels between IgG control treated $Pkd1^{fl/fl}$, *cre+* and $Pkd1^{fl/fl}$, *cre-* animals. In $Pkd1^{fl/fl}$, *cre+* animals, the reduction of plasma Tnfα was paralleled by a decrease in renal *Tnfα* and *Tgfβ* mRNA expression (Figure 3.23 b and c). Importantly, plasma Fgf23 levels were significantly decreased in anti-Tnfα treated $Pkd1^{fl/fl}$, *cre+* (215 $\pm$ 79 pg/ml) and $Pkd1^{fl/fl}$, *cre-* (177 $\pm$ 24 pg/ml) compared to IgG treated $Pkd1^{fl/fl}$, *cre+* (326 $\pm$ 71 pg/ml) and $Pkd1^{fl/fl}$, *cre-* animals (281 $\pm$ 32 pg/ml), respectively (Figure 3.23 d). Furthermore renal *Fgf23* as well as *Nurr1* mRNA expression in anti-Tnfα treated

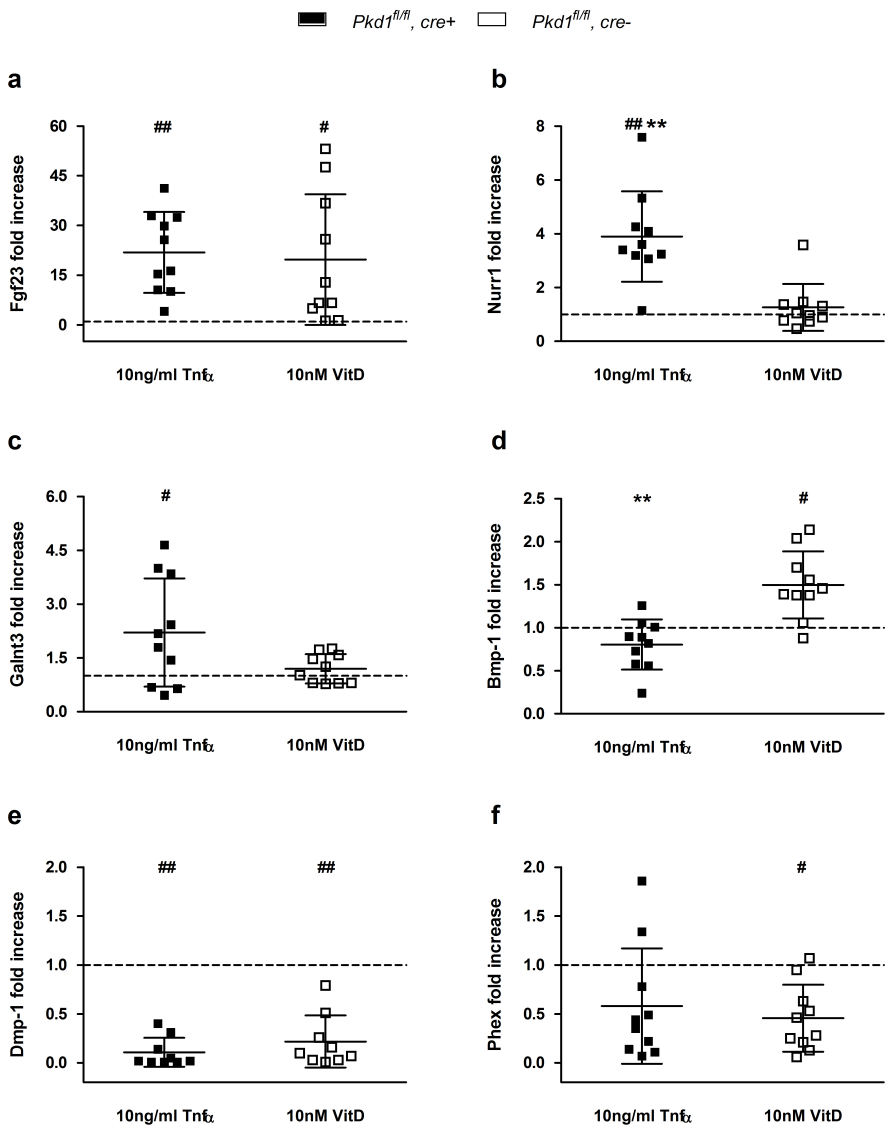

Figure 3.22: Regulation of *Fgf23* in Tnfα and 1,25(OH)$_2$ vitamin D$_3$ stimulated primary mouse osteocytes. Fold increase of *Fgf23* (a), *Nurr1* (b), *Galnt3* (c), *Bmp-1* (d), *Dmp-1* (e), and *Phex* (f) mRNA expression compared to 18S rRNA in primary mouse osteocytes treated with 10 ng/ml Tnfα (black squares) or 1,25(OH)$_2$ vitamin D$_3$ (white squares) for 24 hours (mean ±SD). Single experiments were normalized to their untreated control (dashed line = 1). Number of independent experiments 9-10; * $p<0.05$, ** $p<0.0001$ compared to 1,25(OH)$_2$ vitamin D$_3$ treated cells, # $p<0.05$, ## $p<0.0001$ compared to untreated cells.

Pkd1$^{fl/fl}$, *cre+* animals showed a trend to be suppressed by treatment (Figure 3.23 e and f).

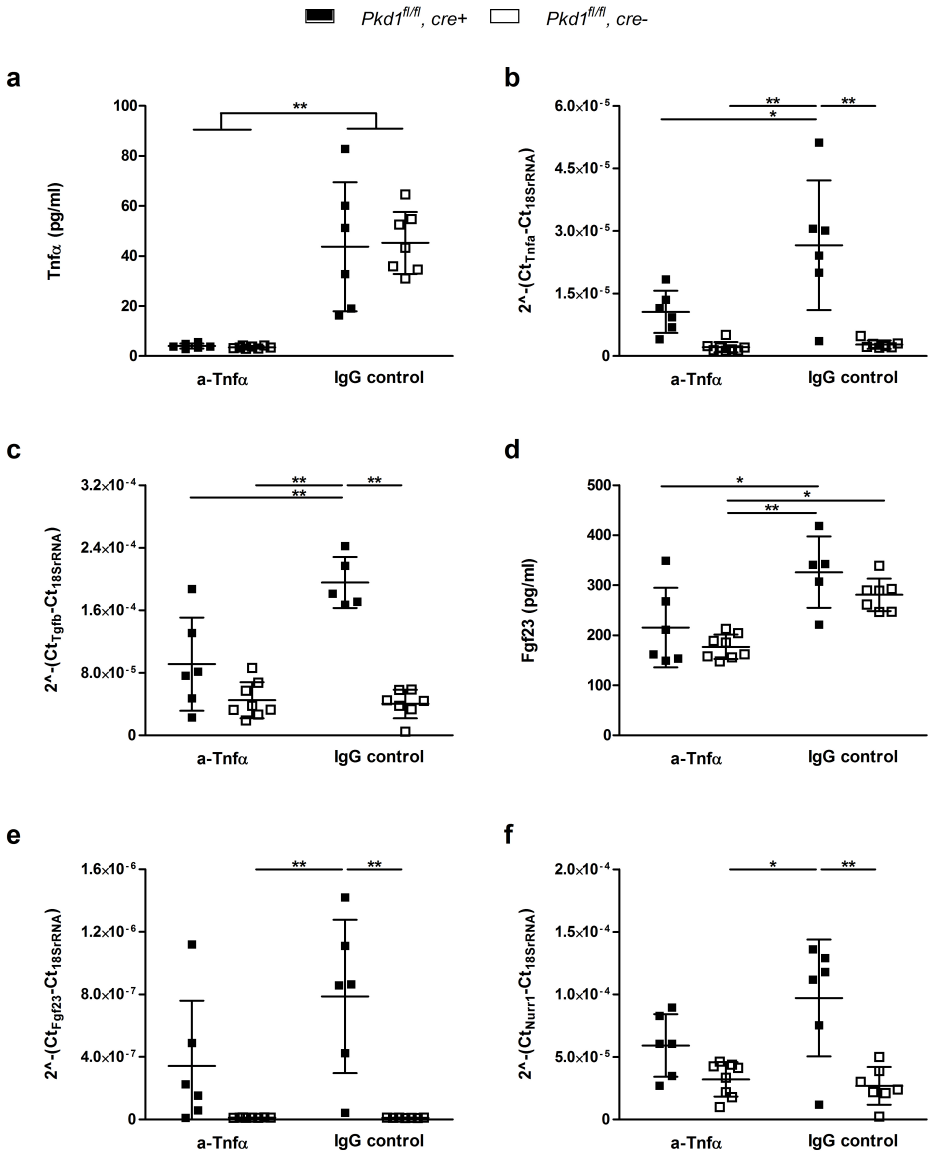

Figure 3.23: The effect of Tnfα neutralization on Fgf23 in *Pkd1* KO mice. Plasma Tnfα (a) and Fgf23 (d) levels as well as renal mRNA expression of *Tnfα* (b), *Tgfβ* (c), *Fgf23* (e), and *Nurr1* (f) 24 hours after injection of 0.5 mg anti-TNFα neutralizing antibody or isotypic IgG control, respectively, in *Pkd1*$^{fl/fl}$, *cre+* (black squares) and *Pkd1*$^{fl/fl}$, *cre-* (white squares) at the age of 12 weeks. Number of animals per group 5-8; * $p<0.05$, ** $p<0.0001$.

3.2.4 Discussion

This study provides new insights into the abnormal regulation of renal *Fgf23* expression in the *Pkd1* conditional KO mouse model and suggests that the proinflammatory cytokine Tnfα triggers renal Fgf23 expression in PKD kidneys and affects plasma Fgf23 levels.

The decrease of renal function in the course of CKD entails stepwise changes in mineral homeostasis [156, 157]. FGF23 rises very early in CKD disease and precedes changes in serum PTH and phosphate levels [157, 158]. In patients with end stage renal disease, serum FGF23 levels are associated with mortality independently of serum phosphate levels suggesting that FGF23 is an important disease modulator [166]. In *Col4a3*$^{-/-}$ KO mice, a CKD animal model, the changes of parameters of mineral homeostasis occur in the same chronology as in humans [160]. Interestingly, the early rise in plasma FGF23 is not accompanied by an increase in *Fgf23* expression in bone, the main site of Fgf23 production [160]. Similarly, our PKD animal model displayed elevated serum FGF23 levels while *Fgf23* expression in bone was unchanged. The cause for higher Fgf23 levels in CKD has remained enigmatic. Several factors such as increased production by bone as well as reduced clearance by the kidney may contribute [253–255]. We and others showed Fgf23 expression in kidneys from PKD and diabetic nephropathy animal models [227, 240]. Our data demonstrate that elevated plasma FGF23 levels in *Pkd1* conditional KO mice paralleled renal *Fgf23* expression as well as an increase in renal expression of typical bone marker genes such as *Runx2* and *Dmp-1*. Whether transformation of renal cells into the osteogenic lineage promotes or underlies Fgf23 expression in kidney remains to be established.

Renal inflammation and local hypoxia are common disease denominators in CKD [243–247, 256, 257]. In PKD, hypoxia is present in tissue sourrounding cysts [243, 244, 256]. Hypoxia increases *Fgf23* expression in UMR-106 rat osteosarcoma cells [139]. Further, C-terminal but not intact plasma FGF23 was increased in rats housed under hypobaric hypoxia conditions [139]. We cultured MC3T3-E1 cells, a mouse preosteoblast cell line as well as primary mouse osteoblasts for 24 and 48 hours in 0.2% hypoxia and we did not observe any stimulatory effect of hypoxia on *Fgf23* expression. On the contrary, hypoxia suppressed the stimulatory effect of 1,25$(OH)_2$ vitamin D_3 on *Fgf23* mRNA expression.

PKD kidneys are also affected by inflammation [245, 257] as confirmed by the increased renal *Tnfα* and *Tgfβ* expression NfκB subunit p65 phosphorylation in our model. Tnfα/NfκB may signal to increase *Nurr1* expression, an orphan nuclear receptor which is involved in the Pth dependent regulation of *Fgf23* expression in bone [133, 239]. We found that *Nurr1* expression was upregulated in PKD kidneys and is predominantly localized in the cell nu-

cleus whereas in wild type kidneys it is localized in the cytoplasm. Nuclear localization of Nurr1 often but not exclusively overlapped with renal Fgf23 protein expression. This finding suggests that Nurr1 may contribute to renal Fgf23 but other factors are likely to be involved.

Ito et al. (2015) showed that inflammatory markers such as Tnfα, IL-1β, and LPS increases *Fgf23* mRNA expression in the IDG-SW3 mouse osteocyte cell line in a dose and time dependent manner [147]. Similarly, we observed a Tnfα induced increase in *Fgf23* mRNA expression in primary mouse osteocytes which was comparable to the well investigated effect of 1,25$(OH)_2$ vitamin D_3 on *Fgf23* expression. However, Tnfα but not 1,25$(OH)_2$ vitamin D_3 increased *Nurr1* and *Galnt3* expression in primary osteocytes. This result suggests that Tnfα but not 1,25$(OH)_2$ vitamin D_3 may regulate *Fgf23* expression in a Nurr1 dependent manner. In addition, Tnfα may also modulate Fgf23 protein stability by regulating the expression of Galnt3. Galnt3 mediates the O-glycosylation of Fgf23 which makes the protein more resistant against proteolytic degradation [102]. In bone, C-terminal Dmp-1 binds with its acidic serine- and asparate-rich motif (ASARM) to the membrane protein Phex and this interaction inhibits *Fgf23* expression [125]. In primary osteocytes, *Phex* expression was decreased by 1,25$(OH)_2$ vitamin D_3 whereas *Dmp-1* expression was strongly decreased by Tnfα and 1,25$(OH)_2$ vitamin D_3. Therefore the upregulation of *Fgf23* expression by Tnfα and 1,25$(OH)_2$ vitamin D_3 is paralleled by the downregulation of its suppressors. The downregulation of *Phex* and *Dmp-1* by inflammatory markers was also observed in the IDG-SW3 cell line [147].

In patients with CKD, TNFα is increasing with ascending FGF23 quartiles and significantly correlates with FGF23 levels independent of renal function and measures of mineral metabolism [142]. A similar observation was made in non CKD stroke patients where markers of inflammation correlate with ascending FGF23 quartiles [143]. Furthermore diseases characterized by inflammation such as inflammatory bowel disease or osteoarthritis are linked to elevated serum FGF23 or increased *FGF23* gene expression levels, respectively [144, 145]. Inoculation of mice with LPS or bacteria leads to an increase in serum Fgf23 levels [149]. In the diabetic nephropathy rat model, renal *Fgf23* expression was reduced with ramipril, an ACE inhibitor [227]. Ramipril lowers blood pressure but additionally reduces inflammatory responses in patients with type 2 diabetes [258]. The

link between Tnfα and Fgf23 is further supported by the finding that the neutralization of Tnfα reduced renal *Tnfα* and *Tgfβ* expression in Pkd animals and concomitantly decreased plasma Fgf23 levels in both PKD diseased and wild type animals. In PKD animals, the decrease in plasma Fgf23 was more pronounced and accompanied by lower renal *Fgf23* and *Nurr1* expression. These results strongly suggest that the inflammatory cytokine Tnfα modulate Fgf23 expression.

In summary, we show that ectopic renal Fgf23 expression is triggered by the inflammatory cytokine Tnfα and that Tnfα neutralization decreases elevated plasma Fgf23 levels in PKD animals.

3.2.5 Methods

Animals

Pkd1 floxed/floxed (*Pkd1$^{fl/fl}$*) tamoxifen inducible *cre* mice were kindly provided by Gregory Germino [201, 202]. Cre recombinase expression is under the control of the β-actin promoter which drives high levels of expression in most tissues [202]. Male and female *Pkd1$^{fl/fl}$, cre+* and *Pkd1$^{fl/fl}$, cre-* mice were used. Cre recombinase activity was induced at postnatal days 15, 17, and 19 by injecting pups with 100 μl tamoxifen (2.5mg/ml) in corn oil causing slow onset disease [202]. Without further interventions, 24 hour urine was collected from 6 and 12 weeks old animals (e.g. 4 or 10 weeks after induction, respectively) which were thereafter sacrificed to collect plasma and organs. For Tnfα blockade, animals were treated at the age of 12 weeks with a single i.p. injection of 0.5mg *InVivo*MAb anti-Tnfα (Clone XT3.11, Lot4653-1/0413, BioXCell, USA) or *InVivo*MAb rat IgG1 (Clone HRPN, Lot 5339/1014, BioXCell, USA) [259, 260]. Twenty-four hours after antibody application, animals were sacrificed and plasma and organs were collected. All animal studies were performed according to protocols approved by the legal authority (Veterinary Office of the Canton of Zurich).

Plasma and urine analysis

Blood and 24 hours urine were collected from *Pkd1$^{fl/fl}$, cre+* and *Pkd1$^{fl/fl}$, cre-* mice at 6 and 12 weeks after birth. Briefly, *Pkd1$^{fl/fl}$, cre* mice were kept for three days in metabolic cages (Tecniplast, Italy) whereas the last day was used for 24 hours urine collection. Afterwards mice were anesthetized with isoflurane and blood was collected from

the heart. Plasma and urine aliquots were rapidly frozen and stored at -80°C until measurement. Urine and plasma laboratory analyses were performed on a UniCel DxC 800 Synchron (Beckman Coulter, Switzerland) by the Zurich Integrative Rodent Physiology (ZIRP) core facility.

The ratio of the maximum rate of tubular phosphate reabsorption to the glomerular filtration rate (TmP/GFR) was calculated as follows:

$TmP/GFR\ in\ mmol/L = P_P - [U_P \times P_{crea}/U_{crea}]$

where P_P, U_P, P_{crea} , and U_{crea} refer to the plasma and urinary concentration of phosphate and creatinine, respectively [230]. The plasma concentration of intact FGF23 (Kainos Laboratories, Japan or Immutopics International, USA), intact PTH (Immutopics International, USA) and Tnfα (Life Technologies Europe, Switzerland) were measured by enzyme-linked immunosorbent assays according to the manufacturers protocols.

Cell culture

All cell culture reagents were from Life Technologies Europe B.V. (Switzerland) unless stated otherwise. Two to four month old $Pkd1^{fl/fl}$, *cre* mice (4-6 per experiment) were sacrificed with carbon dioxide. Tibias and femurs from the hindlegs were harvested. The epiphyses were cut and bones were flashed with Hank's Balanced Salt Solution (HBSS) containing 1% penicillin streptomycin (Pen Strep) to remove the bone marrow. Bones were cut into small pieces of 1-2 mm^2. Bone cell extraction was performed according established protocols [249, 250]. Briefly, small bone pieces were repeatedly digested with either a solution containing 2 mg/ml collagenase type II, 0.05% (w/v) soyabean trypsin inhibitor (Sigma-Aldrich, Switzerland), 20 mM HEPES, 1% Pen Strep in HBSS or 10 nM EDTA, 1% fetal bovin serum (FBS), 1% Pen Strep in phosphate buffered saline (PBS) for 25min at 37^{circ}C. Cells from digestion steps 6-9 or cells and bone pieces from digestion step >9 were cultured for 2 weeks in an osteogenic medium (minimal essential medium α (memα) containing 10% FBS, 1% Pen Strep, 50 μg/ml 2-phospho-L-ascorbic acid trisodium salt (Sigma-Aldrich, Switzerland), and 1mM β-glycerophosphate (Sigma-Aldrich, Switzerland)). After 2 weeks, cells were supplemented for 24 hours with either 10 nM 1,25 $(OH)_2$ vitamin D_3 (CaymanChemical, USA) or 10 ng/ml mouse Tnfα (R&D Systems, USA) and total mRNA was extracted.

MC3T3-E1 subclone 4 preostoblast cells (CRL-2593, Lot 59899932, ATCC France) passage 17/4 were expanded for 4-5 days with memα medium supplemented with 10% FBS and 1% PenStrep. After reaching 80-90% confluence, MC3T3-E1 cells were trypsinized and plated in collagen coated 6 well plates (80'000 cells/well). Medium was changed to osteogenic differentiation medium (memα supplemented with 10% FBS, 1% PenStrep, 50 μg/ml 2-Phospho-L-ascorbic acid trisodium salt (Sigma-Aldrich, Switzerland), and 1 mM beta glycerophosphate (Sigma-Aldrich, Switzerland)). After 2 weeks differentiation along the osteogenic lineage cells were supplemented for 24 or 48 hours with either 10 nM 1,25 $(OH)_2$ vitamin D_3 (CaymanChemical, USA) or an equal amount of EtOH and incubated for 24 or 48 hours under hypoxic (0.2% O_2) or normoxic conditions.

RNA extraction and RT-PCR

Organs were harvested at week 6 and 12 and were rapidly frozen in liquid nitrogen. Tissues were homogenized using either a Precellys homogenizer or a liquid nitrogen cooled mortar and pestle (bone). Total mRNA from bone as well as from cultured cells was extracted with TRIzol (Life Technologies Europe B.V., Switzerland) followed by purification with RNeasy Mini Kit (Qiagen, Switzerland) according to the manufacturers protocol. Total mRNA from kidney was extracted with RNeasy Mini Kit (Qiagen, Switzerland) according to the manufacturers protocol. DNAse digestion was performed using the RNase-free DNAase Set (Qiagen, Switzerland). Total RNA extractions were analyzed for quality, purity, and concentration using the NanoDrop ND-1000 spectrophotometer (Wilmington, Germany). RNA samples were diluted to a final concentration of 100 ng/μl and cDNA was prepared using the TaqMan Reverse Transcriptase Reagent Kit (Applied Biosystems, Roche, Foster City, CA). In brief, in a reaction volume of 40 μl, 300 ng of RNA was used as template and mixed with the following final concentrations of RT buffer (1x): $MgCl_2$ (5.5 mmol/l), random hexamers (2.5 μmol/l), dNTP mix (500 μmol/l each), RNase inhibitor (0.4 U/μl), multiscribe reverse transcriptase (1.25 U/μl), and RNAse-free water. Reverse transcription was performed with thermocycling conditions set at 25°C for 10 min, 48°C for 30 min, and 95°C for 5 min on a thermocycler (Biometra, Germany). Quantitative realtime PCR (RT-PCR) was performed on the ABI PRISM 7700 Sequence Detection System (Applied Biosystems). Primers for genes of interest were designed using Primer

3 software [242, 261]. Primers were chosen to span intron - exon boundaries to exclude genomic DNA contamination. The specificity of all primers was tested and always resulted in a single product of the expected size (data not shown). Probes were labeled with the reporter dye FAM at the 5'-end and the quencher dye TAMRA at the 3'-end (Microsynth, Switzerland). RT-PCR reactions were performed using the KAPA PROBE FAST RT-PCR Kit (KappaBiosystems, USA).

Protein extraction and Western blot analysis

Organs were rapidly frozen in liquid nitrogen. Tissues were homogenized in a homogenization buffer containing 0.27 M sucrose, 2 mM EDTA (pH8), 0.5% NP-40, 60 mM KCl, 15 mM NaCl, 15 mM HEPES (pH 7.5) (all Sigma-Aldrich, Switzerland) and cOmplete protease inhibitor cocktail (Roche, Switzerland) using a Precellys homogenizer. Nuclear proteins were separated by a sucrose cushion and resuspended in a nuclei extraction buffer containing 20 mM HEPES (pH 7.5), 400 mM NaCl, 1 mM EDTA (pH 8), 1 mM DTT and 1 mM PMSF (all Sigma-Aldrich, Switzerland). After measurement of protein concentration (Bio-Rad, Hercules, CA, USA), 60 μg of nuclear proteins were solubilized in loading buffer containing DTT and separated on a 10% polyacrylamide gel. For immunoblotting, proteins were transferred electrophoretically to polyvinylidene fluoride membranes (Immobilon-P, Millipore, Bedford, MA, USA). After blocking with 5% milk powder in Tris-buffered saline/0.1% Tween-20 or 5% bovine serum albumin (BSA) in Tris-buffered saline/0.1% Tween-20 for 60 min, blots were incubated with the primary antibodies: mouse monoclonal anti-Phospho-NFκB p65 (Ser536)(7F1) (Cell Signaling Technology, USA; 1:1000) or rabbit monoclonal NFκB p65 (D14E12) (Cell Signaling Technology, USA; 1:1000) either for 2 h at room temperature or overnight at 4°C. Membranes were then incubated for 1 h at room temperature with secondary goat anti-rabbit or donkey anti-mouse antibodies (1:5000) linked to alkaline phosphatase (Promega, USA) or HRP (Amersham, MA, USA or R&D Systems, USA). The protein signal was detected with the appropriate substrates using the DIANA III-chemiluminescence detection system (Raytest, Straubenhardt, Germany). All images were analyzed using the software Advanced Image Data Analyser AIDA, Raytest to calculate the ratio between phosphorylated protein to total protein.

Immunofluorescence staining

Mouse kidneys were perfused in situ through the left heart ventricle with a fixative solution containing 3% paraformaldehyde in phosphate buffered saline (PBS). Kidneys were embedded in TissueTec and frozen in liquid nitrogen. Five μm cryosections were cut. Slides were rehydreated with PBS, treated for 5 min with 0.5% SDS in PBS followed by 10 min treatment with 0.5% Triton-X-100 in PBS (Sigma-Aldrich, Switzerland). Unspecific sites were blocked with 1% bovine serum albumin (BSA) in PBS for 1 h at room temperature. Primary antibodies were diluted in 1% BSA in PBS (rat anti-FGF23 clone #283507 (R&D Systems, USA) 1:1000; rabbit anti-Nurr1 N-20 sc-991 (Santa-Cruz, USA) 1:200) and kidney sections were incubated with the primary antibody overnight at 4°C. After washing with PBS, sections were incubated with the corresponding secondary antibody (1:500) (anti-rabbit DyLight 594 (Jackson ImmunoResearch, Europe), anti-rat NL493 (R&D Systems, USA)), and DAPI (Life Technologies Europe B.V., Switzerland, 1:1000) for 1 h at room temperature. Slides were washed twice with PBS before they were mounted with Dako glycergel mounting medium (Dako, Switzerland). Sections were visualized on a Leica DM 5500B fluorescence microscope and images processed with ImageJ.

Statistical analysis

Statistics were performed using unpaired Student‘s t-test or ANOVA (GraphPad Prism version 5.0, GraphPad, San Diego, CA). Data are provided as mean ± SD. $P < 0.05$ was considered significant.

3.2.6 Disclosure

All authors declared no competing interests.

3.2.7 Acknowledgments

This study was supported by grants from the the Swiss National Center for Competence in Research NCCR Kidney.CH and the Novartis Foundation for medical-biological research to C. A. Wagner. The use of the ZIRP Core facility for Rodent Physiology is gratefully acknowledged.

3.2.8 Supplementary Data

Supplementary Figures

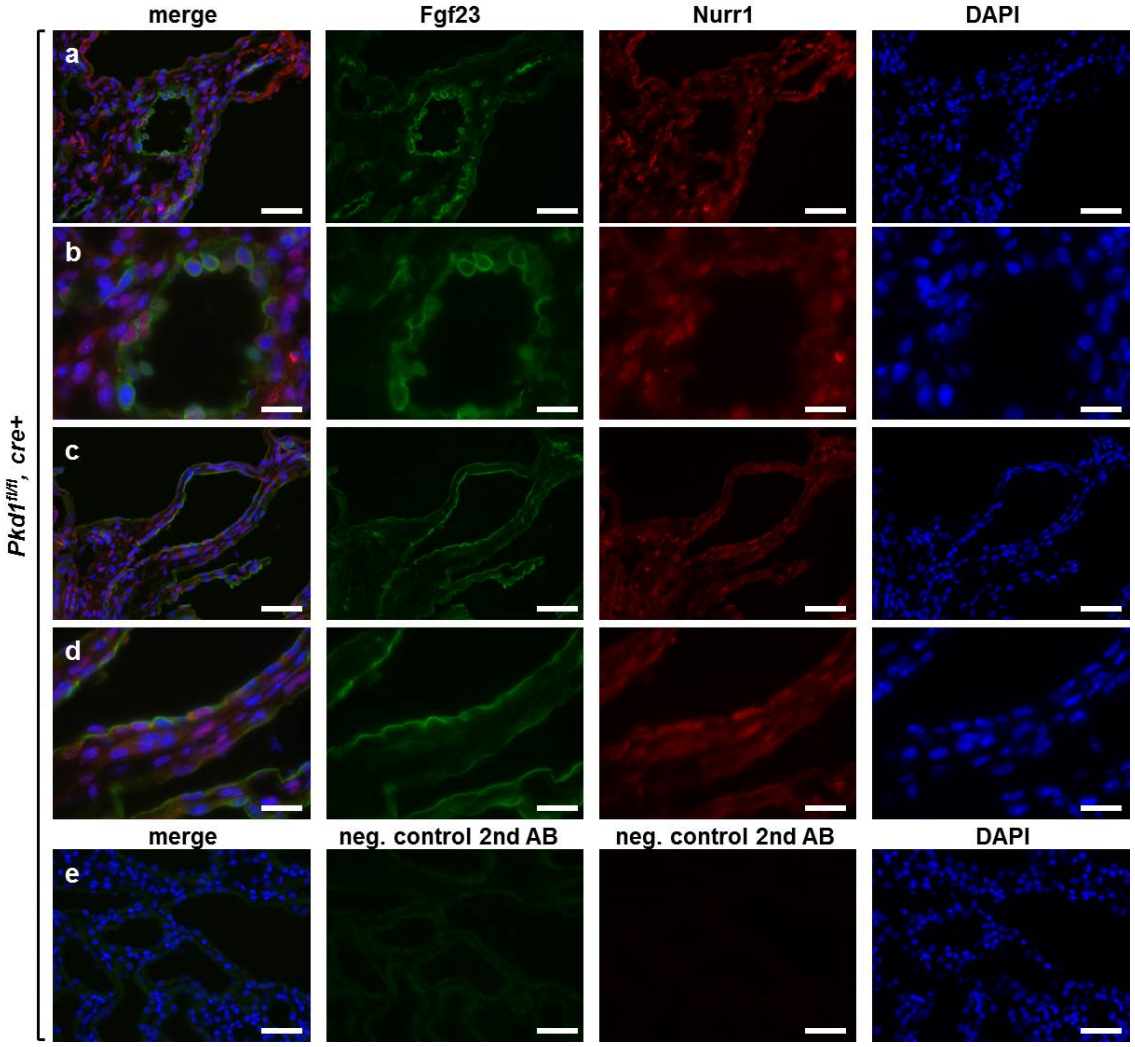

Figure 3.24: Nurr1 staining in kidneys from *Pkd1*$^{fl/fl}$, *cre+* mice. Immunofluorescense staining for FGF23 (green), Nurr1 (red), and DAPI (blue, cell nuclei) merged and single channels: (a-d) kidneys from 12 weeks old *Pkd1*$^{fl/fl}$, *cre+* mice, (e) kidneys from 12 weeks old *Pkd1*$^{fl/fl}$, *cre+* mice incubated with secondary antibodies alone. Original magnification (a, c, e) 400x (scale bar 50 μm) and (b, d) 1000x (scale bar 20 μm).

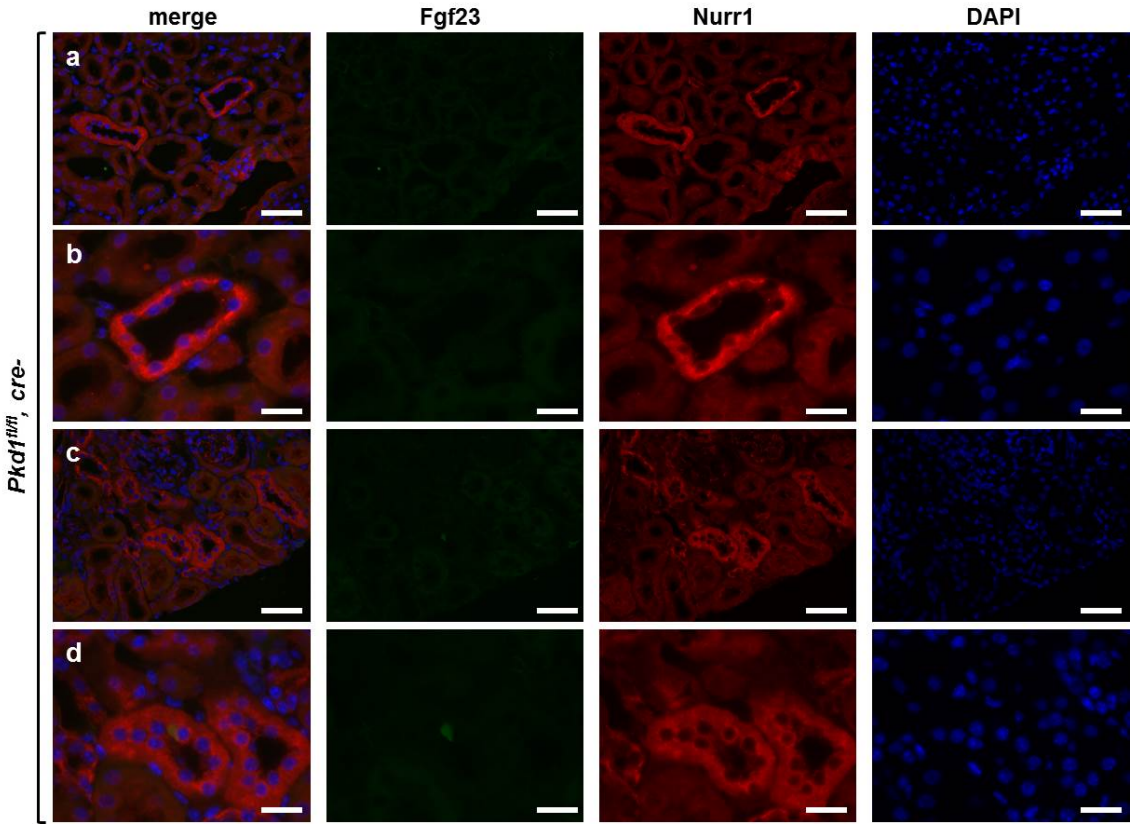

Figure 3.25: Nurr1 staining in kidneys from *Pkd1*$^{fl/fl}$, *cre-* mice. Immunofluorescense staining for FGF23 (green), Nurr1 (red), and DAPI (blue, cell nuclei) merged and single channels: (a-d) kidneys from 12 weeks old *Pkd1*$^{fl/fl}$, *cre-* mice, (e) kidney from 12 weeks old *Pkd1*$^{fl/fl}$, *cre+* mice incubated with secondary antibodies alone. Original magnification (a, c) 400x (scale bar 50 μm) and (b, d) 1000x (scale bar 20 μm).

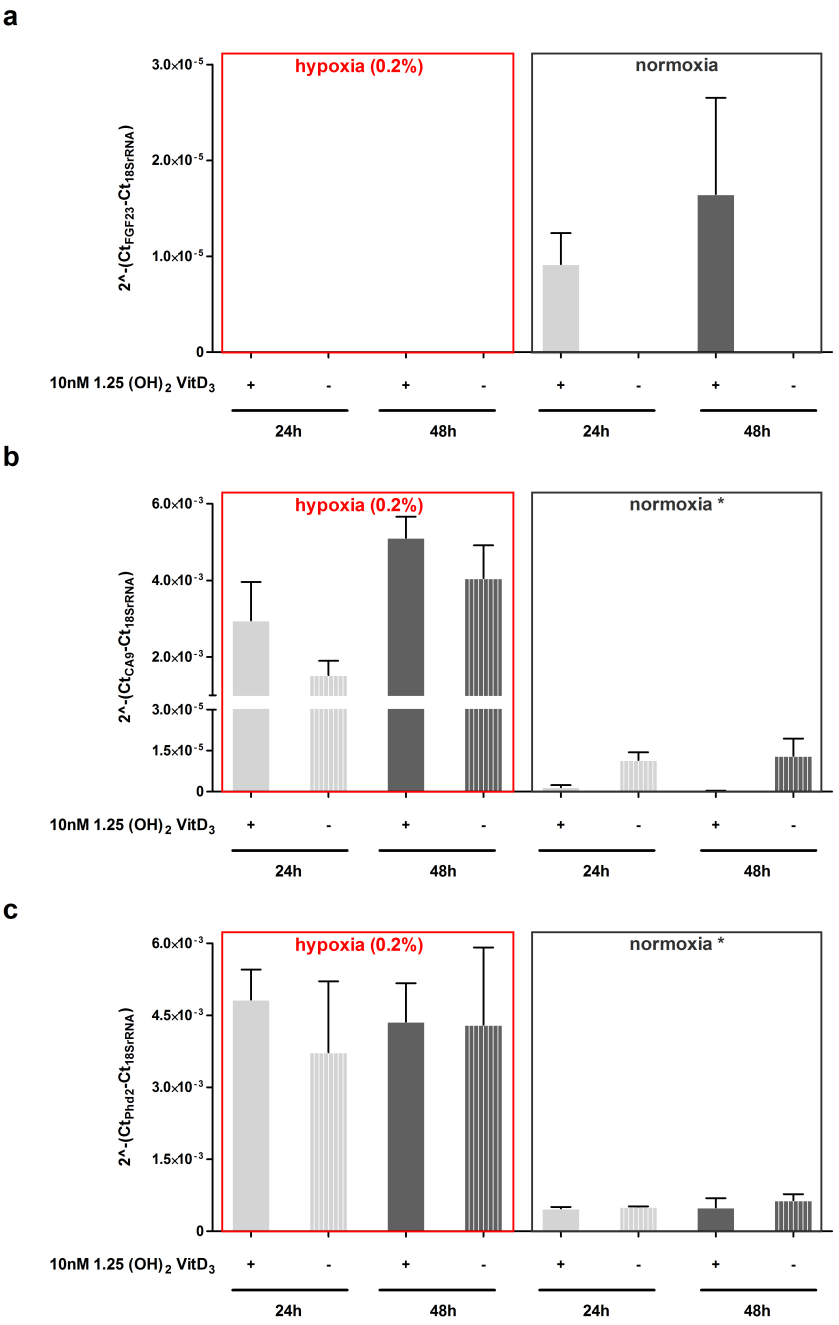

Figure 3.26: 1,25 $(OH)_2$ vitamin D_3 dependent *Fgf23* expression in MC3T3-E1 cells under normoxic and hypoxic conditions. MC3T3-E1 cells were differentiated for two weeks along the osteogenic lineage. Subsequently, cells were supplemented for 24 or 48 hours with 10nM 1,25 $(OH)_2$ vitamin D_3 and incubated in hypoxic (0.2% oxygen) or normoxic conditions. Relative *Fgf23* (a), *Ca9* (b), *Phd2* (c) mRNA expression. Mean ± SD; n=3; * $p<0.05$

Table 3.2: Primer and probe sequences used for RT-PCR

Gene	**Type**	**Sequence**
Mouse Pkd1	Fwd	5'-GGCCAACCTCTCCTCAGTATC-3'
	Rev	5'-GAAGGGTACTGCTGCCACA-3'
	Probe	5'-CTGTGGTGAGGAATATGTCGCCTGC-3'
Mouse Fgf23	Fwd	5'-TCGAAGGTTCCTTTGTATGGAT-3'
	Rev	5'-AGTGATGCTTCTGCGACAAGT-3'
	Probe	5'-TTTTTGGATCGCTTCACT-3'
Mouse Fgf23	Fwd	5'-GTATGGATCTCCACGGCAAC-3'
	Rev	5' AGTGATGCTTCTGCGACAAGT-3'
	Probe	5'-TTTTTGGATCGCTTCACTTCAGCCC-3'
Mouse Galnt3	Fwd	5'-GAGAAAGAGCGAGGGGAAAC-3'
	Rev	5'-GTGGACCATGCTTCATTGTG-3'
	Probe	5'-ACACCCGACCACCTGAATGTATTGAAC-3'
Mouse Phex	Fwd	5'-GCTGCCAGAGAACAAGTGC-3'
	Rev	5'-TCCTCAGCTATGCCAGGAAG-3'
	Probe	5'-CAGTCCTCCACAATTTAGGGTCAATGGTG-3'
Mouse Bmp-1	Fwd	5'-ACAGCAAACAGCCCGAAG-3'
	Rev	5'-TCCAATCACAAACGGGATG-3'
	Probe	5'-CCATCCATCAAAGCTGCAGGAAACTC-3'
Mouse Dmp-1	Fwd	5'-TCTCCCAGTTGCCAGATACC-3'
	Rev	5'-TCTCCAGATTCACTGCTGTCC-3'
	Probe	5'-CTCTGAAGAGAGGACGGGTGATTTGG-3'
Mouse Runx2	Fwd	5'-CCCTGAACTCTGCACCAAGT-3'
	Rev	5'-AGTGGATGGATGGGGATGT-3'
	Probe	5'-TCAGATTACAGATCCCAGGCAGGCA-3'
Mouse Nurr1	Fwd	5'-CATCGACATTTCTGCCTTCTC-3'
	Rev	5'-CTTCCACTCTCTTGGGTTCCT-3'
	Probe	5'-TGCCCTGGCTATGGTCACAGAGAGA-3'
Mouse Tnfα	Fwd	5'-CAGACCCTCACACTCAGATCATCT-3'
	Rev	5'-CCTCCACTTGGTGGTTTGCT-3'
	Probe	5'-ATTCGAGTGACAAGCCTGTAGCCCACGT-3'
Mouse Tgfβ	Fwd	5'-AGAGGTCACCCGCGTGCTA-3'
	Rev	5'-GCTTCCCGAATGTCTGACGTA-3'
	Probe	5'-ACCGCAACAACGCCATCTATGAGAAAACC-3'
Mouse Ca9	Fwd	5'-GCACCTCAGTACTGCTTTCTCC-3'
	Rev	5'-TTCCTCCGAGATTTCTTCCA-3'
	Probe	5'-CCTTTCTGCAGGAGAGCCCAGAAGA-3'
Mouse Phd2	Fwd	5'-TGGGCAACTACAGGATAAACG-3'
	Rev	5'-TGTCACGCATCTTCCATCTC-3'
	Probe	5'-CGAAAGCCATGGTTGCTTGTTACCC-3'

3.3 Publications that did not contribute to this thesis

1. Aldosterone-sensitive NFκB-dependent Orai1 expression in the regulation of FGF23 release.
   Zhang B, Yan J, Umbach AT, Fakhri H, Fajol A, Schmidt S, Salker MS, Chen H, Alexander D, **Spichtig D**, Daryadel A, Wagner CA, Föller M, Lang F.
   J Mol Med, Revision under consideration.

2. Targeting of sodium-glucose cotransporters with phlorizin inhibits polycystic kidney disease progression in Han:SPRD rats.
   Wang X, Zhang S, Liu Y, **Spichtig D**, Kapoor S, Koepsell H, Mohebbi N, Segerer S, Serra AL, Rodriguez D, Devuyst O, Mei C, Wüthrich RP.
   Kidney Int. 2013 Nov;84(5):962-8. doi: 10.1038/ki.2013.199. Epub 2013 May 29. PMID: 23715121

3. Secreted Klotho and FGF23 in chronic kidney disease Stage 1 to 5: a sequence suggested from a cross-sectional study.
   Pavik I, Jaeger P, Ebner L, Wagner CA, Petzold K, **Spichtig D**, Poster D, Wüthrich RP, Russmann S, Serra AL.
   Nephrol Dial Transplant. 2013 Feb;28(2):352-9. doi: 10.1093/ndt/gfs460. Epub 2012 Nov 4. PMID: 23129826

Chapter 4

Discussion

Phosphate is needed for various biological processes such as energy production, cell signaling, mineralization of the endoskeleton as well as membrane and protein synthesis [1–6]. To fulfill its biological actions, serum phosphate levels have to be kept in a narrow range to prevent the body from adverse events due to deficiency or excess. Fgf23, Pth, $1,25(OH)_2$ vitamin D_3, and soluble Klotho build a tight endocrine network with multiple negative feedback loops to control serum phosphate levels by regulating its intestinal absorption, renal excretion and bone turnover (Figure 1.3) [18–20, 46]. In this context the hormonal regulation of phosphate reabsorption by the kidney plays a key role in the maintenance of serum phosphate levels. Both, Fgf23 and Pth lower serum phosphate concentrations by decreasing the abundance of sodium phosphate co-transporters NaPi-IIa and NaPi-IIc in the brush border membrane of proximal tubules in the kidney [41, 44, 49, 83]. $1,25(OH)_2$ vitamin D_3 increases *Fgf23* expression in bone and decreases *Pth* expression in the parathyroid gland both in a VDR dependent manner [58, 63, 77, 128]. In the intestine, $1,25(OH)_2$ vitamin D_3 stimulates dietary phosphate reabsorption [47]. This leads to an overall increase in serum phosphate levels by $1,25(OH)_2$ vitamin D_3. In return, Fgf23 inhibits the synthesis of $1,25(OH)_2$ vitamin D_3 in the kidney by downregulation of *Cyp27b1* and promotes the degradation of $1,25(OH)_2$ vitamin D_3 by upregulation of *Cyp24a1* [77, 79]. Pth stimulates $1,25(OH)_2$ vitamin D_3 production independent of serum Fgf23 levels and increases *Fgf23* expression in bone [51, 52, 129]. In a negative feedback loop, Fgf23 inhibits Pth expression and secretion in the parathyroid gland [91]. The function of soluble Klotho is not yet completely understood. On one hand administration of anti-Klotho antibodies increases Fgf23 levels suggesting that Fgf23 expression is suppressed by Klotho and on the other hand *in*

vivo overexpression of circulating Klotho leads to an increase in *Fgf23* expression in bone [69, 141]. Taken all together, Fgf23 and Pth lower serum phosphate concentrations while 1,25$(OH)_2$ vitamin D_3 is doing the opposite. Thereby these hormones regulate each other in multiple negative feedback loops and imbalance of the hormonal network due to disease or congenital disorders leads to severe disturbances of phosphate homeostasis. Exactly this can be observed in CKD where the decrease of renal function is entailed by stepwise changes in mineral homeostasis (see Figure 1.7) [156, 157]. The changes of mineral homeostasis in CKD start with a gradual decline of plasma and urine concentrations of soluble Klotho [46, 158, 159]. Subsequently, FGF23 plasma levels increase in CKD stage G2 to G3a which suppress in the kidney 1,25$(OH)_2$ vitamin D_3 synthesis and increase its degradation [157]. The decrease in 1,25$(OH)_2$ vitamin D_3 levels and resistance to FGF23 initiate the pathogenesis of secondary hyperparathyroidism [156, 157]. Plasma PTH levels increase in CKD stage G3b to G4 and therefore occurs later in the course of CKD compared to the rise in plasma FGF23 [157]. Serum phosphate decreases in an initial phase in consequence of high FGF23 levels [157]. In a second phase when eGFR drops below 59.1ml/min per 1.73 m^2 phosphate levels gradually increase and patients with advanced CKD suffer from hyperphosphatemia [156, 157]. Both, elevated FGF23 and phosphate levels contribute to the higher mortality risk in ESRD [155, 166].

ADPKD is a monogenetic disorder which is characterized by bilateral kidney enlargement where functional renal tissue is progressively replaced by growing cysts [171, 177]. ADPKD is a cause for CKD and the progression of the disease leads to ESRD [151]. Genetic testing and imaging methods allow ADPKD diagnosis before a detectable decline in renal function occurs for which reason ADPKD is a useful model to study the entire evolution of CKD and the concomitant changes in mineral homeostasis [189]. Pavik et al. (2011) found that ADPKD patients with a nearly preserved renal function (CKD stage G1 and G2) have 4-fold increased FGF23 levels compared to non-diabetic patients and patients with diabetes mellitus type 2 and a similar CKD stage [184]. At the same time, plasma 1,25$(OH)_2$ vitamin D_3 and PTH levels were normal in all CKD patients [184]. Within the ADPKD study group, only those with normal soluble Klotho levels showed a mild decrease in plasma phosphate concentration whereas the majority of ADPKD patients had low serum Klotho levels [184, 185]. Administration of anti-Klotho antibodies in mice leads to an increase

in plasma Fgf23 levels [69]. In a translational approach, the reduction of soluble Klotho would explain the early increase in serum FGF23 levels in ADPKD patients. However, the early rise in plasma FGF23 levels is a specific manifestation for ADPKD and cannot be explained by decrease in renal function as this patients have a preserved eGFR [184]. The goal of the first study was to examine the role of high FGF23 in ADPKD rodent models such as Han:SPRD rats and *Pkd1* conditional KO mice and to analyze the mechanisms which may contribute to the early and excessive elevation of FGF23 in ADPKD.

4.1 PKD animal models

The Han:SPRD *cy/+* rat is a well-established PKD animal model with a spontaneous mutation in the *Pkdr1* gene which encodes the SamCystein protein [216, 217]. Homozygous Han:SPRD *cy/cy* rats have a rapid cyst development and die from renal failure within a month after birth [218]. Heterozygous Han:SPRD *cy/+* rats have little tubular changes after 4 weeks thereafter cyst development progresses so that after 8 weeks significant cyst formation can be observed [218]. Most of the cysts can be localized to proximal tubules in the inner cortex [218]. Despite the cyst growth heterozygous animals survive more than a year [218]. The Han:SPRD *cy/+* rat model has been widely used for examining mechanisms and therapies for ADPKD [220–223]. The aim of this study was to investigate Fgf23 metabolism at an early time point of the disease and therefore we analyzed animals between 2 and 8 weeks of age.

The *Pkd1* KO mouse model is the orthologue model for human ADPKD disease. Unfortunately, homozygous *Pkd1* KO animals develop edema as well as renal cysts in an embryonic state and die already in utero whereas heterozygous *Pkd1* mice rarely develop cystic kidneys before 6 months [198–200]. To bypass these problems Piontek et al. (2004) developed the *Pkd1* conditional KO mouse model [201]. In this mouse model, *Pkd1* exons 2 to 4 are flanked by unidirectional loxP sites which can be excised by *Cre* recombinase [201]. This leads to a complete *Pkd1* null allele and renal cyst formation [201]. In this study we used the $Pkd1^{fl/fl}$ mouse carrying a tamoxifen inducible Cre recombinase driven by the beta-actin promoter. The time point of *Pkd1* inactivation defines the kinetics of kidney cyst formation and an induction until day 12 post partum results in severe cystic disease within 3 weeks whereas an induction after day 14 results in a late onset cystic dis-

ease where cysts appear after 3 month and become severe after 6 month [202, 203]. Since we wanted to investigate the sequential hormonal changes observed in CKD, we decided for a late induction of Cre recombinase at postnatal days 15, 17 and 19. With our protocol we observed slightly different cyst growth kinetics as reported by Piontek et al. (2007) [202]. *Pkd1*$^{fl/fl}$, *cre+* animals had no considerable tubular changes after 6 weeks and the two kidney per body weight ratio was similar to wild type animals. Within the next four weeks *Pkd1*$^{fl/fl}$, *cre+* animals suffered from severe cyst growth and at week 10 the two kidney per body weight ratio was twice as high as at week 6. At this time point kidney cysts could be easily seen by eye. After 12 weeks, kidneys of *Pkd1*$^{fl/fl}$, *cre+* animals were massively cystic and the two kidney per body weight ratio doubled once more compared to animals at 10 weeks. We used the same tamoxifen concentration as Piontek et al. (2007) but injected it three times directly to the pups whereas Piontek et al. (2007) did it once to the nursing mother. Therefore we suggest that cyst growth kinetics depends not only on the developmental switch at day 12 but also from the overall tamoxifen dose given to the PKD animals. Nevertheless, regardless of the protocol, Cre recombinase induction after day 14 results in a slow disease progression model which is ideal to study the sequential hormonal changes observed in CKD.

4.2 FGF23 metabolism in PKD animals

We observed a 10-fold increase in plasma Fgf23 levels in Han:SPRD *cy/+* rats at week 4 which was accompanied by a 2-fold increase in plasma Pth and normal 1,25$(OH)_2$ vitamin D_3 levels. The progressive cyst growth leads to a decline in renal function which starts in Han:SPRD *cy/+* rats at week 8 [218]. This was consistent with our observation that plasma creatinine and urea concentrations were similar after 4 weeks but started to increase after 6 weeks and further rose at 8 weeks. This implies that the increase in plasma Fgf23 levels occured at a time point when renal function was still near normal. Similarly, in *Pkd1* conditional KO animals we observed elevated plasma Fgf23 and unchanged Pth levels whereas creatinine clearance was normal. Hence, our PKD animal models accurately reproduces the observed increase of FGF23 levels in the early disease course of human ADPKD and allows to approach the underlying mechanisms in more detail.

The physiological function of FGF23 is to lower phosphate levels by decreasing the abun-

dance of sodium phosphate co-transporters at the brush border membrane of proximal tubules in the kidney as well as to inhibit 1,25$(OH)_2$ vitamin D_3 synthesis [61, 65, 77–79]. Elevated FGF23 levels in human caused by gain of function mutations in *FGF23* or excessive secretion of FGF23 in the context of tumor-induced osteomalcia are accompanied by hypophosphatemia, urinary phosphate wasting and low 1,25$(OH)_2$ vitamin D_3 levels [61, 100]. Administration of single dose recombinant Fgf23 in mice leads to a decrease in serum phosphate and 1,25$(OH)_2$ vitamin D_3 levels and to an increase in the fractional excretion of phosphate [64, 77]. Despite the high plasma Fgf23 levels in Han:SPRD *cy/+* rats and *Pkd1* conditional KO mice, plasma phosphate levels as well as TmP/GFR were normal over the entire study period. In Han:SPRD *cy/+* rats, expression and activity of sodium phosphate co-transporters was normal. The majority of cysts in Han:SPRD *cy/+* rats originate from the proximal tubule and display varying degrees of proximal tubular brush border membrane degradation and transition zones from intact brush border membrane to dedifferentiated epithelial cells [218]. Cysts with intact brush border membrane had normal NaPi-IIa protein expression whereas in the same cysts in dedifferentiated epithelial cells NaPi-IIa protein was missing. Furthermore, Han:SPRD *cy/+* rats had no change in vitamin D_3 metabolism. There were neither changes in 1,25$(OH)_2$ vitamin D_3 plasma levels nor in the expression of *Cyp27b1* and *Cyp24a1*. These findings went along with the observation in human ADPKD patients where against expectations, only a small fraction of ADPKD patients with normal renal function and elevated serum FGF23 levels was affected by a renal leak of phosphate and mild hypophosphatemia whereas most of them had a normal renal phosphate handling [184]. Ascending FGF23 quartiles are associated with left ventricular hypertrophy in human CKD patients [225]. In mice, repeatedly intravenous injections of Fgf23 increase the heart weight per tibia length ratio and leads to a thickening of the left ventricular heart wall [225]. The heart does not express Klotho, the obligate co-ligand for Fgf23 signaling therefore Fgf23 exerts its effect in a calcineurin dependent pathway [225]. Despite high Fgf23 levels non of our PKD animal models had a change in heart weight per tibia length ratio suggesting either that Fgf23 requires longer time periods, stronger elevation or that the heart is resistant to high Fgf23 levels. Taken together, PKD animals as well as human ADPKD patients with normal kidney function show resistance against highly elevated FGF23 levels. However, the temporal sequence of

rising FGF23 in PKD and the mechanisms underlying resistance to the biological actions of FGF23 remained at this point unclear.

To further investigate the underlying mechanism of Fgf23 resistance in PKD animals we analyzed the Fgf23 signaling cascade in the kidney. Fgf23 binds in the kidney to the Fgfr-Klotho receptor complex which leads to the dimerization and cross-phosphorylation of Fgfr tyrosine kinase domains and activates among others the downstream signaling molecule FRS2α (Figure 1.5) [69]. Fgf23 binds to the Fgfr isoforms Fgfr1c, Fgfr3c, and Fgfr4 but it has been shown that in the kidney Fgfr1 displays a key function in mediating Fgf23 dependent phosphaturia [84–87]. Fgf23 transgenic mice have no changes in *Fgfr* expression levels in the kidney but rather resist increased Fgf23 signaling by the downregulation of *Klotho* expression [226]. We found that elevated plasma Fgf23 levels in Han:SPRD *cy/+* rats had no effect on *Fgfr1* expression in the kidney. We detected lower renal *Klotho* gene expression levels in PKD animals but at the protein level Klotho abundance was unchanged. In Han:SPRD *cy/+* rat kidney, phosphorylation of the downstream molecule FRS2α was increased suggesting that Fgf23 signaling can be activated but may be blocked further downstream.

Han:SPRD *cy/+* rats had higher plasma Pth levels than control rats which is in contrast to ADPKD patients with normal renal function [184]. This divergence is also observed in other CKD rat models where Fgf23 and Pth rise at the same time point in contrast to human CKD patients where FGF23 rises before PTH in the course of CKD [157, 161]. CKD rat models have a relative fast disease progression which reduces the temporal resolution of hormonal changes in the course of CKD. Therefore shorter measurement intervals or animals with slower disease progression may overcome this gap. Fgf23 decreases Pth expression and secretion by the parathyroid gland in a Klotho dependent as well as in calcineurin dependent pathway [91, 93, 97]. Loss of Klotho might be partially involved in induction of Fgf23 resistances in the parathyroid gland and the concomitant increase in Pth levels.

We further addressed the question what causes elevated plasma Fgf23 levels and took either increased expression or decreased degradation into consideration. Screening for *Fgf23* expression in bone, spleen, kidney, heart, and liver revealed bone, as the major source of *Fgf23* expression whereas small amounts were expressed in spleen [61, 62, 65].

Unexpectedly we detected Fgf23 mRNA and protein expression in the kidneys of PKD animals more precisely in the cells lining the cysts. In the mouse and rat PKD model, *Fgf23* expression was increased in PKD kidneys whereas expression in bone and spleen was similar to control animals suggesting that the kidney may contribute to elevated plasma Fgf23 levels. Similarly, renal Fgf23 expression was reported in a diabetic nephropathy rat model [227]. Fam20c protein phosphorylates Fgf23 which inhibits O-glycosylation and leads to the degradation and inactivation of Fgf23 [108, 114]. We observed neither in bone nor in kidneys of Han:SPRD *cy/+* rats a change in *Fam20c* expression suggesting that local Fgf23 degradation is unchanged. Interestingly, Dmp-1, another bone marker protein, was elevated in the kidneys of Han:SPRD *cy/+* rats but how this correlates with renal Fgf23 expression as well as the mechanism causing ectopic renal Fgf23 expression is so far unknown.

4.3 Regulation of renal Fgf23 expression in PKD

In the second project we examined the causes of renal Fgf23 expression in the *Pkd1* conditional KO mouse model. To identify possible triggers for renal Fgf23 expression we compared our PKD animals with the diabetic nephropathy rat model of Zanchi et al. (2013) which displayed as well renal Fgf23 expression [227]. We hypothesized that hypoxia and inflammation are overlapping conditions in the two CKD animal models and investigated the effect of these two factors on *Fgf23* expression in bone cell culture models as well as in kidneys of *Pkd1* conditional KO mice.

Iron deficiency causes anemia and leads *in vivo* and *in vitro* to an increase in *Fgf23* gene expression in bone [136]. Furthermore, hypoxia directly upregulates *Fgf23* expression in UMR-106 rat osteosarcoma cells [139]. Iron deficiency induced *Fgf23* expression in UMR-106 cells is blocked by MAPK inhibitors and increased by Hif1α activators [136]. To the contrary, we did not see any effect on *Fgf23* expression in primary mouse osteoblasts cultured in 0.2% hypoxia. Furthermore hypoxia repressed 1,25$(OH)_2$ vitamin D_3 induced *Fgf23* expression in MC3T3-E1 mouse preosteoblast cells. Despite the negative results we undertook another effort to investigate whether *Fgf23* may be a direct or indirect Hif1α or Hif2α target gene. Loss of Von Hippel-Lindau (Vhl) protein prevents Hif from hydroxylation and degradation in the cytoplasma which leads to the translocation of Hif to the

nucleus where it activates hypoxia sensitive genes [252]. *Vhl* conditional KO mice have increased expression of Hif target genes due to impaired degradation of Hif [262]. We quantified *Fgf23* expression in kidneys of *Vhl* KO animals as well as in primary kidney cells lacking Vhl but neither the kidneys of Vhl KO animals nor the cells lacking Vhl expressed *Fgf23*. Thus, hypoxia alone is not sufficient to trigger *Fgf23* expression in PKD animals.

In CKD patients, IL-6 and TNFα correlate with FGF23 levels independent of renal function and measures of mineral metabolism [142]. Recently, it has been shown that inflammatory cytokines such as Tnfα, Il-1β, and LPS directly stimulate *Fgf23* expression in the IDG-SW3 osteocyte cell line as well as in *ex vivo* cultured human trabecular bone [147]. We found that Tnfα increases *Fgf23* expression in primary mouse osteocytes similar as 1,25$(OH)_2$ vitamin D_3. Tnfα/NfκB signaling increases the expression of the nuclear receptor and early response gene *Nurr1* which is involved in the Pth dependent regulation of *Fgf23* expression in bone [133, 239]. In response to Tnfα but not 1,25$(OH)_2$ vitamin D_3 primary osteocytes upregulated *Nurr1* expression suggesting that Tnfα dependent upregulation of *Fgf23* is indirect via Nurr1. O-glycosylation of FGF23 by GALNT3 is a critical step in FGF23 processing and prevents premature degradation of Fgf23 [102]. Tnfα stimulated *Galnt3* expression in primary mouse osteocytes and might thereby enhance the stability of Fgf23 protein. Both, *Dmp-1* KO mouse as well as the *Hyp* mouse model suffer from low 1,25$(OH)_2$ vitamin D_3 levels and hypophosphatemic rickets [79, 115–118]. Martin et al (2012) demonstrated that the interaction of C-terminal Dmp-1 with the ASARM sequence of the membrane protein Phex locally represses *Fgf23* expression in bone [125]. In the primary osteocyte cells, *Dmp-1* was repressed by Tnfα and 1,25$(OH)_2$ vitamin D_3 whereas *Phex* expression was only repressed by 1,25$(OH)_2$ vitamin D_3.

The finding that the inflammatory cytokines Tnfα impacts *Fgf23* gene expression as well as the expression of Fgf23 regulatory genes allowed us to go back to our initial hypothesis that inflammation may regulate ectopic Fgf23 expression in the kidneys of *Pkd1* conditional KO animals. At week 6, $Pkd1^{fl/fl}$, *cre+* mice were similar to the control mice and had a normal two kidney per body weight ratio, plasma Fgf23 and Pth levels as well as normal phosphate handling and intact renal function. At week 12, the two kidney per body weight ratio was drastically increased in $Pkd1^{fl/fl}$, *cre+* mice and they

displayed increased plasma Fgf23 levels and decreased Pth levels. Further they had a reduced phosphate reabsorption whereas renal function was slightly decreased as apparent from increased BUN but unchanged creatinine clearance. Tamoxifen administration led to an appropriate downregulation of *Pkd1* gene expression and the remaining expression amounted 19% and 74% after 6 and 12 weeks, respectively. In human ADPKD patients, high *PKD1* expression of the intact allele is persistent in the majority of cysts and may explain the high remaining expression levels in the PKD animals at week 12 [241]. We confirmed the expression of the bone marker genes *Fgf23*, *Runx-2* and *Dmp-1* in the cystic kidneys of 12 weeks old $Pkd1^{fl/fl}$, *cre+* animals whereas the expression of these genes were unchanged in bone.

TNFα is secreted into the cyst fluid of human ADPKD patients and contributes in heterozygous *Pkd2* KO animals to cyst formation and cyst growth [257]. Tnfα induces its own transcription by a NfκB dependent pathway and has a prosurvival effect on embryonic epithelial cells of $Pkd1^{null}$ mice [263]. We proved the presence of inflammatory markers in PKD kidneys and found that *Tnfα* and *Tgfβ* expression as well as phosphorylation of the NfκB subunit p65 is increased in PKD animals at week 12. NfκB binds upon Tnfα activation to the promoter region of the orphan nuclear receptor Nurr1 [239]. Nurr1 is an early response gene and stimulates in bone *Fgf23* expression [133]. In PKD animals *Nurr1* expression is strongly increased at week 12. Furthermore Nurr1 localization switched from the cytoplasm into the nucleus in PKD animals whereas it remained in the cytoplasm in wild type animals. Nuclear localization of Nurr1 is frequently but not exclusively co-localized with Fgf23 expression suggesting that further factors are necessary to induce FGF23 expression in PKD kidneys.

Osteoarthritis and inflammatory bowel disease (IBD) are both diseases characterized by inflammation and elevated TNFα levels and are linked to abnormal FGF23 expression [144, 145]. Chondrocytes derived from osteoarthritis patients display elevated *FGF23* gene expression [144]. In children with IBD plasma FGF23 levels are increased in the acute phase whereas they are normal in the remission phase [145]. The increase in plasma FGF23 levels in the acute phase can be suppressed by treatment with the anti-TNFα antibody infliximab [145]. Renal Fgf23 expression in a diabetic nephropathy rat model was reduced after treatment with ramipril, an ACE inhibitor [227]. Beside blood pres-

sure reduction, ramipril is known to lower inflammation markers in patients with type 2 diabetes due to decreased production of the proinflammatory mediator angiotensin II [258, 264]. Angiotensin II increases Tnfα expression and reduces Klotho expression in the kidney which might explain the effect of ramipril in the diabetic nephropathy rat model [163, 227, 264, 265]. We tested the effect of Tnfα blockade in our PKD model and found that a single injection of anti-Tnfα antibodies lowers plasma Fgf23 levels in *Pkd1* conditional KO animals independent of the genotype and decreases the expression of *Tnfα* and *Tgfβ* in the kidneys of $Pkd1^{fl/fl}$, *cre+* animals. The administration of anti-Tnfα antibodies tended to result in lower *Fgf23* and *Nurr1* expression in the kidneys of PKD animals. Further evidence that Fgf23 is involved in inflammatory processes comes from the observation that serum Fgf23 levels of mice inoculated with LPS, E. coli, or S. aureus were increased [149]. Under this conditions, *Fgf23* expression in spleen turned out to be elevated [149]. Within the spleen mainly the bone marrow derived dendritic cells and to a lower extent macrophages were responsible for increased *Fgf23* expression levels [149]. Our results strongly suggest that Tnfα modulates Fgf23 expression and secretion in polycystic kidney disease but the exact physiological function of Tnfα induced *Fgf23* expression within the inflammatory response has to be elucidated in future.

Chapter 5

Summary

This project originated from the clinical observation that ADPKD patients with normal renal function have elevated plasma FGF23 levels. The aim of this project was to examine the role of high Fgf23 in PKD rodent models such as Han:SPRD *cy/+* rats and *Pkd1* conditional KO mice. We found that plasma Fgf23 levels were increased in Han:SPRD *cy/+* rats at a time point when renal function was apparently normal. Therefore Han:SPRD *cy/+* rats accurately reproduced the observed increase of FGF23 levels in the early disease course of human ADPKD and allow to approach the underlying mechanism in more detail. Despite the high Fgf23 levels, phosphate and calcium handling as well as vitamin D_3 metabolism were unchanged, indicating resistance to Fgf23. We analyzed the early mediators of Fgf23 signaling in the kidney and found no differences in *Fgfr* and Klotho expression and FRS2α phosphorylation was even enhanced in Han:SPRD *cy/+* rats. We evaluated the source of Fgf23 and found that *Fgf23* expression in kidney but not in bone was increased in Han:SPRD *cy/+* rats and $Pkd1^{fl/fl}$, *cre+* mice. We detected Fgf23 protein expression in cells lining renal cysts. This raised the question how the expression and secretion of Fgf23 in bone and the *de novo* Fgf23 expression in kidney are triggered in PKD. We tested the hypothesis that local hypoxia or inflammation triggers ectopic renal Fgf23 expression. First, we investigated the effect of hypoxia and the inflammatory cytokine Tnfα on bone cell culture. Hypoxia did not affect *Fgf23* mRNA expression neither in primary mouse osteoblast nor in MC3T3-E1 mouse preosteoblast cells. The inflammatory cytokine Tnfα increased *Fgf23* as well as *Nurr1* mRNA expression in primary mouse osteocyts. We proved that kidneys of $Pkd1^{fl/fl}$, *cre+* were inflamed by showing increased *Tnfα* and *Tgfβ* expression levels as well as increased phosporylation of the NfκB p65 sub-

unit. Likely, Tnfα is responsible for the increased expression of the orphan nuclear receptor Nurr1 in PKD kidneys. Nurr1 showed predominantly a nuclear localization in cystic kidneys whereas it was distributed in the cytoplasm of healthy kidneys. The neutralization of Tnfα with antibodies reduced Fgf23 plasma levels in PKD and healthy animals and decreased the expression of inflammation markers in cystic kidneys. Furthermore application of anti-Tnfα antibodies tended to lower renal *Fgf23* and *Nurr1* expression. These results suggest that the inflammatory cytokine Tnfα affects Fgf23 expression in cystic kidneys as well as in osteocytes. These findings may have also implications for other forms of CKD where elevated FGF23 an local inflammation are commonly occurring.

5.1 Limitations

In the first experimental study we used the Han:SPRD rat model which is not the orthologue model of human ADPKD disease. However, Han:SPRD *cy/+* rats reproduce the clinical finding of elevated FGF23 levels when renal function is still normal. This may be a hint that not the defective *Pkd1* gene itself causes the abnormality but rather the circumstance of cyst growth. We are not able to explain the resistance in Han:SPRD rats against the highly elevated *Fgf23* levels in the presence of normal renal function. It might be that we missed an early decline in renal function due to hyperfiltration of the remaining nephrons and therefore overestimated creatinine clearence of PKD kidneys. An other possibility is that Fgf23 which is expressed in response to inflammatory stimuli has an other function than the well-known regulation of phosphate and vitamin D_3 metabolism. The *Pkd1* conditional KO mouse is the orthologue model of human ADPKD. Cre recombinase is driven by the beta actin promoter which leads to the *Pkd1* gene ablation in the whole body including bone. Pc1 plays an important role in mechanosensing in bone and it is unknown if Pc1 signaling itself has an impact on Fgf23 expression in bone. Kidney specific *Pkd1* conditional animals would be useful to shed light on this aspect. Such animals have been obtained during the course of the PhD project but due to limitations of time could not be investigated to date.

The final evidence that Nurr1 is involved in the Tnfα dependent *Fgf23* expression would need further experiments which involve the downregulation of Nurr1 with siRNA or shRNA *in vitro* or application of a Nurr1 antagonist *in vivo*. To my knowledge there is no Nurr1

antagonist available so far. Our results regarding the regulation of *Fgf23* in osteocytes are only based on mRNA data, western blot analysis should prove if similar processes happen on protein levels.

5.2 Outlook

In the near future, the role of Nurr1 in the regulation of Tnfα dependent *Fgf23* expression should be clarified. This could be done *in vitro* by using siRNA for Nurr1 knockdown. Nurr1 forms heterodimers with RXR to exert its effect on the regulation of gene expression. Due to the lack of Nurr1 antagonists, a RXR inhibitor may repress as well the effect of Nurr1 on gene expression. A more straight forward but also more time consuming approach would be to use a kidney specific *Nurr1* conditional KO mouse. Further, the events happening in the primary osteocyte cells upon Tnfα stimulation should be analyzed at the protein levels. The initial decline of Klotho levels in CKD might be triggered by abnormal cytokine production and therefore Klotho is a factor which has to be considered in the Tnfα dependent *Fgf23* regulation. The analysis of Klotho protein expression in anti-TNFα treated animals will shed light on this aspect.

In the distant future, it would be interesting to identify and characterize the cells expressing Fgf23 in the kidney as well as to identify the steps leading to the transformation of kidney cells to Fgf23 producing cells. One possibility is that the process of epithelial-mesenchymal transition (EMT) is involved in this event. Further, it would be interesting to analyze the Tnfα dependent *Fgf23* expression in other CKD models as well as in models of inflammatory diseases to get an idea about the physiological role of Fgf23 in inflammatory processes. Finally, the relevance of TNFα induced FGF23 expression in human CKD patients has to be clarified. For this purpose the treatment of CKD patients with TNFα antibodies such as infliximab or etanercept would be one possibility to investigate the effect of TNFα on FGF23 expression in different forms of CKD.

Acknowledgments

First, I would like to thank my supervisor Carsten Wagner for his constant support. Throughout the thesis he was an invaluable adviser and tutor who never failed to encourage me even when facing failed experiments or unpromising results. His support did not stop with the excellent scientific advise, but extended also to all matters around my PhD. I hope to continue this fruitful and very rewarding collaboration at some point in the future.
Next, I would like to thank the members of my committee Orson Moe, Philippe Jaeger, and Olivier Devuyst for asking me critical questions and giving me helpful inputs and suggestions for my project during the committee meetings. In particular, I would like to thank Philippe Jaeger for his great assistance in the first manuscript and Orson Moe and Olivier Devuyst for providing me project relevant cells and animals, respectively.
My thanks go to Rudolf Wuethrich for providing me with space in his laboratory as well as to Andreas Serra who significantly contributed to the improvement of my negotiation skills during my PhD.
I would like to thank Sarah Gabriel and Katja Petzold for all the scientific and non-scientific discussions and for sharing with me the joy and sorrow of a PhD student's life.
Next, I would like to thank all group members of the Nephrology and the Wagner Group for their constant support in the lab, their suggestions and inputs in the lab meetings, and interesting discussions.
A special thank you goes to Matthias Egli for supporting me in all aspects during many years, being an excellent listener, encouraging me after failing and celebrate with me the successes. I am very grateful for the continuous support of my parents throughout my life and for my brother being an idol for me.

Bibliography

[1] Mommaerts W F, Seraidarian K. A STUDY OF THE ADENOSINE TRIPHOSPHATASE ACTIVITY OF MYOSIN AND ACTOMYOSIN. *J Gen Physiol* 1947; **30**: 401–422.

[2] Krebs E G, Beavo J A. Phosphorylation-dephosphorylation of enzymes. *Annu Rev Biochem* 1979; **48**: 923–959.

[3] Danielli J F, Davson H. A contribution to the theory of permeability of thin films. *J Cell Comp Physiol* 1935; **5**: 495–508.

[4] McConnell D, Frajola W J, Deamer D W. Relation between the Inorganic Chemistry and Biochemistry of Bone Mineralization. *Science* 1961; **133**: 281–282.

[5] Termine J D, Posner A S. Infrared analysis of rat bone: age dependency of amorphous and crystalline mineral fractions. *Science* 1966; **153**: 1523–1525.

[6] Berndt T, Kumar R. Phosphatonins and the regulation of phosphate homeostasis. *Annu Rev Physiol* 2007; **69**: 341–359.

[7] Berndt T J, Schiavi S, Kumar R. "Phosphatonins" and the regulation of phosphorus homeostasis. *Am J Physiol Renal Physiol* 2005; **289**: F1170–F1182.

[8] Knochel J P. The pathophysiology and clinical characteristics of severe hypophosphatemia. *Arch Intern Med* 1977; **137**: 203–220.

[9] Kruse K, Kracht U, Göpfert G. Renal threshold phosphate concentration (TmPO4/GFR). *Arch Dis Child* 1982; **57**: 217–223.

[10] Haramati A, Mulroney S E, Webster S K. Developmental changes in the tubular capacity for phosphate reabsorption in the rat. *Am J Physiol* 1988; **255**: F287–F291.

[11] Craddock P R, Yawata Y, VanSanten L, *et al.* Acquired phagocyte dysfunction. A complication of the hypophosphatemia of parenteral hyperalimentation. *N Engl J Med* 1974; **290**: 1403–1407.

[12] Travis S F, Sugerman H J, Ruberg R L, *et al.* Alterations of red-cell glycolytic intermediates and oxygen transport as a consequence of hypophosphatemia in patients receiving intravenous hyperalimentation. *N Engl J Med* 1971; **285**: 763–768.

[13] Mc Collum E V, Simmonds N, Shipley P G, *et al.* STUDIES ON EXPERIMENTAL RICKETS. VIII. THE PRODUCTION OF RICKETS BY DIETS LOW IN PHOSPHORUS AND FAT-SOLUBLE A. *The Journal of Biological Chemistry* 1921; **47**: 507–527.

[14] Pappenheimer A M, McCann G F, Zucker T F, *et al.* EXPERIMENTAL RICKETS IN RATS : IV. THE EFFECT OF VARYING THE INORGANIC CONSTITUENTS OF A RICKETS-PRODUCING DIET. *J Exp Med* 1922; **35**: 421–446.

[15] Hamuro Y, Shino A, Suzuoki Z. Acute induction of soft tissue calcification with transient hyperphosphatemia in the KK mouse by modification in dietary contents of calcium, phosphorus, and magnesium. *J Nutr* 1970; **100**: 404–412.

[16] Jono S, McKee M D, Murry C E, *et al.* Phosphate regulation of vascular smooth muscle cell calcification. *Circ Res* 2000; **87**: E10–E17.

[17] Gates F L, Grant J H. EXPERIMENTAL OBSERVATIONS ON IRRADIATED, NORMAL, AND PARTIALLY PARATHYROIDECTOMIZED RABBITS : III. THE EFFECTS OF INANITION. *J Exp Med* 1927; **45**: 139–150.

[18] Radanovic T, Wagner C A, Murer H, *et al.* Regulation of intestinal phosphate transport. I. Segmental expression and adaptation to low-P(i) diet of the type IIb Na(+)-P(i) cotransporter in mouse small intestine. *Am J Physiol Gastrointest Liver Physiol* 2005; **288**: G496–G500.

[19] Levi M, Lötscher M, Sorribas V, *et al.* Cellular mechanisms of acute and chronic adaptation of rat renal P(i) transporter to alterations in dietary P(i). *Am J Physiol* 1994; **267**: F900–F908.

[20] Lötscher M, Kaissling B, Biber J, *et al.* Role of microtubules in the rapid regulation of renal phosphate transport in response to acute alterations in dietary phosphate content. *J Clin Invest* 1997; **99**: 1302–1312.

[21] Staum B B, Hamburger R J, Goldberg M. Tracer microinjection study of renal tubular phosphate reabsorption in the rat. *J Clin Invest* 1972; **51**: 2271–2276.

[22] Werner A, Moore M L, Mantei N, *et al.* Cloning and expression of cDNA for a Na/Pi cotransport system of kidney cortex. *Proc Natl Acad Sci U S A* 1991; **88**: 9608–9612.

[23] Magagnin S, Werner A, Markovich D, *et al.* Expression cloning of human and rat renal cortex Na/Pi cotransport. *Proc Natl Acad Sci U S A* 1993; **90**: 5979–5983.

[24] Segawa H, Kaneko I, Takahashi A, *et al.* Growth-related renal type II Na/Pi cotransporter. *J Biol Chem* 2002; **277**: 19665–19672.

[25] Ohkido I, Segawa H, Yanagida R, *et al.* Cloning, gene structure and dietary regulation of the type-IIc Na/Pi cotransporter in the mouse kidney. *Pflugers Arch* 2003; **446**: 106–115.

[26] Villa-Bellosta R, Ravera S, Sorribas V, *et al.* The Na+-Pi cotransporter PiT-2 (SLC20A2) is expressed in the apical membrane of rat renal proximal tubules and regulated by dietary Pi. *Am J Physiol Renal Physiol* 2009; **296**: F691–F699.

[27] Custer M, Lötscher M, Biber J, *et al.* Expression of Na-P(i) cotransport in rat kidney: localization by RT-PCR and immunohistochemistry. *Am J Physiol* 1994; **266**: F767–F774.

[28] Madjdpour C, Bacic D, Kaissling B, *et al.* Segment-specific expression of sodium-phosphate cotransporters NaPi-IIa and -IIc and interacting proteins in mouse renal proximal tubules. *Pflugers Arch* 2004; **448**: 402–410.

[29] Forster I C, Hernando N, Biber J, *et al.* Phosphate transporters of the SLC20 and SLC34 families. *Mol Aspects Med* 2013; **34**: 386–395.

[30] Biber J, Hernando N, Forster I. Phosphate transporters and their function. *Annu Rev Physiol* 2013; **75**: 535–550.

[31] Miyamoto K i, Haito-Sugino S, Kuwahara S, *et al.* Sodium-dependent phosphate cotransporters: lessons from gene knockout and mutation studies. *J Pharm Sci* 2011; **100**: 3719–3730.

[32] Bergwitz C, Roslin N M, Tieder M, *et al.* SLC34A3 mutations in patients with hereditary hypophosphatemic rickets with hypercalciuria predict a key role for the sodium-phosphate cotransporter NaPi-IIc in maintaining phosphate homeostasis. *Am J Hum Genet* 2006; **78**: 179–192.

[33] Magen D, Berger L, Coady M J, *et al.* A loss-of-function mutation in NaPi-IIa and renal Fanconi's syndrome. *N Engl J Med* 2010; **362**: 1102–1109.

[34] Schlingmann K P, Ruminska J, Kaufmann M, *et al.* Autosomal-Recessive Mutations in SLC34A1 Encoding Sodium-Phosphate Cotransporter 2A Cause Idiopathic Infantile Hypercalcemia. *J Am Soc Nephrol* 2015; .

[35] Segawa H, Onitsuka A, Kuwahata M, *et al.* Type IIc sodium-dependent phosphate transporter regulates calcium metabolism. *J Am Soc Nephrol* 2009; **20**: 104–113.

[36] Myakala K, Motta S, Murer H, *et al.* Renal-specific and inducible depletion of NaPi-IIc/Slc34a3, the cotransporter mutated in HHRH, does not affect phosphate or calcium homeostasis in mice. *Am J Physiol Renal Physiol* 2014; **306**: F833–F843.

[37] Beck L, Karaplis A C, Amizuka N, *et al.* Targeted inactivation of Npt2 in mice leads to severe renal phosphate wasting, hypercalciuria, and skeletal abnormalities. *Proc Natl Acad Sci U S A* 1998; **95**: 5372–5377.

[38] Segawa H, Onitsuka A, Furutani J, *et al.* Npt2a and Npt2c in mice play distinct and synergistic roles in inorganic phosphate metabolism and skeletal development. *Am J Physiol Renal Physiol* 2009; **297**: F671–F678.

[39] Biber J, Hernando N, Forster I, *et al.* Regulation of phosphate transport in proximal tubules. *Pflugers Arch* 2009; **458**: 39–52.

[40] Bacic D, Lehir M, Biber J, *et al.* The renal Na+/phosphate cotransporter NaPi-IIa is internalized via the receptor-mediated endocytic route in response to parathyroid hormone. *Kidney Int* 2006; **69**: 495–503.

[41] Déliot N, Hernando N, Horst-Liu Z, *et al.* Parathyroid hormone treatment induces dissociation of type IIa Na+-P(i) cotransporter-Na+/H+ exchanger regulatory factor-1 complexes. *Am J Physiol Cell Physiol* 2005; **289**: C159–C167.

[42] Hernando N, Déliot N, Gisler S M, *et al.* PDZ-domain interactions and apical expression of type IIa Na/P(i) cotransporters. *Proc Natl Acad Sci U S A* 2002; **99**: 11957–11962.

[43] Werner A, Kempson S A, Biber J, *et al.* Increase of Na/Pi-cotransport encoding mRNA in response to low Pi diet in rat kidney cortex. *J Biol Chem* 1994; **269**: 6637–6639.

[44] Kempson S A, Lötscher M, Kaissling B, *et al.* Parathyroid hormone action on phosphate transporter mRNA and protein in rat renal proximal tubules. *Am J Physiol* 1995; **268**: F784–F791.

[45] Miyamoto K i, Ito M, Kuwahata M, *et al.* Inhibition of intestinal sodium-dependent inorganic phosphate transport by fibroblast growth factor 23. *Ther Apher Dial* 2005; **9**: 331–335.

[46] Hu M C, Shiizaki K, Kuro-o M, *et al.* Fibroblast growth factor 23 and Klotho: physiology and pathophysiology of an endocrine network of mineral metabolism. *Annu Rev Physiol* 2013; **75**: 503–533.

[47] Bergwitz C, Jüppner H. Regulation of phosphate homeostasis by PTH, vitamin D, and FGF23. *Annu Rev Med* 2010; **61**: 91–104.

[48] Reiss E, Canterbury J M, Bercovitz M A, *et al.* The role of phosphate in the secretion of parathyroid hormone in man. *J Clin Invest* 1970; **49**: 2146–2149.

[49] Segal J H, Pollock A S. Transfection-mediated expression of a dominant cAMP-resistant phenotype in the opossum kidney (OK) cell line prevents parathyroid hormone-induced inhibition of Na-phosphate cotransport. A protein kinase-A-mediated event. *J Clin Invest* 1990; **86**: 1442–1450.

[50] Bounoutas G S, Tawfeek H, Fröhlich L F, *et al.* Impact of impaired receptor internalization on calcium homeostasis in knock-in mice expressing a phosphorylation-deficient parathyroid hormone (PTH)/PTH-related peptide receptor. *Endocrinology* 2006; **147**: 4674–4679.

[51] Miao D, He B, Karaplis A C, *et al.* Parathyroid hormone is essential for normal fetal bone formation. *J Clin Invest* 2002; **109**: 1173–1182.

[52] Bai X, Miao D, Goltzman D, *et al.* Early lethality in Hyp mice with targeted deletion of Pth gene. *Endocrinology* 2007; **148**: 4974–4983.

[53] Haussler M R. Vitamin D receptors: nature and function. *Annu Rev Nutr* 1986; **6**: 527–562.

[54] Yu V C, Delsert C, Andersen B, *et al.* RXR beta: a coregulator that enhances binding of retinoic acid, thyroid hormone, and vitamin D receptors to their cognate response elements. *Cell* 1991; **67**: 1251–1266.

[55] Kliewer S A, Umesono K, Mangelsdorf D J, *et al.* Retinoid X receptor interacts with nuclear receptors in retinoic acid, thyroid hormone and vitamin D3 signalling. *Nature* 1992; **355**: 446–449.

[56] Noda M, Vogel R L, Craig A M, *et al.* Identification of a DNA sequence responsible for binding of the 1,25-dihydroxyvitamin D3 receptor and 1,25-dihydroxyvitamin D3 enhancement of mouse secreted phosphoprotein 1 (SPP-1 or osteopontin) gene expression. *Proc Natl Acad Sci U S A* 1990; **87**: 9995–9999.

[57] Yoshizawa T, Handa Y, Uematsu Y, *et al.* Mice lacking the vitamin D receptor exhibit impaired bone formation, uterine hypoplasia and growth retardation after weaning. *Nat Genet* 1997; **16**: 391–396.

[58] Demay M B, Kiernan M S, DeLuca H F, *et al.* Sequences in the human parathyroid hormone gene that bind the 1,25-dihydroxyvitamin D3 receptor and mediate transcriptional repression in response to 1,25-dihydroxyvitamin D3. *Proc Natl Acad Sci U S A* 1992; **89**: 8097–8101.

[59] Yamashita T, Yoshioka M, Itoh N. Identification of a novel fibroblast growth factor, FGF-23, preferentially expressed in the ventrolateral thalamic nucleus of the brain. *Biochem Biophys Res Commun* 2000; **277**: 494–498.

[60] Itoh N, Ornitz D M. Functional evolutionary history of the mouse Fgf gene family. *Dev Dyn* 2008; **237**: 18–27.

[61] Shimada T, Mizutani S, Muto T, *et al.* Cloning and characterization of FGF23 as a causative factor of tumor-induced osteomalacia. *Proc Natl Acad Sci U S A* 2001; **98**: 6500–6505.

[62] Fon Tacer K, Bookout A L, Ding X, *et al.* Research resource: Comprehensive expression atlas of the fibroblast growth factor system in adult mouse. *Mol Endocrinol* 2010; **24**: 2050–2064.

[63] Liu S, Tang W, Zhou J, *et al.* Fibroblast growth factor 23 is a counter-regulatory phosphaturic hormone for vitamin D. *J Am Soc Nephrol* 2006; **17**: 1305–1315.

[64] Shimada T, Muto T, Urakawa I, *et al.* Mutant FGF-23 responsible for autosomal dominant hypophosphatemic rickets is resistant to proteolytic cleavage and causes hypophosphatemia in vivo. *Endocrinology* 2002; **143**: 3179–3182.

[65] Liu S, Guo R, Simpson L G, *et al.* Regulation of fibroblastic growth factor 23 expression but not degradation by PHEX. *J Biol Chem* 2003; **278**: 37419–37426.

[66] Bhattacharyya N, Chong W H, Gafni R I, *et al.* Fibroblast growth factor 23: state of the field and future directions. *Trends Endocrinol Metab* 2012; **23**: 610–618.

[67] Goetz R, Beenken A, Ibrahimi O A, *et al.* Molecular insights into the klotho-dependent, endocrine mode of action of fibroblast growth factor 19 subfamily members. *Mol Cell Biol* 2007; **27**: 3417–3428.

[68] Schlessinger J, Plotnikov A N, Ibrahimi O A, *et al.* Crystal structure of a ternary FGF-FGFR-heparin complex reveals a dual role for heparin in FGFR binding and dimerization. *Mol Cell* 2000; **6**: 743–750.

[69] Urakawa I, Yamazaki Y, Shimada T, *et al.* Klotho converts canonical FGF receptor into a specific receptor for FGF23. *Nature* 2006; **444**: 770–774.

[70] Kuro-o M, Matsumura Y, Aizawa H, *et al.* Mutation of the mouse klotho gene leads to a syndrome resembling ageing. *Nature* 1997; **390**: 45–51.

[71] Shiraki-Iida T, Aizawa H, Matsumura Y, *et al.* Structure of the mouse klotho gene and its two transcripts encoding membrane and secreted protein. *FEBS Lett* 1998; **424**: 6–10.

[72] Matsumura Y, Aizawa H, Shiraki-Iida T, *et al.* Identification of the human klotho gene and its two transcripts encoding membrane and secreted klotho protein. *Biochem Biophys Res Commun* 1998; **242**: 626–630.

[73] Chen C D, Podvin S, Gillespie E, *et al.* Insulin stimulates the cleavage and release of the extracellular domain of Klotho by ADAM10 and ADAM17. *Proc Natl Acad Sci U S A* 2007; **104**: 19796–19801.

[74] Kurosu H, Ogawa Y, Miyoshi M, *et al.* Regulation of fibroblast growth factor-23 signaling by klotho. *J Biol Chem* 2006; **281**: 6120–6123.

[75] Tenhagen M, van Diest P J, Ivanova I A, *et al.* Fibroblast growth factor receptors in breast cancer: expression, downstream effects, and possible drug targets. *Endocr Relat Cancer* 2012; **19**: R115–R129.

[76] Cancilla B, Davies A, Cauchi J A, *et al.* Fibroblast growth factor receptors and their ligands in the adult rat kidney. *Kidney Int* 2001; **60**: 147–155.

[77] Shimada T, Hasegawa H, Yamazaki Y, *et al.* FGF-23 is a potent regulator of vitamin D metabolism and phosphate homeostasis. *J Bone Miner Res* 2004; **19**: 429–435.

[78] Mirams M, Robinson B G, Mason R S, *et al.* Bone as a source of FGF23: regulation by phosphate? *Bone* 2004; **35**: 1192–1199.

[79] Perwad F, Azam N, Zhang M Y H, *et al.* Dietary and serum phosphorus regulate fibroblast growth factor 23 expression and 1,25-dihydroxyvitamin D metabolism in mice. *Endocrinology* 2005; **146**: 5358–5364.

[80] Andrukhova O, Slavic S, Smorodchenko A, *et al.* FGF23 regulates renal sodium handling and blood pressure. *EMBO Mol Med* 2014; **6**: 744–759.

[81] Andrukhova O, Smorodchenko A, Egerbacher M, *et al.* FGF23 promotes renal calcium reabsorption through the TRPV5 channel. *EMBO J* 2014; **33**: 229–246.

[82] Hu M C, Shi M, Zhang J, *et al.* Klotho: a novel phosphaturic substance acting as an autocrine enzyme in the renal proximal tubule. *FASEB J* 2010; **24**: 3438–3450.

[83] Andrukhova O, Zeitz U, Goetz R, *et al.* FGF23 acts directly on renal proximal tubules to induce phosphaturia through activation of the ERK1/2-SGK1 signaling pathway. *Bone* 2012; **51**: 621–628.

[84] Gattineni J, Bates C, Twombley K, *et al.* FGF23 decreases renal NaPi-2a and NaPi-2c expression and induces hypophosphatemia in vivo predominantly via FGF receptor 1. *Am J Physiol Renal Physiol* 2009; **297**: F282–F291.

[85] Liu S, Vierthaler L, Tang W, *et al.* FGFR3 and FGFR4 do not mediate renal effects of FGF23. *J Am Soc Nephrol* 2008; **19**: 2342–2350.

[86] Gattineni J, Alphonse P, Zhang Q, *et al.* Regulation of renal phosphate transport by FGF23 is mediated by FGFR1 and FGFR4. *Am J Physiol Renal Physiol* 2014; **306**: F351–F358.

[87] Gattineni J, Twombley K, Goetz R, *et al.* Regulation of serum 1,25(OH)2 vitamin D3 levels by fibroblast growth factor 23 is mediated by FGF receptors 3 and 4. *Am J Physiol Renal Physiol* 2011; **301**: F371–F377.

[88] Perwad F, Zhang M Y H, Tenenhouse H S, *et al.* Fibroblast growth factor 23 impairs phosphorus and vitamin D metabolism in vivo and suppresses 25-hydroxyvitamin D-1alpha-hydroxylase expression in vitro. *Am J Physiol Renal Physiol* 2007; **293**: F1577–F1583.

[89] Ranch D, Zhang M Y, Portale A A, *et al.* Fibroblast growth factor 23 regulates renal 1,25-dihydroxyvitamin D and phosphate metabolism via the MAP kinase signaling pathway in Hyp mice. *J Bone Miner Res* 2011; **26**: 1883–1890.

[90] Zhang M Y H, Ranch D, Pereira R C, *et al.* Chronic inhibition of ERK1/2 signaling improves disordered bone and mineral metabolism in hypophosphatemic (Hyp) mice. *Endocrinology* 2012; **153**: 1806–1816.

[91] Ben-Dov I Z, Galitzer H, Lavi-Moshayoff V, *et al.* The parathyroid is a target organ for FGF23 in rats. *J Clin Invest* 2007; **117**: 4003–4008.

[92] Krajisnik T, Björklund P, Marsell R, *et al.* Fibroblast growth factor-23 regulates parathyroid hormone and 1alpha-hydroxylase expression in cultured bovine parathyroid cells. *J Endocrinol* 2007; **195**: 125–131.

[93] Galitzer H, Ben-Dov I Z, Silver J, *et al.* Parathyroid cell resistance to fibroblast growth factor 23 in secondary hyperparathyroidism of chronic kidney disease. *Kidney Int* 2010; **77**: 211–218.

[94] Canalejo R, Canalejo A, Martinez-Moreno J M, *et al.* FGF23 fails to inhibit uremic parathyroid glands. *J Am Soc Nephrol* 2010; **21**: 1125–1135.

[95] Komaba H, Goto S, Fujii H, *et al.* Depressed expression of Klotho and FGF receptor 1 in hyperplastic parathyroid glands from uremic patients. *Kidney Int* 2010; **77**: 232–238.

[96] Krajisnik T, Olauson H, Mirza M A I, *et al.* Parathyroid Klotho and FGF-receptor 1 expression decline with renal function in hyperparathyroid patients with chronic kidney disease and kidney transplant recipients. *Kidney Int* 2010; **78**: 1024–1032.

[97] Olauson H, Lindberg K, Amin R, *et al.* Parathyroid-specific deletion of Klotho unravels a novel calcineurin-dependent FGF23 signaling pathway that regulates PTH secretion. *PLoS Genet* 2013; **9**: e1003975.

[98] A D H R C. Autosomal dominant hypophosphataemic rickets is associated with mutations in FGF23. *Nat Genet* 2000; **26**: 345–348.

[99] Econs M J, McEnery P T. Autosomal dominant hypophosphatemic rickets/osteomalacia: clinical characterization of a novel renal phosphate-wasting disorder. *J Clin Endocrinol Metab* 1997; **82**: 674–681.

[100] White K E, Carn G, Lorenz-Depiereux B, *et al.* Autosomal-dominant hypophosphatemic rickets (ADHR) mutations stabilize FGF-23. *Kidney Int* 2001; **60**: 2079–2086.

[101] Hanisch F G. O-glycosylation of the mucin type. *Biol Chem* 2001; **382**: 143–149.

[102] Kato K, Jeanneau C, Tarp M A, *et al.* Polypeptide GalNAc-transferase T3 and familial tumoral calcinosis. Secretion of fibroblast growth factor 23 requires O-glycosylation. *J Biol Chem* 2006; **281**: 18370–18377.

[103] Topaz O, Shurman D L, Bergman R, *et al.* Mutations in GALNT3, encoding a protein involved in O-linked glycosylation, cause familial tumoral calcinosis. *Nat Genet* 2004; **36**: 579–581.

[104] Ichikawa S, Lyles K W, Econs M J. A novel GALNT3 mutation in a pseudoautosomal dominant form of tumoral calcinosis: evidence that the disorder is autosomal recessive. *J Clin Endocrinol Metab* 2005; **90**: 2420–2423.

[105] Ichikawa S, Guigonis V, Imel E A, *et al.* Novel GALNT3 mutations causing hyperostosis-hyperphosphatemia syndrome result in low intact fibroblast growth factor 23 concentrations. *J Clin Endocrinol Metab* 2007; **92**: 1943–1947.

[106] Garringer H J, Fisher C, Larsson T E, *et al.* The role of mutant UDP-N-acetyl-alpha-D-galactosamine-polypeptide N-acetylgalactosaminyltransferase 3 in regulating serum intact fibroblast growth factor 23 and matrix extracellular phosphoglycoprotein in heritable tumoral calcinosis. *J Clin Endocrinol Metab* 2006; **91**: 4037–4042.

[107] Ichikawa S, Sorenson A H, Austin A M, *et al.* Ablation of the Galnt3 gene leads to low-circulating intact fibroblast growth factor 23 (Fgf23) concentrations and hyperphosphatemia despite increased Fgf23 expression. *Endocrinology* 2009; **150**: 2543–2550.

[108] Tagliabracci V S, Engel J L, Wen J, *et al.* Secreted kinase phosphorylates extracellular proteins that regulate biomineralization. *Science* 2012; **336**: 1150–1153.

[109] Ishikawa H O, Xu A, Ogura E, *et al.* The Raine syndrome protein FAM20C is a Golgi kinase that phosphorylates bio-mineralization proteins. *PLoS One* 2012; **7**: e42988.

[110] Simpson M A, Hsu R, Keir L S, *et al.* Mutations in FAM20C are associated with lethal osteosclerotic bone dysplasia (Raine syndrome), highlighting a crucial molecule in bone development. *Am J Hum Genet* 2007; **81**: 906–912.

[111] Simpson M A, Scheuerle A, Hurst J, *et al.* Mutations in FAM20C also identified in non-lethal osteosclerotic bone dysplasia. *Clin Genet* 2009; **75**: 271–276.

[112] Rafaelsen S H, Raeder H, Fagerheim A K, *et al.* Exome sequencing reveals FAM20c mutations associated with fibroblast growth factor 23-related hypophosphatemia, dental anomalies, and ectopic calcification. *J Bone Miner Res* 2013; **28**: 1378–1385.

[113] Wang X, Wang S, Li C, *et al.* Inactivation of a novel FGF23 regulator, FAM20C, leads to hypophosphatemic rickets in mice. *PLoS Genet* 2012; **8**: e1002708.

[114] Tagliabracci V S, Engel J L, Wiley S E, *et al.* Dynamic regulation of FGF23 by Fam20C phosphorylation, GalNAc-T3 glycosylation, and furin proteolysis. *Proc Natl Acad Sci U S A* 2014; **111**: 5520–5525.

[115] Du L, Desbarats M, Viel J, *et al.* cDNA cloning of the murine Pex gene implicated in X-linked hypophosphatemia and evidence for expression in bone. *Genomics* 1996; **36**: 22–28.

[116] Eicher E M, Southard J L, Scriver C R, *et al.* Hypophosphatemia: mouse model for human familial hypophosphatemic (vitamin D-resistant) rickets. *Proc Natl Acad Sci U S A* 1976; **73**: 4667–4671.

[117] Liu S, Zhou J, Tang W, *et al.* Pathogenic role of Fgf23 in Hyp mice. *Am J Physiol Endocrinol Metab* 2006; **291**: E38–E49.

[118] Feng J Q, Ward L M, Liu S, *et al.* Loss of DMP1 causes rickets and osteomalacia and identifies a role for osteocytes in mineral metabolism. *Nat Genet* 2006; **38**: 1310–1315.

[119] Terasawa M, Shimokawa R, Terashima T, *et al.* Expression of dentin matrix protein 1 (DMP1) in nonmineralized tissues. *J Bone Miner Metab* 2004; **22**: 430–438.

[120] Qin C, Brunn J C, Cook R G, *et al.* Evidence for the proteolytic processing of dentin matrix protein 1. Identification and characterization of processed fragments and cleavage sites. *J Biol Chem* 2003; **278**: 34700–34708.

[121] Steiglitz B M, Ayala M, Narayanan K, *et al.* Bone morphogenetic protein-1/Tolloid-like proteinases process dentin matrix protein-1. *J Biol Chem* 2004; **279**: 980–986.

[122] Toyosawa S, Shintani S, Fujiwara T, *et al.* Dentin matrix protein 1 is predominantly expressed in chicken and rat osteocytes but not in osteoblasts. *J Bone Miner Res* 2001; **16**: 2017–2026.

[123] Martin A, Liu S, David V, *et al.* Bone proteins PHEX and DMP1 regulate fibroblastic growth factor Fgf23 expression in osteocytes through a common pathway involving FGF receptor (FGFR) signaling. *FASEB J* 2011; **25**: 2551–2562.

[124] Wöhrle S, Henninger C, Bonny O, *et al.* Pharmacological inhibition of fibroblast growth factor (FGF) receptor signaling ameliorates FGF23-mediated hypophosphatemic rickets. *J Bone Miner Res* 2013; **28**: 899–911.

[125] Martin A, David V, Li H, *et al.* Overexpression of the DMP1 C-terminal fragment stimulates FGF23 and exacerbates the hypophosphatemic rickets phenotype in Hyp mice. *Mol Endocrinol* 2012; **26**: 1883–1895.

[126] Fedarko N S, Jain A, Karadag A, *et al.* Three small integrin binding ligand N-linked glycoproteins (SIBLINGs) bind and activate specific matrix metalloproteinases. *FASEB J* 2004; **18**: 734–736.

[127] Lanske B, Razzaque M S. Molecular interactions of FGF23 and PTH in phosphate regulation. *Kidney Int* 2014; **86**: 1072–1074.

[128] Kolek O I, Hines E R, Jones M D, *et al.* 1alpha,25-Dihydroxyvitamin D3 upregulates FGF23 gene expression in bone: the final link in a renal-gastrointestinal-skeletal axis that controls phosphate transport. *Am J Physiol Gastrointest Liver Physiol* 2005; **289**: G1036–G1042.

[129] Kawata T, Imanishi Y, Kobayashi K, *et al.* Parathyroid hormone regulates fibroblast growth factor-23 in a mouse model of primary hyperparathyroidism. *J Am Soc Nephrol* 2007; **18**: 2683–2688.

[130] López I, Rodríguez-Ortiz M E, Almadén Y, *et al.* Direct and indirect effects of parathyroid hormone on circulating levels of fibroblast growth factor 23 in vivo. *Kidney Int* 2011; **80**: 475–482.

[131] Lavi-Moshayoff V, Wasserman G, Meir T, *et al.* PTH increases FGF23 gene expression and mediates the high-FGF23 levels of experimental kidney failure: a bone parathyroid feedback loop. *Am J Physiol Renal Physiol* 2010; **299**: F882–F889.

[132] Saji F, Shigematsu T, Sakaguchi T, *et al.* Fibroblast growth factor 23 production in bone is directly regulated by 1alpha,25-dihydroxyvitamin D, but not PTH. *Am J Physiol Renal Physiol* 2010; **299**: F1212–F1217.

[133] Meir T, Durlacher K, Pan Z, *et al.* Parathyroid hormone activates the orphan nuclear receptor Nurr1 to induce FGF23 transcription. *Kidney Int* 2014; .

[134] Tetradis S, Bezouglaia O, Tsingotjidou A. Parathyroid hormone induces expression of the nuclear orphan receptor Nurr1 in bone cells. *Endocrinology* 2001; **142**: 663–670.

[135] Pirih F Q, Aghaloo T L, Bezouglaia O, *et al.* Parathyroid hormone induces the NR4A family of nuclear orphan receptors in vivo. *Biochem Biophys Res Commun* 2005; **332**: 494–503.

[136] Farrow E G, Yu X, Summers L J, *et al.* Iron deficiency drives an autosomal dominant hypophosphatemic rickets (ADHR) phenotype in fibroblast growth factor-23 (Fgf23) knock-in mice. *Proc Natl Acad Sci U S A* 2011; **108**: E1146–E1155.

[137] Braithwaite V, Jarjou L M A, Goldberg G R, *et al.* Iron status and fibroblast growth factor-23 in Gambian children. *Bone* 2012; **50**: 1351–1356.

[138] Wolf M, Koch T A, Bregman D B. Effects of iron deficiency anemia and its treatment on fibroblast growth factor 23 and phosphate homeostasis in women. *J Bone Miner Res* 2013; **28**: 1793–1803.

[139] Clinkenbeard E L, Farrow E G, Summers L J, *et al.* Neonatal iron deficiency causes abnormal phosphate metabolism by elevating FGF23 in normal and ADHR mice. *J Bone Miner Res* 2014; **29**: 361–369.

[140] Brownstein C A, Adler F, Nelson-Williams C, *et al.* A translocation causing increased alpha-klotho level results in hypophosphatemic rickets and hyperparathyroidism. *Proc Natl Acad Sci U S A* 2008; **105**: 3455–3460.

[141] Smith R C, O'Bryan L M, Farrow E G, *et al.* Circulating αKlotho influences phosphate handling by controlling FGF23 production. *J Clin Invest* 2012; **122**: 4710–4715.

[142] Munoz Mendoza J, Isakova T, Ricardo A C, *et al.* Fibroblast growth factor 23 and Inflammation in CKD. *Clin J Am Soc Nephrol* 2012; **7**: 1155–1162.

[143] Hanks L J, Casazza K, Judd S E, *et al.* Associations of fibroblast growth factor-23 with markers of inflammation, insulin resistance and obesity in adults. *PLoS One* 2015; **10**: e0122885.

[144] Iliopoulos D, Malizos K N, Oikonomou P, *et al.* Integrative microRNA and proteomic approaches identify novel osteoarthritis genes and their collaborative metabolic and inflammatory networks. *PLoS One* 2008; **3**: e3740.

[145] El-Hodhod M A A, Hamdy A M, Abbas A A, *et al.* Fibroblast growth factor 23 contributes to diminished bone mineral density in childhood inflammatory bowel disease. *BMC Gastroenterol* 2012; **12**: 44.

[146] Uno J K, Kolek O I, Hines E R, *et al.* The role of tumor necrosis factor alpha in down-regulation of osteoblast Phex gene expression in experimental murine colitis. *Gastroenterology* 2006; **131**: 497–509.

[147] Ito N, Wijenayaka A R, Prideaux M, *et al.* Regulation of FGF23 expression in IDG-SW3 osteocytes and human bone by pro-inflammatory stimuli. *Mol Cell Endocrinol* 2015; **399**: 208–218.

[148] Dai B, David V, Martin A, *et al.* A comparative transcriptome analysis identifying FGF23 regulated genes in the kidney of a mouse CKD model. *PLoS One* 2012; **7**: e44161.

[149] Masuda Y, Ohta H, Morita Y, *et al.* Expression of fgf23 in activated dendritic cells and macrophages in response to immunological stimuli in mice. *Biol Pharm Bull* 2015; **38**: 687–693.

[150] Levin A, Stevens P E. Summary of KDIGO 2012 CKD Guideline: behind the scenes, need for guidance, and a framework for moving forward. *Kidney Int* 2014; **85**: 49–61.

[151] System U S R D. United States Renal Data System, 2014 USRDS annual data report: An overview of the epidemiology of kidney disease in the United States. National Institutes of Health, National Institute of Diabetes and Digestive and Kidney Diseases, Bethesda, MD, 2014, http://www.usrds.org/2014/view/Default.aspx 08.05.2015, 2014.

[152] Jha V, Garcia-Garcia G, Iseki K, *et al.* Chronic kidney disease: global dimension and perspectives. *Lancet* 2013; **382**: 260–272.

[153] G B D M, of Death Collaborators C. Global, regional, and national age-sex specific all-cause and cause-specific mortality for 240 causes of death, 1990-2013: a systematic analysis for the Global Burden of Disease Study 2013. *Lancet* 2015; **385**: 117–171.

[154] Foley R N, Chen S C, Solid C A, *et al.* Early mortality in patients starting dialysis appears to go unregistered. *Kidney Int* 2014; **86**: 392–398.

[155] Block G A, Klassen P S, Lazarus J M, *et al.* Mineral metabolism, mortality, and morbidity in maintenance hemodialysis. *J Am Soc Nephrol* 2004; **15**: 2208–2218.

[156] Gutierrez O, Isakova T, Rhee E, *et al.* Fibroblast growth factor-23 mitigates hyperphosphatemia but accentuates calcitriol deficiency in chronic kidney disease. *J Am Soc Nephrol* 2005; **16**: 2205–2215.

[157] Isakova T, Wahl P, Vargas G S, *et al.* Fibroblast growth factor 23 is elevated before parathyroid hormone and phosphate in chronic kidney disease. *Kidney Int* 2011; **79**: 1370–1378.

[158] Pavik I, Jaeger P, Ebner L, *et al.* Secreted Klotho and FGF23 in chronic kidney disease Stage 1 to 5: a sequence suggested from a cross-sectional study. *Nephrol Dial Transplant* 2013; **28**: 352–359.

[159] Hu M C, Shi M, Zhang J, *et al.* Klotho deficiency causes vascular calcification in chronic kidney disease. *J Am Soc Nephrol* 2011; **22**: 124–136.

[160] Stubbs J R, He N, Idiculla A, *et al.* Longitudinal evaluation of FGF23 changes and mineral metabolism abnormalities in a mouse model of chronic kidney disease. *J Bone Miner Res* 2011; .

[161] Hasegawa H, Nagano N, Urakawa I, *et al.* Direct evidence for a causative role of FGF23 in the abnormal renal phosphate handling and vitamin D metabolism in rats with early-stage chronic kidney disease. *Kidney Int* 2010; **78**: 975–980.

[162] Tsujikawa H, Kurotaki Y, Fujimori T, *et al.* Klotho, a gene related to a syndrome resembling human premature aging, functions in a negative regulatory circuit of vitamin D endocrine system. *Mol Endocrinol* 2003; **17**: 2393–2403.

[163] Hu M C, Kuro-o M, Moe O W. Secreted klotho and chronic kidney disease. *Adv Exp Med Biol* 2012; **728**: 126–157.

[164] Bricker N S. On the pathogenesis of the uremic state. An exposition of the "trade-off hypothesis". *N Engl J Med* 1972; **286**: 1093–1099.

[165] Gutierrez O M. Fibroblast growth factor 23 and disordered vitamin D metabolism in chronic kidney disease: updating the "trade-off" hypothesis. *Clin J Am Soc Nephrol* 2010; **5**: 1710–1716.

[166] Gutiérrez O M, Mannstadt M, Isakova T, *et al.* Fibroblast growth factor 23 and mortality among patients undergoing hemodialysis. *N Engl J Med* 2008; **359**: 584–592.

[167] Shalhoub V, Shatzen E M, Ward S C, *et al.* FGF23 neutralization improves chronic kidney disease-associated hyperparathyroidism yet increases mortality. *J Clin Invest* 2012; **122**: 2543–2553.

[168] Meyer R Jr, Gray R W, Kiebzak G M, *et al.* Altered vitamin D, cyclic nucleotide and trace mineral metabolism in the X-linked hypophosphatemic mouse. *Adv Exp Med Biol* 1980; **128**: 351–359.

[169] Farrow E G, Summers L J, Schiavi S C, *et al.* Altered renal FGF23-mediated activity involving MAPK and Wnt: effects of the Hyp mutation. *J Endocrinol* 2010; **207**: 67–75.

[170] Ketteler M, Biggar P H, Liangos O. FGF23 antagonism: the thin line between adaptation and maladaptation in chronic kidney disease. *Nephrol Dial Transplant* 2013; **28**: 821–825.

[171] Torres V E, Harris P C, Pirson Y. Autosomal dominant polycystic kidney disease. *Lancet* 2007; **369**: 1287–1301.

[172] Reeders S T, Breuning M H, Davies K E, *et al.* A highly polymorphic DNA marker linked to adult polycystic kidney disease on chromosome 16. *Nature* 1985; **317**: 542–544.

[173] Peters D J, Spruit L, Saris J J, *et al.* Chromosome 4 localization of a second gene for autosomal dominant polycystic kidney disease. *Nat Genet* 1993; **5**: 359–362.

[174] Kimberling W J, Kumar S, Gabow P A, *et al.* Autosomal dominant polycystic kidney disease: localization of the second gene to chromosome 4q13-q23. *Genomics* 1993; **18**: 467–472.

[175] Hughes J, Ward C J, Peral B, *et al.* The polycystic kidney disease 1 (PKD1) gene encodes a novel protein with multiple cell recognition domains. *Nat Genet* 1995; **10**: 151–160.

[176] Mochizuki T, Wu G, Hayashi T, *et al.* PKD2, a gene for polycystic kidney disease that encodes an integral membrane protein. *Science* 1996; **272**: 1339–1342.

[177] Grantham J J, Torres V E, Chapman A B, *et al.* Volume progression in polycystic kidney disease. *N Engl J Med* 2006; **354**: 2122–2130.

[178] Grantham J J, Chapman A B, Torres V E. Volume progression in autosomal dominant polycystic kidney disease: the major factor determining clinical outcomes. *Clin J Am Soc Nephrol* 2006; **1**: 148–157.

[179] Bell P E, Hossack K F, Gabow P A, *et al.* Hypertension in autosomal dominant polycystic kidney disease. *Kidney Int* 1988; **34**: 683–690.

[180] Gabow P A, Chapman A B, Johnson A M, *et al.* Renal structure and hypertension in autosomal dominant polycystic kidney disease. *Kidney Int* 1990; **38**: 1177–1180.

[181] Ecder T, Schrier R W. Hypertension in autosomal-dominant polycystic kidney disease: early occurrence and unique aspects. *J Am Soc Nephrol* 2001; **12**: 194–200.

[182] Goldblatt H, Lynch J, Hanzal R F, *et al.* STUDIES ON EXPERIMENTAL HYPERTENSION : I. THE PRODUCTION OF PERSISTENT ELEVATION OF SYSTOLIC BLOOD PRESSURE BY MEANS OF RENAL ISCHEMIA. *J Exp Med* 1934; **59**: 347–379.

[183] Gabow P A, Johnson A M, Kaehny W D, *et al.* Risk factors for the development of hepatic cysts in autosomal dominant polycystic kidney disease. *Hepatology* 1990; **11**: 1033–1037.

[184] Pavik I, Jaeger P, Kistler A D, *et al.* Patients with autosomal dominant polycystic kidney disease have elevated fibroblast growth factor 23 levels and a renal leak of phosphate. *Kidney Int* 2011; **79**: 234–240.

[185] Pavik I, Jaeger P, Ebner L, *et al.* Soluble klotho and autosomal dominant polycystic kidney disease. *Clin J Am Soc Nephrol* 2012; **7**: 248–257.

[186] Cornec-Le Gall E, Audrézet M P, Chen J M, *et al.* Type of PKD1 mutation influences renal outcome in ADPKD. *J Am Soc Nephrol* 2013; **24**: 1006–1013.

[187] Hateboer N, v Dijk M A, Bogdanova N, *et al.* Comparison of phenotypes of polycystic kidney disease types 1 and 2. European PKD1-PKD2 Study Group. *Lancet* 1999; **353**: 103–107.

[188] Rossetti S, Burton S, Strmecki L, *et al.* The position of the polycystic kidney disease 1 (PKD1) gene mutation correlates with the severity of renal disease. *J Am Soc Nephrol* 2002; **13**: 1230–1237.

[189] Rule A D, Torres V E, Chapman A B, *et al.* Comparison of methods for determining renal function decline in early autosomal dominant polycystic kidney disease: the consortium of radiologic imaging studies of polycystic kidney disease cohort. *J Am Soc Nephrol* 2006; **17**: 854–862.

[190] Gonzalez S D Jlez-Perrett, Kim K, Ibarra C, *et al.* Polycystin-2, the protein mutated in autosomal dominant polycystic kidney disease (ADPKD), is a Ca2+-permeable nonselective cation channel. *Proc Natl Acad Sci U S A* 2001; **98**: 1182–1187.

[191] Tsiokas L, Arnould T, Zhu C, *et al.* Specific association of the gene product of PKD2 with the TRPC1 channel. *Proc Natl Acad Sci U S A* 1999; **96**: 3934–3939.

[192] Hanaoka K, Qian F, Boletta A, *et al.* Co-assembly of polycystin-1 and -2 produces unique cation-permeable currents. *Nature* 2000; **408**: 990–994.

[193] Ibraghimov-Beskrovnaya O, Dackowski W R, Foggensteiner L, *et al.* Polycystin: in vitro synthesis, in vivo tissue expression, and subcellular localization identifies a large membrane-associated protein. *Proc Natl Acad Sci U S A* 1997; **94**: 6397–6402.

[194] Yoder B K, Hou X, Guay-Woodford L M. The polycystic kidney disease proteins, polycystin-1, polycystin-2, polaris, and cystin, are co-localized in renal cilia. *J Am Soc Nephrol* 2002; **13**: 2508–2516.

[195] Tsiokas L, Kim E, Arnould T, *et al.* Homo- and heterodimeric interactions between the gene products of PKD1 and PKD2. *Proc Natl Acad Sci U S A* 1997; **94**: 6965–6970.

[196] Nauli S M, Alenghat F J, Luo Y, *et al.* Polycystins 1 and 2 mediate mechanosensation in the primary cilium of kidney cells. *Nat Genet* 2003; **33**: 129–137.

[197] Nauli S M, Rossetti S, Kolb R J, *et al.* Loss of polycystin-1 in human cyst-lining epithelia leads to ciliary dysfunction. *J Am Soc Nephrol* 2006; **17**: 1015–1025.

[198] Lu W, Peissel B, Babakhanlou H, *et al.* Perinatal lethality with kidney and pancreas defects in mice with a targetted Pkd1 mutation. *Nat Genet* 1997; **17**: 179–181.

[199] Lu W, Shen X, Pavlova A, *et al.* Comparison of Pkd1-targeted mutants reveals that loss of polycystin-1 causes cystogenesis and bone defects. *Hum Mol Genet* 2001; **10**: 2385–2396.

[200] Boulter C, Mulroy S, Webb S, *et al.* Cardiovascular, skeletal, and renal defects in mice with a targeted disruption of the Pkd1 gene. *Proc Natl Acad Sci U S A* 2001; **98**: 12174–12179.

[201] Piontek K B, Huso D L, Grinberg A, *et al.* A functional floxed allele of Pkd1 that can be conditionally inactivated in vivo. *J Am Soc Nephrol* 2004; **15**: 3035–3043.

[202] Piontek K, Menezes L F, Garcia-Gonzalez M A, *et al.* A critical developmental switch defines the kinetics of kidney cyst formation after loss of Pkd1. *Nat Med* 2007; **13**: 1490–1495.

[203] Lantinga-van Leeuwen I S, Leonhard W N, van der Wal A, *et al.* Kidney-specific inactivation of the Pkd1 gene induces rapid cyst formation in developing kidneys and a slow onset of disease in adult mice. *Hum Mol Genet* 2007; **16**: 3188–3196.

[204] Bacic D, Capuano P, Baum M, *et al.* Activation of dopamine D1-like receptors induces acute internalization of the renal Na+/phosphate cotransporter NaPi-IIa in mouse kidney and OK cells. *Am J Physiol Renal Physiol* 2005; **288**: F740–F747.

[205] Baum M, Schiavi S, Dwarakanath V, *et al.* Effect of fibroblast growth factor-23 on phosphate transport in proximal tubules. *Kidney Int* 2005; **68**: 1148–1153.

[206] Berndt T J, Bielesz B, Craig T A, *et al.* Secreted frizzled-related protein-4 reduces sodium-phosphate co-transporter abundance and activity in proximal tubule cells. *Pflugers Arch* 2006; **451**: 579–587.

[207] Capuano P, Radanovic T, Wagner C A, *et al.* Intestinal and renal adaptation to a low-Pi diet of type II NaPi cotransporters in vitamin D receptor- and 1alphaOHase-deficient mice. *Am J Physiol Cell Physiol* 2005; **288**: C429–C434.

[208] Murer H, Hernando N, Forster I, *et al.* Proximal tubular phosphate reabsorption: molecular mechanisms. *Physiol Rev* 2000; **80**: 1373–1409.

[209] Murer H, Hernando N, Forster I, *et al.* Regulation of Na/Pi transporter in the proximal tubule. *Annu Rev Physiol* 2003; **65**: 531–542.

[210] Picard N, Capuano P, Stange G, *et al.* Acute parathyroid hormone differentially regulates renal brush border membrane phosphate cotransporters. *Pflugers Arch* 2010; **460**: 677–687.

[211] Nowik M, Lecca M R, Velic A, *et al.* Genome-wide gene expression profiling reveals renal genes regulated during metabolic acidosis. *Physiol Genomics* 2008; **32**: 322–334.

[212] Farrow E G, Davis S I, Summers L J, *et al.* Initial FGF23-mediated signaling occurs in the distal convoluted tubule. *J Am Soc Nephrol* 2009; **20**: 955–960.

[213] Olauson H, Lindberg K, Amin R, *et al.* Targeted deletion of Klotho in kidney distal tubule disrupts mineral metabolism. *J Am Soc Nephrol* 2012; **23**: 1641–1651.

[214] Shigematsu T, Kazama J J, Yamashita T, *et al.* Possible involvement of circulating fibroblast growth factor 23 in the development of secondary hyperparathyroidism associated with renal insufficiency. *Am J Kidney Dis* 2004; **44**: 250–256.

[215] Evenepoel P, Meijers B, Viaene L, *et al.* Fibroblast growth factor-23 in early chronic kidney disease: additional support in favor of a phosphate-centric paradigm for the pathogenesis of secondary hyperparathyroidism. *Clin J Am Soc Nephrol* 2010; **5**: 1268–1276.

[216] Bihoreau M T, Ceccherini I, Browne J, *et al.* Location of the first genetic locus, PKDr1, controlling autosomal dominant polycystic kidney disease in Han:SPRD cy/+ rat. *Hum Mol Genet* 1997; **6**: 609–613.

[217] Brown J H, Bihoreau M T, Hoffmann S, *et al.* Missense mutation in sterile alpha motif of novel protein SamCystin is associated with polycystic kidney disease in (cy/+) rat. *J Am Soc Nephrol* 2005; **16**: 3517–3526.

[218] Schäfer K, Gretz N, Bader M, *et al.* Characterization of the Han:SPRD rat model for hereditary polycystic kidney disease. *Kidney Int* 1994; **46**: 134–152.

[219] Ahrabi A K, Jouret F, Marbaix E, *et al.* Glomerular and proximal tubule cysts as early manifestations of Pkd1 deletion. *Nephrol Dial Transplant* 2010; **25**: 1067–1078.

[220] Torres V E, Bengal R J, Litwiller R D, *et al.* Aggravation of polycystic kidney disease in Han:SPRD rats by buthionine sulfoximine. *J Am Soc Nephrol* 1997; **8**: 1283–1291.

[221] Turner C M, Ramesh B, Srai S K S, *et al.* Altered ATP-sensitive P2 receptor subtype expression in the Han:SPRD cy/+ rat, a model of autosomal dominant polycystic kidney disease. *Cells Tissues Organs* 2004; **178**: 168–179.

[222] Wahl P R, Serra A L, Le Hir M, *et al.* Inhibition of mTOR with sirolimus slows disease progression in Han:SPRD rats with autosomal dominant polycystic kidney disease (ADPKD). *Nephrol Dial Transplant* 2006; **21**: 598–604.

[223] Wu M, Arcaro A, Varga Z, *et al.* Pulse mTOR inhibitor treatment effectively controls cyst growth but leads to severe parenchymal and glomerular hypertrophy in rat polycystic kidney disease. *Am J Physiol Renal Physiol* 2009; **297**: F1597–F1605.

[224] Vogel M, Kränzlin B, Biber J, *et al.* Altered expression of type II sodium/phosphate cotransporter in polycystic kidney disease. *J Am Soc Nephrol* 2000; **11**: 1926–1932.

[225] Faul C, Amaral A P, Oskouei B, *et al.* FGF23 induces left ventricular hypertrophy. *J Clin Invest* 2011; **121**: 4393–4408.

[226] Marsell R, Krajisnik T, Göransson H, *et al.* Gene expression analysis of kidneys from transgenic mice expressing fibroblast growth factor-23. *Nephrol Dial Transplant* 2008; **23**: 827–833.

[227] Zanchi C, Locatelli M, Benigni A, *et al.* Renal Expression of FGF23 in Progressive Renal Disease of Diabetes and the Effect of Ace Inhibitor. *PLoS One* 2013; **8**: e70775.

[228] Pathare G, Föller M, Michael D, *et al.* Enhanced FGF23 serum concentrations and phosphaturia in gene targeted mice expressing WNK-resistant SPAK. *Kidney Blood Press Res* 2012; **36**: 355–364.

[229] Pathare G, Föller M, Daryadel A, *et al.* OSR1-sensitive renal tubular phosphate reabsorption. *Kidney Blood Press Res* 2012; **36**: 149–161.

[230] Brodehl J, Krause A, Hoyer P F. Assessment of maximal tubular phosphate reabsorption: comparison of direct measurement with the nomogram of Bijvoet. *Pediatr Nephrol* 1988; **2**: 183–189.

[231] Biber J, Stieger B, Haase W, *et al.* A high yield preparation for rat kidney brush border membranes. Different behaviour of lysosomal markers. *Biochim Biophys Acta* 1981; **647**: 169–176.

[232] Biber J, Stieger B, Stange G, *et al.* Isolation of renal proximal tubular brush-border membranes. *Nat Protoc* 2007; **2**: 1356–1359.

[233] Hilfiker H, Hattenhauer O, Traebert M, *et al.* Characterization of a murine type II sodium-phosphate cotransporter expressed in mammalian small intestine. *Proc Natl Acad Sci U S A* 1998; **95**: 14564–14569.

[234] Law S W, Conneely O M, DeMayo F J, *et al.* Identification of a new brain-specific transcription factor, NURR1. *Mol Endocrinol* 1992; **6**: 2129–2135.

[235] Torii T, Kawarai T, Nakamura S, *et al.* Organization of the human orphan nuclear receptor Nurr1 gene. *Gene* 1999; **230**: 225–232.

[236] Wilson T E, Fahrner T J, Johnston M, *et al.* Identification of the DNA binding site for NGFI-B by genetic selection in yeast. *Science* 1991; **252**: 1296–1300.

[237] Honkaniemi J, Sharp F R. Global ischemia induces immediate-early genes encoding zinc finger transcription factors. *J Cereb Blood Flow Metab* 1996; **16**: 557–565.

[238] Ohkubo T, Sugawara Y, Sasaki K, *et al.* Early induction of nerve growth factor-induced genes after liver resection-reperfusion injury. *J Hepatol* 2002; **36**: 210–217.

[239] McEvoy A N, Murphy E A, Ponnio T, *et al.* Activation of nuclear orphan receptor NURR1 transcription by NF-kappa B and cyclic adenosine 5'-monophosphate response element-binding protein in rheumatoid arthritis synovial tissue. *J Immunol* 2002; **168**: 2979–2987.

[240] Spichtig D, Zhang H, Mohebbi N, *et al.* Renal expression of FGF23 and peripheral resistance to elevated FGF23 in rodent models of polycystic kidney disease. *Kidney Int* 2014; **85**: 1340–1350.

[241] Ong A C, Harris P C, Davies D R, *et al.* Polycystin-1 expression in PKD1, early-onset PKD1, and TSC2/PKD1 cystic tissue. *Kidney Int* 1999; **56**: 1324–1333.

[242] Koressaar T, Remm M. Enhancements and modifications of primer design program Primer3. *Bioinformatics* 2007; **23**: 1289–1291.

[243] Belibi F, Zafar I, Ravichandran K, *et al.* Hypoxia-inducible factor-1? (HIF-1?) and autophagy in polycystic kidney disease (PKD). *Am J Physiol Renal Physiol* 2011; **300**: F1235–F1243.

[244] Raina S, Honer M, Krämer S D, *et al.* Anti-VEGF antibody treatment accelerates polycystic kidney disease. *Am J Physiol Renal Physiol* 2011; **301**: F773–F783.

[245] Zeier M, Fehrenbach P, Geberth S, *et al.* Renal histology in polycystic kidney disease with incipient and advanced renal failure. *Kidney Int* 1992; **42**: 1259–1265.